THESIS FOR THE DEGREE OF DOCTOR OF PHILOSOPHY

# Location-aware Communications

L. Srikar Muppirisetty

CHALMERS

Communication Systems Group
Department of Electrical Engineering
Chalmers University of Technology
Göteborg, Sweden, 2017

L. Srikar Muppirisetty
LOCATION-AWARE COMMUNICATIONS

ISBN 978-91-7597-670-9
Doktorsavhandlingar vid Chalmers tekniska högskola
Series No. 4127
ISSN 0346-718X
Technical Report No. R015/2017
Communication Systems Group
Department of Electrical Engineering
Chalmers University of Technology
SE–412 96 Göteborg
Sweden
Telephone: +46–(0)31–772 10 00



Front Cover: The figure on the front cover is the main idea of Location-aware communication. The user has an expected navigation path. The background shows the long-term average channel quality, including base station specific path-loss, and a spatial field for shadowing.

Printed by Chalmers Reproservice
Göteborg, Sweden, November 2017.

To my beloved wife Haritha and son Shreyansh.

"All truths are easy to understand once they are discovered; the point is to discover them."

-Galileo Galilei

# Abstract

5G networks will be characterized by a wide variety of use cases, as well as orders-of-magnitude increase in mobile data volume per area, number of connected devices, and typical user data rate, all compared to current mobile communication systems. In particular, they are expected to offer 1000 times higher mobile data volume per unit area, 10-100 times higher number of connecting devices and user data rate, 10 times longer battery life and 5 times reduced latency. With such high number of connected devices, scalability and reduction of signalling overhead become important issues, as well as minimization of total energy consumption to enable green and affordable cost for network operation. In this thesis, we argue how location information can be exploited to address some of the aforementioned challenges. The thesis aims at bridging the gap between the research topics of positioning and communication, and understand how and to what extent location information with uncertainty may aid communication capabilities across the different layers of the protocol stack in 5G networks.

In the first part of thesis, we review the basics of the wireless channel and its predictability and describe various traditional resource allocation schemes. We discuss the channel characteristics of wireless propagation channel and then show how location information is related to predicting the long-term channel components such as path-loss and shadowing. We then present statistical channel models based on location information for cellular and ad-hoc networks. The statistical channel models are complemented with channel measurements for validation purposes, carried out for both cellular and ad-hoc networks. Upon the establishment of the relationship between the location and channel, we then describe a machine learning framework called Gaussian processes (GP) and show how it can be used for spatial channel prediction for cellular and ad-hoc networks with perfect location information. The framework can be used to predict different channel quality metrics (CQM) such as received signal strength, root-mean-square (RMS) delay spread, and interference levels.

Location information can be used in two types of resource allocation schemes, namely reactive and proactive resource allocation. In reactive networks, the resource allocation starts when a user requests for a service, whereas in proactive networks, the resource allocation is planned before the user requests for a service. We first show the drawbacks with the traditional resource allocation schemes and then show how location information can be used to mitigate these. The location information can either be used directly or through predicted CQM for reactive and proactive resource allocation. Specifically, we show the potential of location information for various resource allocation schemes for the 5G candidate technologies such as: (i) scheduling and routing in device-to-device communications and show how location information can be used to reduce signalling overhead and latency; (ii) initial access is a challenging problem for millimeter wave communications due to its high directivity, we review works where location information is used to speed up the initial discovery phase; (iii) location information can also be used for interference management in heterogeneous networks with low signalling overhead; (iv) interference mitigation through location-aided pilot allocation in

massive multiple-input and multiple-output (MIMO) systems; (v) efficient utilization of network resources with location-aware proactive caching and long-term predictive resource allocation.

The second part of the thesis includes six research papers based on location-aware communications. Paper A discusses the challenges of 5G networks, which include an increase in traffic and number of devices, robustness for mission-critical services, and a reduction in total energy consumption and latency. We argue how location information can be leveraged in addressing several of the key challenges in 5G with location-aware channel prediction by maintaining a channel database. We provide a broad overview of using location-aware channel prediction in addressing the aforementioned challenges across different layers of the protocol stack. In Paper B, we first show a location-aware channel prediction framework with perfect location information using the GP tool from machine learning. We then discuss its weakness in poor quality channel predictions when location uncertainty is not considered. Finally, we propose a new framework based on GP to handle location uncertainty that enhances the channel quality predictions for cellular networks. Paper C extends the framework from Paper B to ad-hoc networks. Paper D studies the use of location information for reactive resource allocation in massive MIMO systems. Specifically, a location-based approach to mitigate the pilot contamination problem for uplink MIMO is described. We show that the proposed pilot assignment strategy offers improved channel estimation performance as well as enhanced downlink sum rate even when the number of antennas is finite. Paper E and Paper F concentrate on the use of location information for proactive resource allocation. In Paper E, we develop optimal proactive strategies based on the predictable user demand preferences and channel characteristics for content prefetching at the user terminal. We demonstrate that the designed proactive schedulers offer better performance in terms of cost and load, in contrast to a baseline reactive scheduler. In Paper F, we propose and evaluate a location-aware user-centric proactive resource allocation approach, in which the users are proactive and seek good channel quality by moving to locations where the signal quality is good. The approach utilizes the GP framework for channel prediction from Paper B. We show that the proposed method improves the number of satisfied users and the overall network throughput.

**Keywords:** 5G, Gaussian processes, resource allocation, reactive resource allocation, proactive resource allocation, millimeter wave communications, initial access, massive MIMO, pilot contamination, proactive caching, heterogeneous networks.

# Publications

The thesis is based on the following appended papers:

[A] R. Di Taranto, L. S. Muppirisetty, R. Raulefs, D. Slock, T. Svensson, and H. Wymeersch, "Location-aware communications for 5G networks", in *IEEE Signal Processing Magazine*, vol. 31, no. 6, pp. 102-112, Nov. 2014.

[B] L. S. Muppirisetty, H. Wymeersch, and T. Svensson, "Spatial wireless channel prediction under location uncertainty", in *IEEE Transactions on Wireless Communications*, vol. 15, no. 2, pp. 1031-1044, Feb. 2016.

[C] M. Fröhle, L. S. Muppirisetty, and H. Wymeersch, "Channel gain prediction for multi-agent networks in the presence of location uncertainty", in *Proceedings of IEEE International Conference on Acoustics, Speech and Signal Processing (ICASSP)*, pp. 3911-3915, Mar. 2016.

[D] L. S. Muppirisetty, T. Charalambous, J. Karout, G. Fodor, and H. Wymeersch, "Location-aided pilot contamination avoidance for massive MIMO systems", Submitted to *IEEE Transactions on Wireless Communications.*

[E] L. S. Muppirisetty, J. Tadrous, A. Eryilmaz, and H. Wymeersch, "Proactive resource allocation with predictable channel statistics", in preparation.

[F] L. S. Muppirisetty, S. Yiu, and H. Wymeersch, "LAPRA: Location-aware proactive resource allocation", in *Proceedings of IEEE Global Communications Conference (GLOBECOM)*, Dec. 2016.

Other contributions by the author (not included in this thesis):

[G] S. Ahmad, R. Reinhagen, L. S. Muppirisetty, and H. Wymeersch, "Predictive resource allocation evaluation with real channel measurements", in *Proceedings of IEEE International Conference on Communications (ICC)*, pp. 1-5, May 2017.

[H] L. S. Muppirisetty, H. Wymeersch, J. Karout, and G. Fodor, "Location-Aided Pilot Contamination Elimination for Massive MIMO Systems", in *Proceedings of IEEE Global Communications Conference (GLOBECOM)*, pp. 1-5, Dec. 2015.

[I] L. S. Muppirisetty, J. Tadrous, A. Eryilmaz, and H. Wymeersch, "On proactive caching with demand and channel uncertainties", in *Proceedings of 53rd Annual Allerton Conference on Communication, Control, and Computing (Allerton)*, pp. 1174-1181, Sept. 2015.

[J] G. E. Garcia, L. S. Muppirisetty, E. M. Schiller, and H. Wymeersch, "On the trade-off between accuracy and delay in cooperative UWB localization: performance bounds and scaling laws", in *IEEE Transactions on Wireless Communications*, vol. 13, no. 8, pp. 4574-4585, Aug. 2014.

[K] L. S. Muppirisetty, R. Di Taranto, and H. Wymeersch, "Robust link scheduling with channel estimation and location information", in *Proceedings of Forty Seventh Asilomar Conference on Signals, Systems and Computers*, pp. 1695-1699, Nov. 2013.

[L] G. E. Garcia, L. S. Muppirisetty, and H. Wymeersch, "On trade-off between accuracy and delay in cooperative UWB navigation", in *Proceedings of IEEE Wireless Communications and Networking Conference*, pp. 1603-1608, Apr. 2013.

[M] C. Lindberg, L. S. Muppirisetty, K. Dahlen, V. Savic, and H. Wymeersch, "MAC delay in belief consensus for distributed tracking", in *Proceedings of 10th Workshop on Positioning, Navigation and Communication*, pp. 1-6, Mar. 2013.

[N] G. E. Garcia, L. S. Muppirisetty, and H. Wymeersch, "On the trade-off between accuracy and delay in UWB navigation", in *IEEE Communications Letters*, vol. 17, no. 1, pp. 39-42, Jan. 2013.

# Contents

# Acknowledgments

"No matter what accomplishments you make, somebody helped you."

-Althea Gibson

First and foremost, I would like to express my deepest gratitude to my main supervisor, Prof. Henk Wymeersch for giving me this opportunity of pursuing Ph.D. studies in the Communication Systems (ComSys) group. Thank you very much for your guidance, encouragement, and for giving me the freedom to explore and work on new and interesting problems. I am very lucky to have you as my supervisor. One great quality in you is that you make sure that your students never feel that they are alone and you provide extra needed support during difficult times. Even though you were quite busy, you always make up the time to discuss research ideas. I am still unable to figure out, how you can be quite efficient in replying to emails in quick time. I hope I will be efficient like you one day.

I would like to express my great appreciation to my co-supervisor Prof. Tommy Svensson. It is very nice and fun to work with you again after my masters. I also want to take this opportunity to thank all my collaborators. It was a great learning experience working with Dr. Themistoklis Charalambous. Special thanks to Dr. Rocco Di Taranto, for many interesting discussions and collaborations. My gratitude also goes to Prof. Atilla Eryilmaz and Dr. John Tadrous. Thank you, Atilla for hosting me at your group at The Ohio State University. It was so amazing to work with you John, although we never met physically. Thank you for all your support. Also, I would like to thank Dr. Simon Yiu and Dr. Doru Calin for hosting me for an internship at Bell Labs. Thanks a lot Simon for many interesting discussions and taking good care of me during my stay at Bell Labs. It was my dream come true to work with such an innovative organization. I would like to give my special thanks to Dr. Gabor Fodor, it was my pleasure working with you. I would like to give a special mention to Dr. Johnny Karout, it was very nice to work with you again after our master thesis.

Thanks to Christopher for being the best office mate possible. I would also like to thank COOPNET team members for many interesting discussions and for the constructive feedback on the articles. My heartfelt thanks to the current and former members of the Comsys group for the consistent support during last few years. A big thank you to Markus, Erik Steinmetz, Keerthi, Themis, Naga, John, and Christopher for proofreading the various chapters of this thesis.

I would like to thank my Indian friends at ComSys: Naga, Abu, Satya, Keerthi, Rahul, Rajet, and Tilak for very interesting lunch discussions.

I would like to acknowledge Prof. Erik Ström for his efforts to provide an excellent and stimulating research environment. Many thanks to Agneta, Natasha, for all their help. It is very hard to imagine the department without you.

I owe a big thanks to Naga and Prasad for all your help when I needed the most. Also, special gratitude goes to Sneha, Ankur, Keerthi, Gyan, Sejal, Naga, Pravin Karthik, Selva, Sunil, and Prasad for all the wonderful weekends and fun parties.

Finally, my outmost gratitude and love goes to my precious family: Thanks, Dad, Mom, and brother for believing in me and for your support and encouragement all these years. I would also like to thank my in-laws for their support. Most importantly, I would like to thank my wife Haritha, for her understanding, support and unconditional love. You left everything behind in India for me and joined me on this beautiful journey. I know, you are more excited than me, when I started this. I understand how much struggle you have gone through due to this to enter the Swedish job market. As a result, you did your masters and now part of Volvo as software graduate trainee, I am very proud of your achievement. I would like to thank you for all your support to manage Shreyansh last year. Honestly, without your support, I could not have made to this point. You are my biggest strength and source of joy. Thank you with all my heart and soul.

Finally, my little champ Shreyansh, you are my stress buster and it is real fun playing with you. I am greatly indebted to you for all your support, especially the last year. We are very lucky to have you. I am so much amazed at your understanding and never complain about anything. I guess you are the most cheerful kid I have ever seen and your innocence makes us even more joyous every day. I wish you a healthy and successful life.

*L. Srikar Muppirisetty*
*Gothenburg, November, 2017.*

*This research was supported, in part, by the European Research Council, under Grant No. 258418 (COOPNET).*

# Acronyms

| | |
|---|---|
| ABS | almost blank sub-frames |
| AoA | angle-of-arrival |
| AoD | angle-of-departure |
| ARIMA | auto regressive integrated moving average |
| BF | beamforming |
| BIP | binary integer programming |
| BS | base station |
| cGP | classical GP |
| CoMP | coordinated multipoint |
| CQM | channel quality metrics |
| CSI | channel state information |
| D2D | device-to-device |
| eICIC | enhanced ICIC |
| FAP | femtocell access point |
| GBS | gain based scheduler |
| Gbps | giga-bit per second |
| GP | Gaussian processes |
| GPS | global positioning system |
| HetNet | heterogeneous network |
| IA | initial access |
| ICIC | inter-cell interference coordination |
| IM | interference management |
| LBS | location based scheduler |
| LOS | line of sight |
| MAC | medium access control |
| MDT | minimization of drive test |
| MIMO | multi-input multi-output |
| MUE | macro cell user |
| mmWave | millimeter wave |
| pdf | probability density function |
| PRA | proactive RA |
| QoS | quality of service |
| RA | resource allocation |

| | |
|---|---|
| REM | radio environment map |
| RF | radio frequency |
| RLSP | robust link scheduling problem |
| RMS | root mean square |
| RRA | reactive RA |
| RSRP | received signal received power |
| STDMA | spatial time division multiple access |
| SINR | signal to interference plus noise ratio |
| SNR | signal to noise ratio |
| SP | service provider |
| TV | television |
| TDD | time division duplex |
| TDMA | time division multiple access |
| uGP | uncertain GP |
| UWB | ultrawide bandwidth |

# Part I

# Overview

# Chapter 1

# Introduction

## 1.1 Motivation

Location-awareness has received intense interest from the research community, in particular with respect to cognitive radio [1], where radio environment map (REM) enabled databases are being used to exploit TV white spaces [2]. REM provides various network and user-related context information such as geo-location data, propagation models, interference maps, spectral usage regulations, user and service policies [3]. REM has been applied to various problems such as interference management in two-tier cellular networks [3], coverage hole detection and prediction [4], and compensating time-varying Doppler spread for railways [5] to name a few. However, recent studies have revealed that location information (part of context information) can be harnessed in not only cognitive networks, but also cellular and ad-hoc configurations [6]. In particular, location-aware resource allocation techniques can reduce overheads and delays due to their ability to predict channel quality beyond traditional time scales. In [7], it was demonstrated that a communication system can benefit from location information if it can exploit not only short-term channel coherence, but also mid-term/long-term coherence of the users' location and movement. This is achieved by the mobile devices reporting back their current location and their navigation routes and destinations to base stations (BSs). The concept of location-aware communication is shown in Fig. 1.1, where a user provides its up-to-date location to the BS, which, based on a spatial channel model, can allocate resources among users.

5G networks will be the first generation to benefit from location information that is sufficiently precise to be leveraged in wireless network design and optimization. 5G networks will be characterized by a wide variety of use cases, as well as orders-of-magnitude increase in mobile data volume per area, number of connected devices, and typical user data rate, all compared to current mobile communication systems. In particular, they are expected to offer 1000 times higher mobile data volume per unit area, 10-100 times higher number of connecting devices and user data rate, 10 times longer battery life and 5 times reduced latency [8]. Moreover,

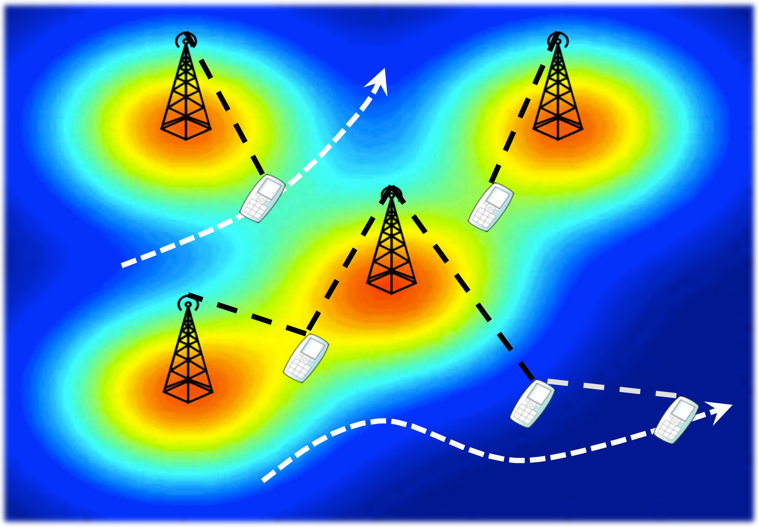

**Figure 1.1:** *Location-aware communication: the main idea.* The user has an expected navigation path. The background shows the long-term average channel quality, including BS specific path-loss, and a spatial field for shadowing. The BSs can adjust their transmission strategy (at different levels of the protocol stack) if accurate and up-to-date location information is available.

scalability and reduction of signalling overhead must be accounted for, as well as minimization of (total) energy consumption to enable affordable cost for network operation [9].

Location-information can be the key to address this challenge, and complement existing methods at time and space scales that are currently not considered. We envision that context information in general, and location information in particular can be utilized by these networks across all layers of the communication protocol stack, since location and communication are tightly coupled (see Fig. 1.2). This vision is based on two assumptions: (i) the availability of location information; (ii) the possibility for the network operator to collect and store geo-tagged channel quality information. The first assumption is met by the introduction of sophisticated network localization methods (see [10] and references therein) and new localization technologies (such as Galileo [11], 5G localization [12]), which enable sufficient resolution to capture path-loss and shadowing. The second assumption is based on minimization of drive test (MDT) feature in 3GPP Release 10 [13]. In MDT, users collect radio measurements and associated location information in order to assess network performance.

The geo-tagged channel quality metrics (CQM) (received signal strength, RMS delay spread, interference levels etc.) from users enables the construction of a dynamic database, and this allows the prediction of CQM at arbitrary locations and future times. In order to predict the CQM in locations where no previous

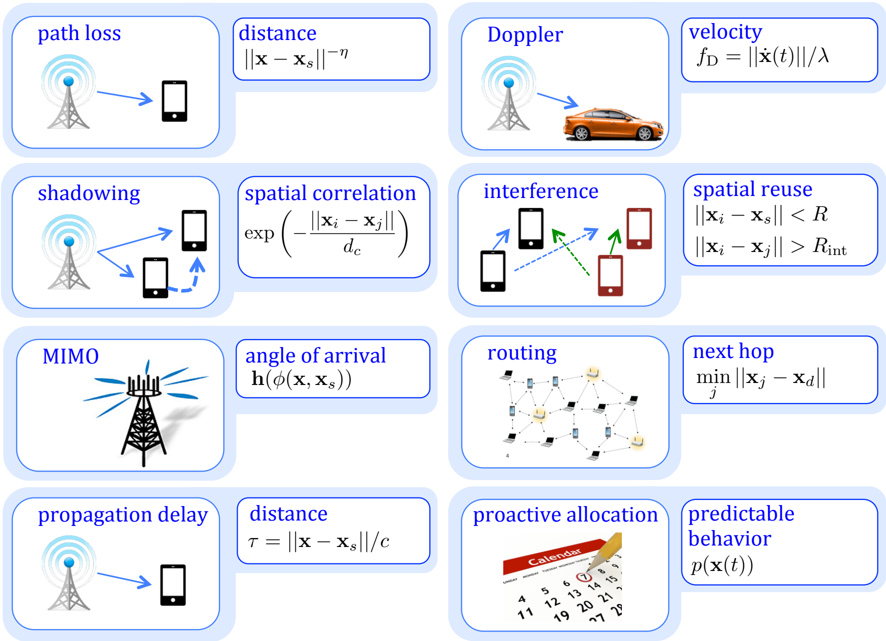


**Figure 1.2:** The figure is based on [9]. Communication systems are tied to location information in many ways, including through distances, delays, velocities, angles, and predictable user behavior. The notations are as follows (starting from the top left downward): $\mathbf{x}$ is the user location, $\mathbf{x}_s$ is the BS or sender location, $\eta$ is the path-loss exponent; $\mathbf{x}_i$ and $\mathbf{x}_j$ are two user locations, $d_c$ is a correlation distance; $\phi(.)$ is an angle of arrival between a user and a BS, $\mathbf{h}$ is a multi-input multi-output (MIMO) channel; $c$ is the speed of light and $\tau$ a propagation delay; $f_\mathrm{D}$ is a Doppler shift, $\dot{\mathbf{x}}(t)$ is the user velocity, $\lambda$ is the carrier wavelength; $R$ is a communicate range, $R_\mathrm{int}$ is an interference range; $\mathbf{x}_d$ is a destination; $p(\mathbf{x}(t))$ is a distribution of a user location at a future time $t$.

CQM was available, a flexible location-aware predictive engine is needed. However, localization is subject to errors as the algorithms need to cope with harsh propagation conditions, delays, receiver dynamics and is also highly dependent on the environment. The accuracies of various common localization technologies are as follows: the global positioning system (GPS) is the most widely used localization technology in outdoor scenarios, whose accuracy is around few meters [14]; ultrawide bandwidth (UWB) systems provide sub-meter accuracy and are mainly used in indoor scenarios [15]; WiFi-based positioning gives accuracy on the order of few meters [15]. Undoubtedly, the uncertainty in the localization must be accounted for when developing the location-aware predictive engine. The location-aware CQM predictions can be utilized in several areas such as in handling proactive caching strategies [16–18] and in anticipatory networks for predictive resource allocation [19–28].

## 1.2 Scope and Aim of the Thesis

The thesis aims in bridging the gap between the interaction of the research topics of positioning and communication, and understand how and to what extent location information with uncertainty may aid communication capabilities across the different layers of the protocol stack in 5G networks. In particular, we analyze statistical channel models, which tie locations to channels. Furthermore, we develop a framework for spatial prediction of wireless channels with uncertain location information for cellular and ad-hoc networks. We also investigate the role of location information in reactive as well as proactive resource allocation for 5G networks. Specifically, we study the use of location information in various use cases, such as location-aided pilot allocation methods to reduce uplink interference in massive MIMO systems, optimal proactive strategies based on the predictable user demand preferences and channel characteristics for content prefetching, and location-aware predictive resource allocation for media streaming.

## 1.3 Organization of the Thesis

There are two choices for a doctoral student to write the PhD thesis: one is monograph and the other is a collection of papers. This thesis is written as collection of papers and is divided into two parts. Part I gives an introduction and motivation to the topic and necessary background material to understand the appended papers in part II of the thesis. Part I is structured as follows. In Chapter 2, we introduce basics of wireless channels and provide statistical channel models for cellular and ad-hoc networks. We also provide the channel measurements that are obtained as part of a measurement campaign to support the channel models. Later, in Chapter 3, we use Gaussian processes, a regression tool from machine learning, and show its use in predicting channel gain based on location information for cellular and ad-hoc networks. In Chapter 4, we demonstrate the potential of location information to reduce the drawbacks in the traditional reactive resource allocation schemes. In Chapter 5, we investigate the use of location information for various proactive resource allocation methods. Finally, the contributions of this thesis are summarized in Chapter 6.

## 1.4 Notation

The following notation is used in the introductory part of the thesis.

- Vectors and matrices are written in bold (e.g., a vector $\mathbf{k}$ and a matrix $\mathbf{K}$); $\mathbf{K}^{\mathrm{T}}$ denotes transpose of $\mathbf{K}$; $|\mathbf{K}|$ denotes determinant of $\mathbf{K}$; $[\mathbf{K}]_{ij}$ denotes entry $(i, j)$ of $\mathbf{K}$.

- $\mathbf{I}$ denotes identity matrix of appropriate size; $\mathbf{1}$ and $\mathbf{0}$ are vectors of ones and zeros, respectively, of appropriate size.
- $\|.\|$ denotes $L_2$-norm unless otherwise stated.
- $\|.\|_{\mathrm{F}}$ denotes the Frobenius norm.
- $\mathbb{E}[.]$ denotes the expectation operator.
- Cov[.] denotes covariance operator (i.e., $\mathrm{Cov}[\mathbf{y}_1, \mathbf{y}_2] = \mathbb{E}[\mathbf{y}_1\mathbf{y}_2^{\mathrm{T}}] - \mathbb{E}[\mathbf{y}_1]\,\mathbb{E}[\mathbf{y}_2]^{\mathrm{T}}$).
- $\mathcal{N}(\mathbf{x}; \mathbf{m}, \Sigma)$ denotes a Gaussian distribution evaluated in $\mathbf{x}$ with mean vector $\mathbf{m}$ and covariance matrix $\Sigma$ and $\mathbf{x} \sim \mathcal{N}(\mathbf{m}, \Sigma)$ denotes that $\mathbf{x}$ is drawn from a Gaussian distribution with mean vector $\mathbf{m}$ and covariance matrix $\Sigma$.
- A sequence of elements $\{a_1, a_2, \ldots\}$ is written in short as $\{a_j\}_j$.
- The positive operator is denoted as $(x)^+ = \max(0, x)$.
- The cardinality of a set $\mathcal{A}$ is denoted by $|\mathcal{A}|$.
- The sets of real and complex numbers are denoted by $\mathbb{R}$ and $\mathbb{C}$, respectively; the $n$-dimensional Euclidean and complex spaces are denoted by $\mathbb{R}^n$ and $\mathbb{C}^n$, respectively.
- $\mathbf{x} \preceq \mathbf{y}$ means that $x_i \leq y_i$, $\forall i$.
- $\{\}_t$ denotes a collection of elements, and $()_t$ denotes a sequence of elements.

# Chapter 2

# Wireless Channel Propagation Models

## 2.1 Introduction

In this chapter, we review the basics of wireless propagation channels. The characteristics of wireless radio channels have been studied quite extensively in the literature ([29–33] and references therein). A common way to model the wireless propagation channel is as a stochastic process with three major dynamics which occur at different length scales namely path-loss, shadowing, and small-scale fading. On a larger length scale, path-loss captures power attenuation of the radio signal with distance, which decays linearly with the logarithm of the distance from the transmitter [1]. Shadowing captures the medium length scale power variations of the signal around the path-loss, which occur due to obstacles in the propagation environment such as hills, buildings, trees, etc. Path-loss and shadowing vary over longer distances and are hence called large-scale fading. Finally, small-scale fading captures power fluctuations on a shorter (typically in the scale of the wavelength of the carrier) length scale due to multi-path propagation effects of the signal in the environment. The large-scale fading allows to model the average channel characteristics whereas small-scale fading allows to capture instantaneous channel characteristics. In the rest of the chapter, we introduce the statistical channel models for cellular and ad-hoc networks. Furthermore, we exemplify these models with the measurements we have collected as part of a measurement campaign.

[1] Under the assumption of omnidirectional receivers embracing the transmitter.

## 2.2 Statistical Channel Model with Static Transmitter

Consider a geographical region $\mathcal{A} \subset \mathbb{R}^2$, where a transmitter is located at $\mathbf{x}_{\mathrm{TX}} \in \mathbb{R}^2$ and is static (usually the case for BSs in cellular networks) and transmits a signal with power $P_{\mathrm{TX}}$ to $i$-th receiver located at $\mathbf{x}_{\mathrm{RX},i} \in \mathbb{R}^2$ through a wireless propagation channel. The received power $P_{\mathrm{RX}}(\mathbf{x}_{\mathrm{TX}}, \mathbf{x}_{\mathrm{RX},i}, t)$ at receiver $i$ and time $t$ can be expressed as [29]

$$P_{\mathrm{RX}}(\mathbf{x}_{\mathrm{TX}}, \mathbf{x}_{\mathrm{RX},i}, t) = P_{\mathrm{TX}}\, g_0\, ||\mathbf{x}_{\mathrm{TX}} - \mathbf{x}_{\mathrm{RX},i}||^{-\eta}\, \psi(\mathbf{x}_{\mathrm{TX}}, \mathbf{x}_{\mathrm{RX},i}, t)\, |h(\mathbf{x}_{\mathrm{TX}}, \mathbf{x}_{\mathrm{RX},i}, t)|^2, \tag{2.1}$$

where $g_0$ is a constant that captures antenna and other propagation gains, $\eta$ is the path-loss exponent, $\psi(\mathbf{x}_{\mathrm{TX}}, \mathbf{x}_{\mathrm{RX},i}, t)$ is the location-dependent shadowing and $h(\mathbf{x}_{\mathrm{TX}}, \mathbf{x}_{\mathrm{RX},i}, t)$ is the component from small-scale fading.

In this thesis, we assume measurements are averaged over small-scale fading, either in time (measurements taken over a time window) or frequency (measurements represent average power over a large frequency band). Therefore, the resulting received signal power from the transmitter to receiver $i$ can be expressed in dB scale as

$$P_{\mathrm{RX}}(\mathbf{x}_{\mathrm{TX}}, \mathbf{x}_{\mathrm{RX},i})[\mathrm{dBm}] = L_0 - 10\,\eta\, \log_{10}(||\mathbf{x}_{\mathrm{TX}} - \mathbf{x}_{\mathrm{RX},i}||) + \Psi(\mathbf{x}_{\mathrm{TX}}, \mathbf{x}_{\mathrm{RX},i}), \tag{2.2}$$

where $L_0 = P_{\mathrm{TX}}[\mathrm{dBm}] + G_0$ with $G_0 = 10\,\log_{10}(g_0)$ and $\Psi(\mathbf{x}_{\mathrm{TX}}, \mathbf{x}_{\mathrm{RX},i}) = 10\,\log_{10}(\psi(\mathbf{x}_{\mathrm{TX}}, \mathbf{x}_{\mathrm{RX},i}))$. The log-normal distribution is a common choice for modeling shadowing in wireless systems in which it is assumed that the received power in dB is Gaussian distributed. Thus, shadowing in logarithm domain follows a zero mean Gaussian distribution with variance $\sigma_\Psi^2$ i.e., $\Psi(\mathbf{x}_{\mathrm{TX}}, \mathbf{x}_{\mathrm{RX},i}) \sim \mathcal{N}(0, \sigma_\Psi^2)$. Spatial correlations of shadowing are studied extensively and well-established models exist in the literature (see [34] for an overview). The Gudmundson model [35] is a widely used shadowing correlation model in cellular communications, where the transmitter is static. According to this model, the spatial auto covariance function of the shadowing between receivers at locations $\mathbf{x}_{\mathrm{RX},i}$ and $\mathbf{x}_{\mathrm{RX},j}$ follows an exponential decay function as

$$\begin{aligned} C(\mathbf{x}_{\mathrm{RX},i}, \mathbf{x}_{\mathrm{RX},j}) &= \mathbb{E}[\Psi(\mathbf{x}_{\mathrm{TX}}, \mathbf{x}_{\mathrm{RX},i}), \Psi(\mathbf{x}_{\mathrm{TX}}, \mathbf{x}_{\mathrm{RX},j}) | \mathbf{x}_{\mathrm{RX},i}, \mathbf{x}_{\mathrm{RX},j}] \\ &= \sigma_\Psi^2 \exp\left(-\frac{||\mathbf{x}_{\mathrm{RX},i} - \mathbf{x}_{\mathrm{RX},j}||}{d_c}\right), \end{aligned} \tag{2.3}$$

where $d_c$ is the correlation distance. Later in this chapter, we will describe the covariance function for ad-hoc networks.

A typical one dimensional simulated channel realization using (2.2) is depicted in Fig. 2.1. The transmitter is fixed and receiver is moved along a straight line. It can be observed that received power decays with distance and also the measurements vary slowly with distance indicating spatial correlation. Thus, it is possible to predict the large-scale fading component (path-loss and shadowing) of the wireless channel from the location. In Chapter 3, we show how this can be

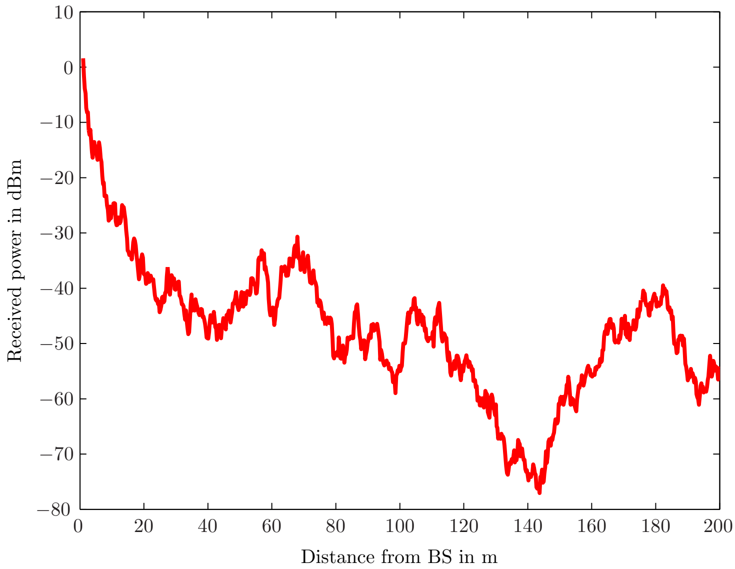


**Figure 2.1:** A typical one dimensional channel realization with fixed transmitter placed at origin. The received signal power experienced by a receiver moving along a straight line from the transmitter. The following parameters are used to generate the channel realization, $L_0 = -10$, $\eta = 2.5$, $d_c = 30$ m, $\sigma_\Psi = 10$.

achieved using a spatial regression framework when perfect location information is available. Furthermore, to understand the validity of the statistical channel model on real measurements we have conducted a measurement campaign, which we will detail in the next section.

## Channel Measurement Campaign

In this section, we describe the outdoor measurement campaign we have conducted in Gothenburg, Sweden during spring of 2016 [36]. The measurements are performed with off-the-shelf smartphones. The application on the smart phone provides a noisy observation of received power

$$y(\mathbf{x}_{\mathrm{TX}}, \mathbf{x}_{\mathrm{RX},i}) = P_{\mathrm{RX}}(\mathbf{x}_{\mathrm{TX}}, \mathbf{x}_{\mathrm{RX},i}) + n, \tag{2.4}$$

where $n \sim \mathcal{N}(0, \sigma_n^2)$ and $\sigma_n^2$ is the measurement variance.

For the channel measurement campaign, we have considered two different scenarios (see Fig. 2.2 for the maps of the routes). The first one is a route stretching from Korsvägen to Wavrinskys Plats. This is a tram route and the reason to chose this track is that it involves passing through a tunnel. The second one is a pedestrian path along the Gibraltargatan street, which is a street that runs parallel to Chalmers Johanneberg Campus. This route was chosen mainly as there are many tall buildings on one side of this road which block the signals from a cellular BS.

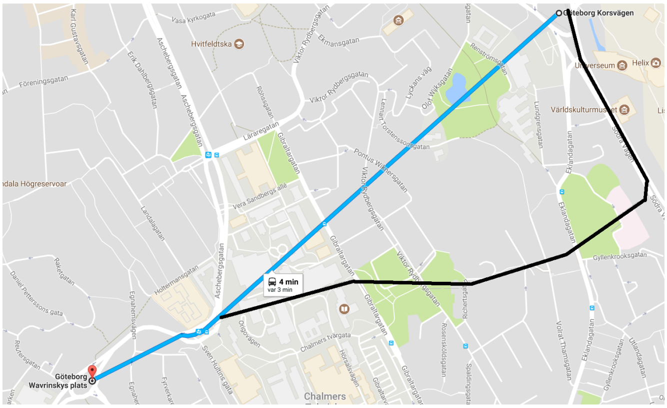


(a)

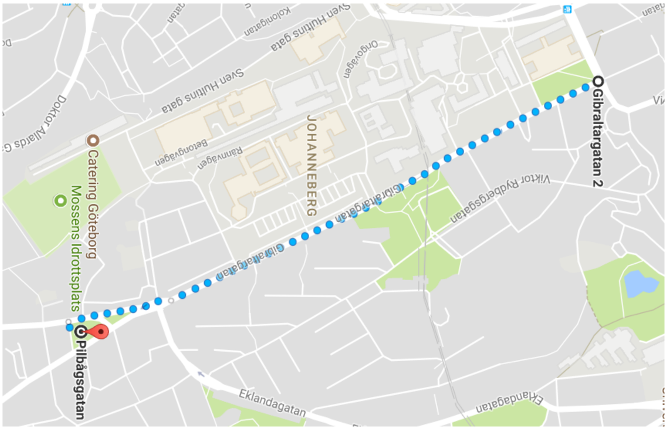


(b)

**Figure 2.2:** Maps of the routes for the measurement campaign. (a): Korsvägen to Wavrinskys Plats, (b): Pilbågsgatan to Läraregatan.

This scenario helps to capture the shadowing behavior of the channel. The length of the street is 1.2 km from bus stop Pilbågsgatan till the end of the street towards Läraregatan.

### Methodology

In this section, we describe how the measurements were collected as part of the campaign. The measurements were gathered using a Google Nexus 5X smartphone and data was logged using GNet Track Pro application by Gyokov solutions. The application allowed logging of the received signal received power (RSRP), GPS location and many other parameters including Cell ID of the serving BS and a heat map to show the variation of received signal strength along a route. This made the application an excellent choice to perform the measurements. For the two scenarios, the measurement iterations were carried out during various times of the day to collect sufficient data to extract statistics. This was done until the characteristics, the mean and variance, for each location could be assumed to be approximated from the measurements. These measurements were then mapped to a one dimensional space with the distance from a fixed point as one of the parameters. The starting and ending points are located at known fixed geographical locations, allowing the same track to be recorded several times.

#### Measurement Results

Fig. 2.3 shows the RSRP values along the two considered routes. We observe large variations of the RSRP, depending on the position. We also see that over the span of multiple days, the RSRP at a given position is relatively stable, with variations due to environmental factors as well as GPS location errors. Peaks in the RSRP are due to a direct line of sight (LOS) connection with BSs, while valleys are due to shadowing by large buildings and other structures which block the signal. To complement these measurements, we have also analyzed the channel statistics after removing the mean from the RSRP measurements. In Fig. 2.4, we show the autocorrelation function and probability density function (pdf) of shadowing. We see that the RSRP values decorrelate around 160 meters for the pedestrian path and 250 meters for the tunnel route. The measurements confirm the strong correlation of shadowing and also concurs with similar suburban measurement results for shadowing in the literature [29]. The mean-removed RSRP measurements are approximated with a Gaussian distribution and we can observe clearly that they follow this distribution. The estimate of the standard deviation of shadowing is 3.6 dB for the pedestrian path and 5.7 dB for the tunnel route.

We experience a problem with the tunnel scenario, as the application could not get GPS signals. Once smartphone enters the tunnel the GPS is lost and goes to an indoor mode, where location is tracked by means of some tracking algorithm. In this thesis, we only considered the pedestrian path as the GPS measurements were of good quality throughout the path.

We can conclude from the measurement findings, that the received power is spatially correlated and hence it can be predicted provided the user path is known.

## 2.3 Statistical Channel Model with Mobile Transmitter

In the case of cellular networks, the BS is static and the receiver is moving, whereas for ad-hoc networks, both transmitter and receiver can be moving [37]. The power relation (2.2) between the transmitter and receiver still holds as the path-loss only depends on the relative distance between the transmitter and receiver. However, (2.3) is only suitable for networks with static transmitter. In the following, we describe a couple of models of the shadowing for ad-hoc networks. The first model is similar to the Gudmundson model but modified to account for the mobility

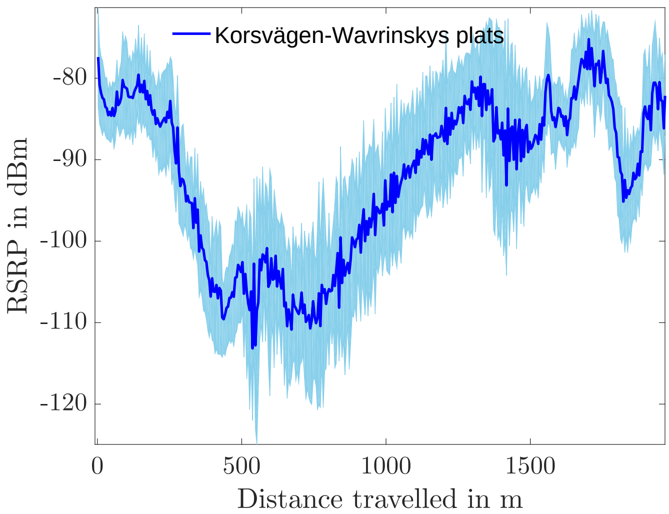


(a)

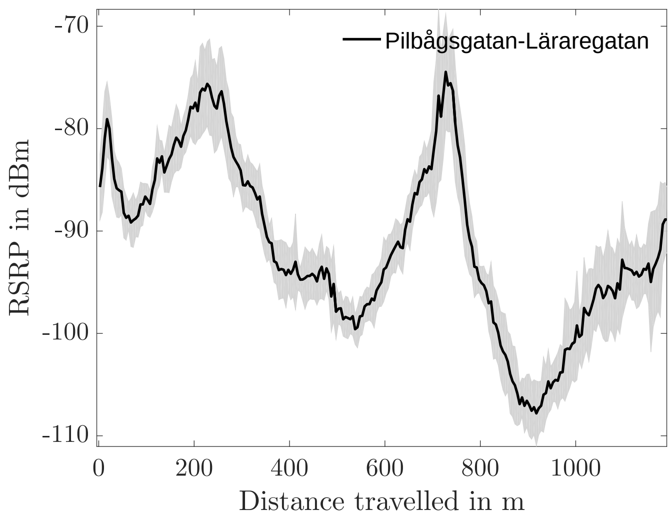


(b)

**Figure 2.3:** We have conducted channel measurement campaign using a smartphone, where the RSRP are measured for two different scenarios. Inset (a): the user is moving in tram (Korsvg̈en-Wavrinskys plats) involving a tunnel. Inset (b): the user is walking along a pedestrian path (Pilbågsgatan-Lr̈aregatan). The solid line is the mean RSRP with measurements averaged over different times of the day and at different days. The shaded region captures the standard deviation of the measurements. We can clearly observe in both the scenarios that the RSRP is correlated due to shadowing.

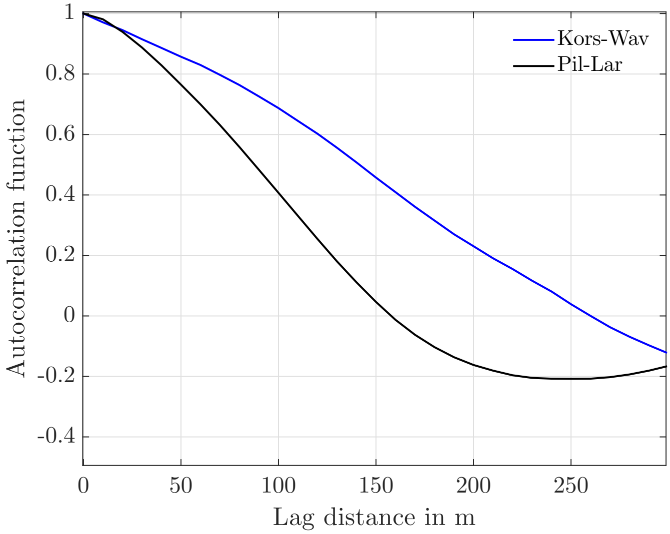


(a)

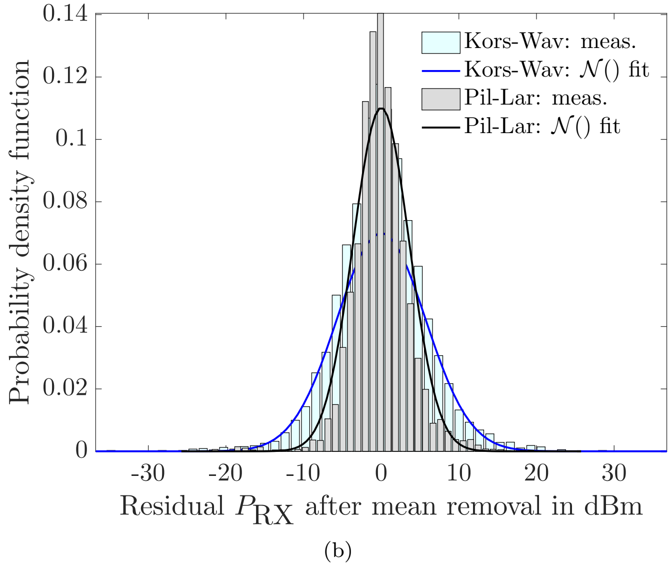


(b)

**Figure 2.4:** Inset (a): autocorrelation function, (b): pdf function, of the RSRP measurements after removing the mean.

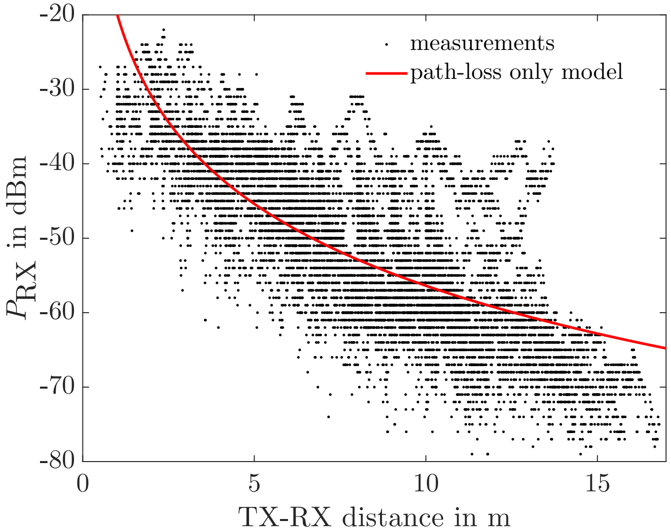


(a)

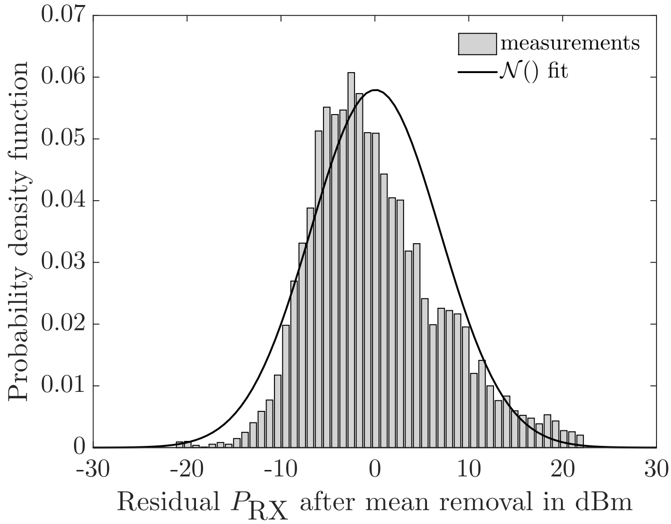


(b)

**Figure 2.5:** The figures are taken with permission from [43]. Inset (a) The received power in shown w.r.t. to the distance between transmitter and receiver. The measurements are shown in black dots and and a simple linear fit with distance is shown in red solid line. Inset (b) shows pdf function of the measurements after removing the mean and a Gaussian fit to the measurements.

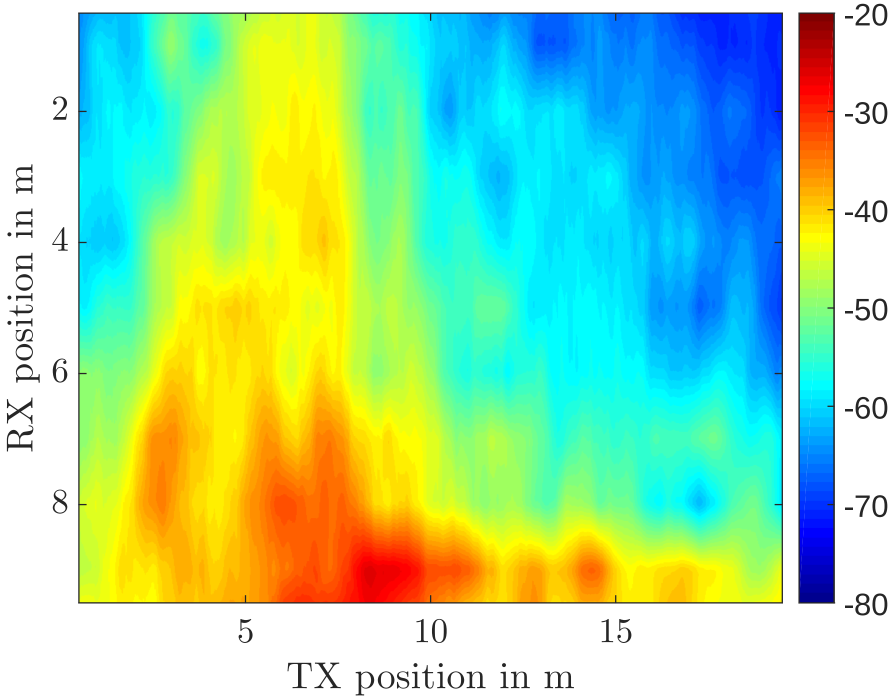


**Figure 2.6:** The figure is taken with permission from [44]. The received power measurements from the indoor campaign for different transmitter and receiver locations. The measurements are averaged out spatially to remove the small-scale fading component from the channel.

of both transmitter and receiver. This model relies on the assumption that the channel between transmitter and receiver is reciprocal. This assumption is valid for the scenarios with static propagation conditions and homogeneous transmitter and receiver devices using the same frequency band [38]. The channel reciprocity holds when $\Psi(\mathbf{x}_{\mathrm{TX}}, \mathbf{x}_{\mathrm{RX}}) = \Psi(\mathbf{x}_{\mathrm{RX}}, \mathbf{x}_{\mathrm{TX}})$.

The traditional Gudmundson model can be extended for ad-hoc networks to include the mobility of transmitter and receiver. Under the assumption that the relative distance between transmitter and receiver is much larger when compared to the displacements of the transmitter and receiver, we can write the spatial covariance of the shadowing as [39, 40]

$$\begin{aligned}
&C(\mathbf{x}_{\mathrm{TX},i}, \mathbf{x}_{\mathrm{RX},i}, \mathbf{x}_{\mathrm{TX},j}, \mathbf{x}_{\mathrm{RX},j}) \\
&= \mathbb{E}[\Psi(\mathbf{x}_{\mathrm{TX},i}, \mathbf{x}_{\mathrm{RX},i}), \Psi(\mathbf{x}_{\mathrm{TX},j}, \mathbf{x}_{\mathrm{RX},j}) | \mathbf{x}_{\mathrm{TX},i}, \mathbf{x}_{\mathrm{RX},i}, \mathbf{x}_{\mathrm{TX},j}, \mathbf{x}_{\mathrm{RX},j}] \\
&= \sigma_\Psi^2 \exp\left(-\frac{||\mathbf{x}_{\mathrm{RX},i} - \mathbf{x}_{\mathrm{RX},j}||}{d_c}\right) \exp\left(-\frac{||\mathbf{x}_{\mathrm{TX},i} - \mathbf{x}_{\mathrm{TX},j}||}{d_c}\right).
\end{aligned} \tag{2.5}$$

This model has been applied for robot communication [37], where transmitter and receiver do not share a common end node.

Another spatial channel model for ad-hoc networks is proposed in [41], in which it is assumed that shadowing experienced on the links in a network are due to an underlying spatial loss field $\Phi(\mathbf{x})$. Under this model, the covariance function between arbitrary locations $\mathbf{x}_i$ and $\mathbf{x}_j$ is defined as

$$\mathbb{E}\{\Phi(\mathbf{x}_i), \Phi(\mathbf{x}_j)\} = \frac{\sigma_\Psi^2}{d_c} \exp(-\frac{||\mathbf{x}_i - \mathbf{x}_j||_2}{d_c}).$$

Then shadowing for a link between a pair of nodes is obtained as a weighted line integral of the spatial loss field $\Phi(\mathbf{x})$ as

$$\Psi(\mathbf{x}_i, \mathbf{x}_j) = \frac{1}{||\mathbf{x}_j - \mathbf{x}_i||^{1/2}} \int_{\mathbf{x}_i}^{\mathbf{x}_j} \Phi(\mathbf{x})\, \mathrm{d}\mathbf{x}.$$

The construction of spatial loss field $\Phi(\mathbf{x})$ based on the measurements of arbitrary link pairs between nodes using radio tomographic imaging is demonstrated in [42], and [41] details the learning of the parameters of the loss field $\Phi(\mathbf{x})$.

## Channel Measurement Campaign

A measurement campaign of channel measurements for the ad-hoc networks has been carried out in [43]. The indoor measurements were performed in a hallway at the Department of Signals and Systems of Chalmers University of Technology.

### Methodology

For the channel measurements, the receiver is placed at several locations on a straight line on the hall way. The transmitter is also placed at several locations on a straight line perpendicular to the hall way. Then, for each receiver and transmitter position, the received signal power is measured using commodity hardware radio of type Netgear N150 Wireless adapter. The floor plan and the measurement parameters can be found in [43].

### Measurement Results

In Fig. 2.5 (a), we depict the received power w.r.t. to the distance between transmitter and receiver locations. A simple linear curve fitting is done against measurements. It was found that the deterministic path-loss component $L_0 = -19.88$

dB and the path-loss exponent $\eta = 3.65$. The measurements after removing the path-loss component are approximated with a Gaussian distribution. From Fig. 2.5 (b) we can observe clearly that shadowing measurements follow Gaussian distribution but with some positive skewness. The standard deviation $\sigma_\Psi$ of shadowing was estimated to be 6.88 dB. In Fig. 2.6, the channel measurements for different transmitter and receiver locations are shown.

## 2.4 Summary

In this chapter, we reviewed the basics of the wireless channel and its predictability. We discussed the channel characteristics of the wireless propagation channel and then showed how location information is related to predicting the long-term channel components such as path-loss and shadowing. We then presented statistical channel models based on location information for cellular and ad-hoc networks. The statistical channel models were complemented with channel measurements for validation purposes, carried out for both cellular and ad-hoc networks.

# Chapter 3

# Wireless Channel Prediction using Gaussian Processes

In this chapter, we describe Gaussian processes (GP), a tool for spatial regression from the machine learning field. Spatial regression tools generally comprise a training/learning phase in which the underlying parameters are estimated based on the available training database and a testing/prediction phase in which predictions are made at the test inputs using learned parameters and a training database. GP is one of the powerful and commonly used spatial regression frameworks, since it is generally considered to be flexible and provides confidence information on the predictions [45]. First, we give a brief introduction on how to make predictions using GP, after that we connect it to location-aware channel prediction for large scale fading component of the wireless channel.

## 3.1 Gaussian Processes Basics

**Definition 1** *A GP is a collection of random variables, any finite number of which have a joint Gaussian distribution [45].*

Let $f(\mathbf{x})$ be a stochastic process, for $\mathbf{x} \in \mathbb{R}^D$ with mean function $\mu(\mathbf{x}) = \mathbb{E}[f(\mathbf{x})]$ and covariance function $C(\mathbf{x}_i, \mathbf{x}_j) = \mathbb{E}[(f(\mathbf{x}_i) - \mu(\mathbf{x}_i))\,(f(\mathbf{x}_j) - \mu(\mathbf{x}_j))]$. We write a GP $f(\mathbf{x})$ as

$$f(\mathbf{x}) \sim \mathcal{GP}(\mu(\mathbf{x}), C(\mathbf{x}_i, \mathbf{x}_j)). \tag{3.1}$$

Let $y_i$ be the noisy observation of $f(\mathbf{x}_i)$, which is written as $y_i = f(\mathbf{x}_i) + n_i$, where $n_i$ is a zero mean additive white Gaussian noise with variance $\sigma_n^2$. We introduce $\mathbf{X} = [\mathbf{x}_1^{\mathrm{T}}, \mathbf{x}_2^{\mathrm{T}}, \ldots, \mathbf{x}_N^{\mathrm{T}}]^{\mathrm{T}}$ as the collection of $N$ measurement inputs and $\mathbf{y} = [y_1, y_2, \ldots, y_N]^{\mathrm{T}}$ be the vector of noisy observations at those inputs. The resulting training database is thus $\{\mathbf{X}, \mathbf{y}\}$. Due to the GP model, the joint distribution of the $N$ training observations exhibits a Gaussian distribution [45]

$$p(\mathbf{y}|\mathbf{X}, \Theta) = \mathcal{N}(\boldsymbol{\mu}(\mathbf{X}), \mathbf{K}), \tag{3.2}$$

where $\boldsymbol{\mu}(\mathbf{X}) = [\mu(\mathbf{x}_1), \mu(\mathbf{x}_2), \ldots, \mu(\mathbf{x}_N)]^T$ is the mean vector and $\mathbf{K}$ is the covariance matrix given as

$$\mathbf{K} = \begin{bmatrix} C(\mathbf{x}_1,\mathbf{x}_1)+\sigma_n^2 & C(\mathbf{x}_1,\mathbf{x}_2) & \cdots & C(\mathbf{x}_1,\mathbf{x}_N) \\ C(\mathbf{x}_2,\mathbf{x}_1) & C(\mathbf{x}_2,\mathbf{x}_2)+\sigma_n^2 & \cdots & C(\mathbf{x}_2,\mathbf{x}_N) \\ \vdots & \vdots & \ddots & \vdots \\ C(\mathbf{x}_N,\mathbf{x}_1) & C(\mathbf{x}_N,\mathbf{x}_2) & \cdots & C(\mathbf{x}_N,\mathbf{x}_N)+\sigma_n^2 \end{bmatrix}, \tag{3.3}$$

with entries $[\mathbf{K}]_{ij} = C(\mathbf{x}_i, \mathbf{x}_j) + \sigma_n^2\, \delta_{ij}$, where $\delta_{ij} = 1$ for $i = j$ and zero otherwise. There are many choices for a covariance function of which squared exponential is the most widely used in machine learning, and is written as [45, Chapter 4]

$$C(\mathbf{x}_i, \mathbf{x}_j) = \sigma_f^2 \,\exp\left(-\frac{\|\mathbf{x}_i - \mathbf{x}_j\|^2}{2\, l^2}\right), \tag{3.4}$$

where $l$ is the correlation length and $\sigma_f^2$ is the variance of the process.

### 3.1.1 Learning

The objective during learning is to infer the model parameters $\Theta = [\sigma_n, \sigma_f, l]$ from observations at known inputs. The model parameters can be learned through maximum likelihood estimation, given a training database, by minimizing the negative log-likelihood function with respect to $\Theta$:

$$\begin{aligned} \hat{\Theta} &= \arg\min_{\Theta}\{-\log(p(\mathbf{y}|\mathbf{X}, \Theta)\} \qquad (3.5) \\ &= \arg\min_{\Theta}\left\{\frac{N}{2}\log(2\pi) + \frac{1}{2}\log|\mathbf{K}| + \frac{1}{2}(\mathbf{y} - \boldsymbol{\mu}(\mathbf{X}))^T\, \mathbf{K}^{-1}\, (\mathbf{y} - \boldsymbol{\mu}(\mathbf{X}))\right\} \end{aligned}$$

The likelihood function is usually not convex and can contain multiple local maxima/minima, even though they might explain the measurements, the predictions will be poor. Once $\Theta$ is estimated from $\{\mathbf{X}, \mathbf{y}\}$, the training process is complete.

### 3.1.2 Prediction

Once $\hat{\Theta}$ is obtained, we can determine the predictive distribution of $f(\mathbf{x}_*)$ at new and arbitrary test input $\mathbf{x}_*$, given the training database $\{\mathbf{X}, \mathbf{y}\}$. We first form the joint distribution as [45, Chapter 2]

$$\begin{bmatrix} \mathbf{y} \\ f(\mathbf{x}_*) \end{bmatrix} \sim \mathcal{N}\left(\begin{bmatrix} \boldsymbol{\mu}(\mathbf{X}) \\ \mu(\mathbf{x}_*) \end{bmatrix}, \begin{bmatrix} \mathbf{K} & \mathbf{k}_* \\ \mathbf{k}_*^{\mathrm{T}} & k_{**} \end{bmatrix}\right), \tag{3.6}$$

where $\mathbf{k}_*$ is the $N \times 1$ vector of cross-covariance $C(\mathbf{x}_*, \mathbf{x}_i)$ between $\mathbf{x}_*$ and the training inputs $\mathbf{x}_i$, and $k_{**}$ is the prior variance, given by $k_{**} = C(\mathbf{x}_*, \mathbf{x}_*) = \sigma_f^2$.

Conditioning the joint Gaussian distribution (3.6) on the observations $\mathbf{y}$, we obtain the Gaussian posterior predictive distribution $p(f(\mathbf{x}_*)|\mathbf{X}, \mathbf{y}, \hat{\Theta}, \mathbf{x}_*) \sim \mathcal{N}(\bar{f}(\mathbf{x}_*),$

$\tilde{f}(\mathbf{x}_*)$) for a test input $\mathbf{x}_*$. The mean and variance of this distribution turn out to be [45, Chapter 2]

$$\bar{f}(\mathbf{x}_*) = \mu(\mathbf{x}_*) + \mathbf{k}_*^{\mathrm{T}} \mathbf{K}^{-1} (\mathbf{y} - \boldsymbol{\mu}(\mathbf{X}), \tag{3.7}$$

$$\tilde{f}(\mathbf{x}_*) = k_{**} - \mathbf{k}_*^{\mathrm{T}} \mathbf{K}^{-1} \mathbf{k}_*. \tag{3.8}$$

Fig. 3.1 demonstrates an example of regression using a GP. Observe the decrease in predictive variance for test inputs which are closer to the training inputs.

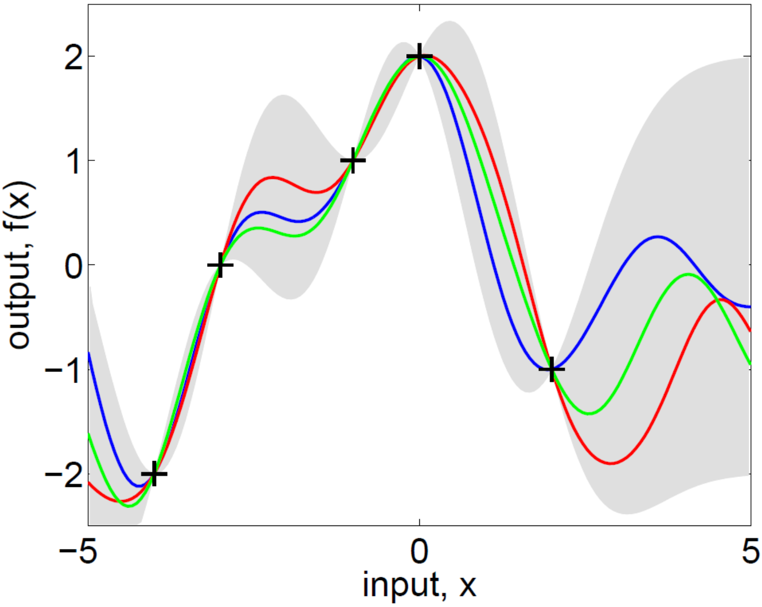


**Figure 3.1:** Example of a GP regression [46]: marked in (+) are 5 training inputs, solid line depicts the predictive mean and shaded area represents the point wise predictive mean plus and minus two times the predictive standard deviation for each input value.

## 3.2 Channel Prediction for Static Transmitter using GP

As large-scale fading component of the wireless channel is spatially correlated over tens of meters for outdoor scenarios [29], spatial regression tools such as GP can be utilized for its prediction. In the following, we show the steps for a location-aware channel prediction framework for cellular networks using GP.

1. Model $P_{\mathrm{RX}}(\mathbf{x})$ as $P_{\mathrm{RX}}(\mathbf{x}) \sim \mathcal{GP}(\mu(\mathbf{x}), C(\mathbf{x}_i, \mathbf{x}_j))$ GP with input $\mathbf{x}$:

(a) $\mu(\mathbf{x}) = L_0 - 10\,\eta\,\log_{10}(||\mathbf{x}_{\mathrm{TX}} - \mathbf{x}_{\mathrm{RX}}||)$,

(b) $$\begin{aligned} C(\mathbf{x}_i, \mathbf{x}_j) &= \mathbb{E}[\Psi(\mathbf{x}_{\mathrm{TX}}, \mathbf{x}_{\mathrm{RX},i}), \Psi(\mathbf{x}_{\mathrm{TX}}, \mathbf{x}_{\mathrm{RX},j}) | \mathbf{x}_{\mathrm{RX},i}, \mathbf{x}_{\mathrm{RX},j}] \\ &= \sigma_\Psi^2 \exp\left(-\frac{||\mathbf{x}_{\mathrm{RX},i} - \mathbf{x}_{\mathrm{RX},j}||}{d_c}\right). \end{aligned}$$

2. Data collection:

   (a) $y(\mathbf{x}_{\mathrm{TX}}, \mathbf{x}_{\mathrm{RX},i}) = P_{\mathrm{RX}}(\mathbf{x}_{\mathrm{TX}}, \mathbf{x}_{\mathrm{RX},i}) + n_i,\ n_i \sim \mathcal{N}(0, \sigma_n^2)$,

   (b) $\mathbf{y} = [y(\mathbf{x}_{\mathrm{TX}}, \mathbf{x}_{\mathrm{RX},1}), y(\mathbf{x}_{\mathrm{TX}}, \mathbf{x}_{\mathrm{RX},2}), \ldots, y(\mathbf{x}_{\mathrm{TX}}, \mathbf{x}_{\mathrm{RX},N})]^{\mathrm{T}}$ and $\mathbf{X} = [\mathbf{x}_{\mathrm{RX},1}^{\mathrm{T}}, \mathbf{x}_{\mathrm{RX},2}^{\mathrm{T}}, \ldots, \mathbf{x}_{\mathrm{RX},N}^{\mathrm{T}}]^{\mathrm{T}}$.

3. Training:

   (a) Learn the channel parameters $\Theta = [\sigma_n, d_c, L_0, \eta, \sigma_\Psi]$ for $\{\mathbf{X}, \mathbf{y}\}$.

4. Prediction at new location $\mathbf{x}_*$:

   (a) $\bar{P}_{\mathrm{RX}}(\mathbf{x}_*) = \mu(\mathbf{x}_*) + \mathbf{k}_*^{\mathrm{T}}\,\mathbf{K}^{-1}\,(\mathbf{y} - \boldsymbol{\mu}(\mathbf{X}))$,

   (b) $\tilde{P}_{\mathrm{RX}}(\mathbf{x}_*) = k_{**} - \mathbf{k}_*^{\mathrm{T}}\,\mathbf{K}^{-1}\,\mathbf{k}_*$.

Fig. 3.2 demonstrates an example of radio channel prediction using a GP [9]. A BS is placed in the center and a 2D radio propagation field is simulated with sampling points on a square grid of 200 m $\times$ 200 m and a resolution of 4 m. Based on measurements at marked locations, the mean and standard deviation of the prediction are obtained for any location. Observe the increased uncertainty in the right panel of Fig. 3.2 in regions where few measurements are available. In the next section, we show the channel prediction using GP for ad-hoc networks.

## 3.3 Channel Prediction for Mobile Transmitter using GP

Let us denote the locations of transmitter and receiver pair as $\mathbf{x} = [\mathbf{x}_{\mathrm{TX}}^{\mathrm{T}}, \mathbf{x}_{\mathrm{RX}}^{\mathrm{T}}]^{\mathrm{T}}$. The following steps show the use of GP as a tool for location-aware channel prediction for ad-hoc networks.

1. Model $P_{\mathrm{RX}}(\mathbf{x})$ as $P_{\mathrm{RX}}(\mathbf{x}) \sim \mathcal{GP}(\mu(\mathbf{x}), C(\mathbf{x}_i, \mathbf{x}_j))$ GP with input $\mathbf{x}$:

   (a) $\mu(\mathbf{x}) = L_0 - 10\,\eta\,\log_{10}(||\mathbf{x}_{\mathrm{TX}} - \mathbf{x}_{\mathrm{RX}}||)$,

   (b) $$\begin{aligned} C(\mathbf{x}_i, \mathbf{x}_j) &= \mathbb{E}[\Psi(\mathbf{x}_{\mathrm{TX},i}, \mathbf{x}_{\mathrm{RX},i}), \Psi(\mathbf{x}_{\mathrm{TX},j}, \mathbf{x}_{\mathrm{RX},j}) | \mathbf{x}_{\mathrm{TX},i}, \mathbf{x}_{\mathrm{RX},i}, \mathbf{x}_{\mathrm{TX},j}, \mathbf{x}_{\mathrm{RX},j}] \\ &= \sigma_\Psi^2 \exp\left(-\frac{||\mathbf{x}_{\mathrm{RX},i} - \mathbf{x}_{\mathrm{RX},j}||}{d_c}\right) \exp\left(-\frac{||\mathbf{x}_{\mathrm{TX},i} - \mathbf{x}_{\mathrm{TX},j}||}{d_c}\right). \end{aligned}$$

2. Data collection:

   (a) $y(\mathbf{x}_i) = P_{\mathrm{RX}}(\mathbf{x}_{\mathrm{TX},i}, \mathbf{x}_{\mathrm{RX},i}) + n_i,\ n_i \sim \mathcal{N}(0, \sigma_n^2)$,

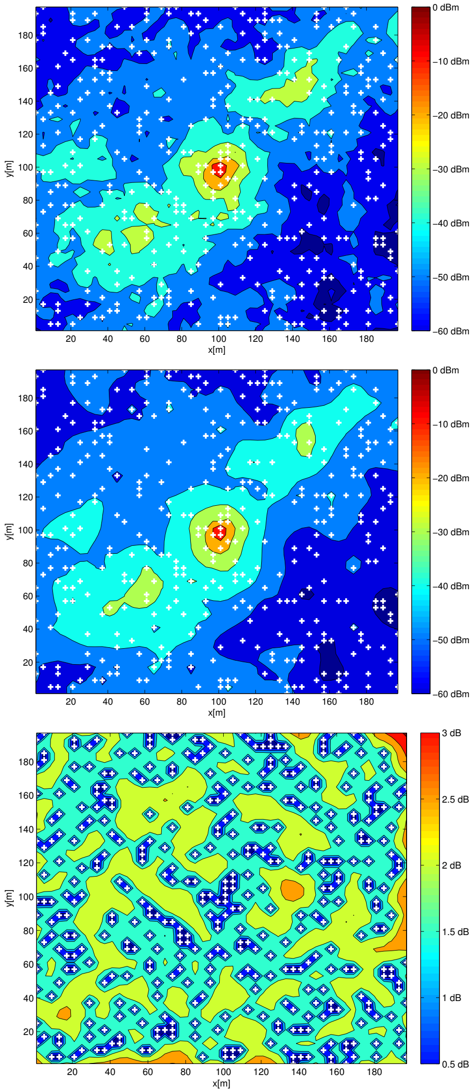


**Figure 3.2:** Radio channel prediction in dB scale, with hyperparameters $\Theta = [\sigma_n = 0.1, d_c = 70 \text{ m}, L_0 = 10 \text{ dB}, \eta = 3, \sigma_\Psi = 9 \text{ dB}]$, $N = 400$ measurements (+ signs). The channel prediction is performed at a resolution of 4 m. Top panel: the true channel field. Middle panel: the mean of the predicted channel field $\bar{P}_{\text{RX}}(\mathbf{x}_*)$. Bottom panel: the standard deviation (obtained from the square root of $(\tilde{P}_{\text{RX}}(\mathbf{x}_*))$ of the predicted channel field.

(b) $\mathbf{y} = [y(\mathbf{x}_1), y(\mathbf{x}_2), \ldots, y(\mathbf{x}_N)]^{\mathrm{T}}$ and $\mathbf{X} = [\mathbf{x}_1^{\mathrm{T}}, \mathbf{x}_2^{\mathrm{T}}, \ldots, \mathbf{x}_N^{\mathrm{T}}]^{\mathrm{T}}$ .

3. Training:

   (a) Learn the channel parameters $\Theta = [\sigma_n, d_c, L_0, \eta, \sigma_\Psi]$ for $\{\mathbf{X}, \mathbf{y}\}$.

4. Prediction at new location $\mathbf{x}_*$:

   (a) $\bar{P}_{\mathrm{RX}}(\mathbf{x}_*) = \mu(\mathbf{x}_*) + \mathbf{k}_*^{\mathrm{T}}\, \mathbf{K}^{-1}\, (\mathbf{y} - \boldsymbol{\mu}(\mathbf{X}))$,
   (b) $\tilde{P}_{\mathrm{RX}}(\mathbf{x}_*) = k_{**} - \mathbf{k}_*^{\mathrm{T}}\, \mathbf{K}^{-1}\, \mathbf{k}_*$.

**Remark on channel reciprocity**

As mentioned in Section 2.3, for the ad-hoc channel model to be valid, it should hold channel reciprocity. This condition is not inherently considered by the GP framework, as $\mathbf{x} = [\mathbf{x}_{\mathrm{TX}}^{\mathrm{T}}, \mathbf{x}_{\mathrm{RX}}^{\mathrm{T}}]^{\mathrm{T}}$ and $\mathbf{x} = [\mathbf{x}_{\mathrm{RX}}^{\mathrm{T}}, \mathbf{x}_{\mathrm{TX}}^{\mathrm{T}}]^{\mathrm{T}}$ are two different inputs. To incorporate the channel reciprocity in to the GP framework, we add additional channel measurement (by interchanging the role of transmitter and receiver) to the database for every measurement associated transmitter and receiver pair.

## 3.4 Channel Prediction with Location Uncertainty

It is clear that while GP are flexible, but they have some limitations. The first limitation of GP is its computational complexity. The prediction step of GP requires inversion of the $N \times N$ covariance matrix $\mathbf{K}$, whose complexity scale as $\mathcal{O}(N^3)$. To alleviate the computational complexity, various sparse GP techniques have been proposed in [47–49]. While in [50] the connection between GP and Kalman filtering is studied.

Another limitation of GP is that they cannot handle well the uncertainty in the inputs. The works in [51, 52] study the impact of input uncertainty, which show that GP is adversely affected, both in training and testing. Some approaches tackle this through linearizing the output around the mean of the input [53, 54], but they are limited to mildly non-linear scenarios. The input uncertainty to GP in our case translates to location uncertainty. In Paper B, we demonstrate that not considering location uncertainty in GP leads to poor learning of the channel parameters and poor prediction of channel gain values at other locations. We then discuss how to handle this location uncertainty in the GP channel prediction framework both for cellular networks and ad-hoc networks. In Paper B and C, we develop channel prediction frameworks based on GP that incorporate location uncertainty for cellular and ad-doc networks respectively.

## 3.5 Summary

In this chapter, we described the basics of the GP tool and showed how it can be utilized for spatial channel prediction for cellular and ad-hoc networks with perfect location information. We also discussed the limitations of the GP especially the computational complexity and its incapability to handle the uncertainty in location information.

In the next chapter, we focus on the use of location information for reactive resource allocation in 5G networks.

# Chapter 4

# Location-aware Reactive Resource allocation

In this chapter, we describe resource allocation (RA) in wireless communications for 5G. We then discuss how location information has been exploited in the literature for various RA applications. In particular, we provide a case study on the use of location information in medium access control (MAC) layer link scheduling and pilot decontamination in massive MIMO systems.

## 4.1 5G and Resource Allocation

As mentioned in Section 1.1, 5G networks will be characterized by a wide variety of use cases and high requirements on data rate, number of connected devices, latency, and battery life. To meet these highly ambitious requirements, 5G networks need a mixture of new concepts and technologies. The following are some potential candidate solutions to meet these requirements in 5G [55].

- Device-to-device (D2D) communications offer devices in proximity to communicate with each other directly rather than hopping through a BS.
- Massive MIMO, where a large number of antenna elements at the BS are incorporated to achieve higher data rates, improved coverage, and energy efficiency.
- Millimeter wave (mmWave) communications, where new multi-GHz frequency bands in the mmWave spectrum are considered to further boost the data rates on the order of Gbps.
- Network densification with coordination and cooperation techniques between various kinds of network elements in an ultra-dense heterogeneous network (HetNet).

These candidate technologies should exploit the available resources in the network in the best possible way to achieve target requirements. RA is one of the main ingredients in wireless communications because it optimizes available resources at the network to improve overall quality of service (QoS) of the user. Resources include time, frequency, power, rate (modulation and coding), pilot sequences, and beamforming (BF) codebooks. Typical RA applications would include power control, rate control, and multiple access [29].

RA can be classified mainly into two categories, reactive RA (RRA) and proactive RA (PRA). A RRA system is described in [56] as follows *"The Reactive Resource Allocation design pattern maintains the performance of a computing system within required bounds by observing when the system's performance is close to crossing, or has crossed, a threshold; determining how best to reallocate the available resources to prevent or correct any requirement violation; and then directing that resource reallocation"*. In RRA, the RA starts when the user requests for a service. Typically, RRA schemes are employed in traditional wireless communication systems. Traditional RA methods rely on instantaneous CSI (path-loss, shadowing, and small-scale fading), demand, interference, etc (see Fig. 4.1). In this chapter, we review RRA based on location information and, in the next chapter, PRA schemes based on location information are explored.

The RA schemes that are challenging and need new approaches to tackle them for the aforementioned 5G candidate technologies are:

- Link scheduling and routing are important RA problems for D2D communications due to large numbers of connected devices in 5G. In link scheduling, multiple links are scheduled in the same time slot as long as they do not cause much mutual interference to each other. For perfect link scheduling, we need the complete CSI between the links to be scheduled and choose the best possible links to schedule to avoid outages. Routing is a procedure where data packets are transferred from source to destination via multiple intermediate nodes through a wireless communication channel. Again to find the best possible route, we need to estimate the CSI between all the nodes in the network. The main drawbacks with traditional CSI-based methods are signalling overhead and feedback delay [9].

- Massive MIMO offers numerous advantages and its main limitation is interference during uplink channel estimation. Pilot sequences are a scarce resource and they are reused in the surrounding cells for channel estimation, thereby leading to interference. Therefore, there is a need to carefully assign the pilots to users in order to limit the interference during channel estimation. Pilot allocation due to random assignment will lead to pilot contamination [57].

- Initial access (IA) is the procedure to synchronize transmitter and receiver, and to establish a connection, before starting to communicate. IA is a big concern in mmWave due to very narrow transmitter beams. In traditional methods, the transmitter sweeps through the entire angular space with beams to discover the receiver. Therefore, they take larger discovery time for IA [58].

- HetNets offer advantages such as increased system capacity and coverage. However, managing interference among cross-tier networks is a challenge. Traditionally, cooperation and coordination among different networks elements is applied to mitigate the interference. The drawbacks of these methods are large signalling overhead and the need for fast and low latency backhaul links [59].

Utilizing location information is a possible approach to address the aforementioned challenges of various RA schemes. In location-aware RA, location information of various network entities is utilized for RA. The location information can be used either directly or can be used to predict other CQM (CQI, interference, angle-of-arrival (AoA)). The predicted CQM are utilized in the RA through a database (see Chapter 3). Location-aided RA methods are based on path-loss and shadowing since small-scale fading is relatively difficult to capture through location. Location-aware RA techniques can reduce overheads and delays due to their ability to predict channel quality beyond traditional time scales. Location information can be harnessed to reduce interference and signalling overhead, to avoid penalties due to feedback delays, or to synchronize coordinated communication schemes [9]. In the rest of the chapter, we review location-aware RA schemes for: MAC layer scheduling and routing in D2D communications, pilot allocation in massive MIMO networks, IA in mmWave communications, and interference management in HetNets.

## 4.2 Location-aware D2D Communications

### 4.2.1 Background

D2D communications is one of the important promising technologies for 5G, which exploits the proximity of the devices to communicate with each other [60,61]. The device here refers to a user mobile, laptop, tablet etc. D2D communications offer three advantages [61]: (i) due to close proximity, devices can communicate with low power, low latency, and can achieve higher data rates, this is called proximity gain; (ii) since same resources can be used both by the cellular users and D2D users, D2D communications provide reuse gain; (iii) such communications also offer hop gain, since the devices can communicate directly rather than via a BS.

D2D communications are facilitated in the licensed or unlicensed spectrum (see Fig. 4.2). D2D communications under unlicensed spectrum is a well studied research area. Ad-hoc and personal area networks fall into this category. In this case, there is no need of support from the network. D2D communication for the cellular networks under licensed spectrum is recently proposed, as this offer better spectrum utilization and provides energy efficiency. For D2D communication in the the licensed band, network assistance is necessary in providing node synchronization and assisting security procedures.

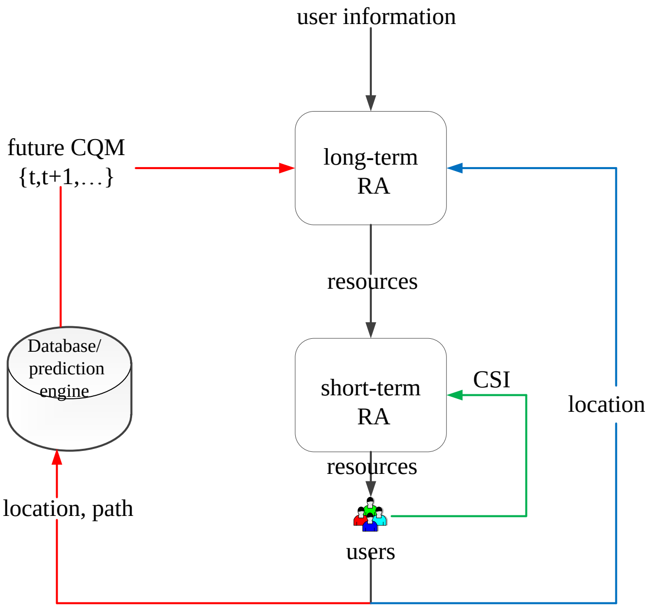


**Figure 4.1:** Comparison of reactive and proactive resource allocation. The green line path is the traditional RRA based on instantaneous CSI. The blue line path is the location-aware RRA and red line path is the location-aware PRA.

RA in D2D is divided in two modes, namely network-scheduled and autonomous D2D [61]. In the network-scheduled D2D, the BS acts as a centralized controller and optimizes and configures the resources to be used by the devices. On the other hand, in autonomous D2D mode, the devices themselves select resources from the pool without interacting with the BS. We review the main location-aware RA schemes, i.e., scheduling and routing for D2D communications. Since scheduling and routing for D2D under licensed spectrum is a fairly recent topic, we instead concentrate on matured D2D RA under unlicensed spectrum. The traditional D2D scheduling and routing rely on the assumption of complete knowledge of the channels between the device pairs. This assumption in practice is realized via additional signalling overhead and latency. We now show how location information can be leveraged to find low-latency data paths for routing as well as how it can be harnessed to reduce signalling overhead in link scheduling for network-controlled D2D communication under unlicensed spectrum.

### 4.2.2 Location-aware Scheduling for D2D

With more and more devices communicating with each other, scalability, efficiency, and latency are important challenges while designing efficient protocols for MAC. In this section, we provide an overview of some of the existing works on the usage

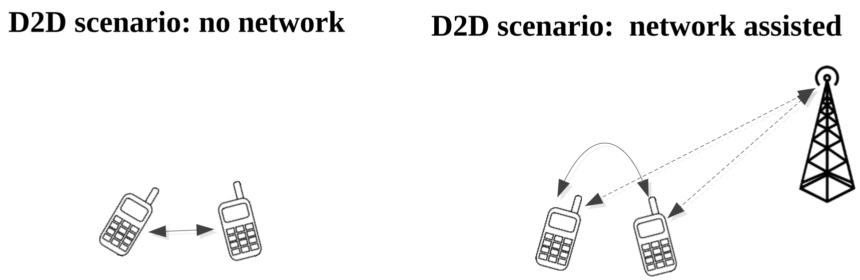


**Figure 4.2:** D2D communication comparison in unlicensed spectrum (inspired from [61]).

of location information at the MAC layer to address the main design challenges. In particular, multicasting, scheduling, and selection protocols are considered. We can make a distinction between approaches that tie locations to channel and approaches where locations are exploited in a different way.

In the first group, we find works such as [6, 62–64]. In [6], a location-aided round-robin scheduling algorithm for fractional frequency reuse is proposed, where allowing temporary sharing of resources between cell-center and cell-edge users is shown to achieve higher total throughput with less and less frequent feedback than the conventional method. In [62], location-based multicasting is considered, assuming a disk model, and is shown to both reduce the number of contention phases and increase the reliability of packet delivery, especially in dense networks. Time division with spatial reuse is considered in [64], which investigates location-aware joint scheduling and power control for IEEE 802.15.3, leading to lower latencies and higher throughput compared to a traditional round-robin type scheduling mechanism. Location information is also beneficial in reducing the overhead associated with node selection mechanisms (e.g., users, relays), by allowing BSs to make decisions based solely on the users' locations [6]. Finally, location information is a crucial ingredient in predicting interference levels in small/macro cell coexistence, in multi-cell scenarios, and in all cognitive radio primary/secondary systems. For example, [6, 65] demonstrate that the use of location information significantly improves inter-cell interference coordination techniques. These works indicate that significant gains in terms of throughput and latency can be reaped from location-aware MAC in wireless networks, provided appropriate channel models are used.

In the second group, we find approaches that utilize location information in a different way [63, 66, 67]. These works relate to vehicular networks. In [63], a family of highly efficient location-based MAC protocols is proposed, whereby vehicles broadcast information to other vehicles only when they pass through specified, predetermined transmission areas. When the traffic flow rate increases, the proposed location-based protocols have a smaller message delivery time, compared to conventional random access schemes. A similar idea is proposed in [66], where a decentralized location-based channel access protocol for inter-vehicle communication is studied. Channel allocation is done based on vehicles' instantaneous geographic location, and unique channels are associated to geographic cells. Communication delay is bounded and fairness among the vehicles is maintained as each vehicle gets a channel regularly to transmit. Finally, [67] introduces the concept of geocasting, whereby multicast regions are formed based on geographical location of the nodes and packets are sent to all the nodes in the group. Specialized location-based multicasting schemes are proposed to decrease the delivery overhead of packets when compared to the multicast flooding mechanisms.

In what follows, we show how location information is used in the robust link scheduling problem (RLSP) based on spatial time division multiple access (STDMA) [68]. STDMA is a collision-free scheme in which links are allocated time slots, and concurrent transmissions are allowed as long as they do not cause significant mutual interference [69].

### Case Study: Robust Link Scheduling [70]

We consider a wireless network of $N$ nodes, represented by a communication graph $G = (V, E)$ consisting of a set $V$ of vertices (nodes) and a given set $E \subseteq V \times V$ representing the links between nodes, which are to be scheduled. The objective is to find the minimum number of time slots required to schedule all the links in the network using STDMA. We introduce $x_{ijt} \in \{0, 1\}$, with $x_{ijt} = 1$ if time slot $t$ is assigned to link $(i, j) \in E$, and $y_t \in \{0, 1\}$, where $y_t = 1$ indicates that time slot $t$ is used. Let $\mathcal{T}$ be a feasible set of $T$ time slots i.e., $\mathcal{T} = \{1, 2, 3, \dots, T\}$. Following [71], the RLSP can be written as binary integer programming (BIP) problem as

$$\begin{aligned}
\text{minimize} \quad & \mathbf{y}^{\mathrm{T}}\mathbf{1} && \text{(4.1a)}\\
\text{subject to} \quad & \sum_{(i,j)\in E} x_{ijt} \le y_t\,|E| && \text{(4.1b)}\\
& \sum_{t\in\mathcal{T}} x_{ijt} = 1 && \text{(4.1c)}\\
& \mathrm{SINR}_{ij}(\tilde{\mathbf{g}}, \mathbf{x}) \ge \gamma && \text{(4.1d)}\\
& \mathbf{g}^{-} \preceq \tilde{\mathbf{g}} \preceq \mathbf{g}^{+} && \text{(4.1e)}\\
& \sum_{j:(i,j)\in E} x_{ijt} + \sum_{k:(k,i)\in E} x_{kit} \le 1 && \text{(4.1f)}\\
& x_{ijt} \in \{0,1\},\ y_t \in \{0,1\}, && \text{(4.1g)}
\end{aligned}$$

where $\mathbf{g}^{-}$ and $\mathbf{g}^{+}$ are vectors of pessimistic and optimistic channel gains respectively, which will be discussed shortly, and

$$\mathrm{SINR}_{ij}(\tilde{\mathbf{g}}, \mathbf{x}) = \frac{\tilde{g}_{ij} x_{ijt} P + (1 - x_{ijt}) M_{ij}}{\sum_{(m \neq i,n)} \tilde{g}_{mj} x_{mnt} P + W}, \tag{4.2}$$

where we tacitly assume that $\tilde{g}_{ij} = 0$, when a link is not available to the scheduler, $g_{ij}$ is the channel gain between nodes $i$ and $j$, $P$ is the fixed power transmitted by node $i$, $W$ is the noise power at the receiver, and $\gamma$ is the target SNR requirement. The scalar $M_{ij}$ is introduced to enable a BIP formulation of the RLSP.

We note the following: (4.1a) aims to minimize the total number of time slots required to schedule all the links in $E$; (4.1b) specifies that the number of links scheduled in one slot should not be more than the total number of links $|E|$; (4.1c) states that every link must be assigned a slot in the schedule; (4.1d) is the SINR requirement for successful transmission; (4.1e) states that the channel gains lie between[1] pessimistic and optimistic values; (4.1f) states that a node cannot transmit and receive at the same time; and (4.6c) imposes the integer requirements on the optimization variables.

Observe that links for which $\mathrm{SNR}_{ij}(g_{ij}^{-}) < \gamma$ are not feasible, where $\mathrm{SNR}_{ij}(g_{ij}) = g_{ij}P/W$. Therefore, problem (4.1) becomes infeasible. These links are removed from (4.1) to obtain a feasible problem and have them scheduled in a pure TDMA fashion. We denote the number of removed links by $t_{\mathrm{T}}$. Note that due to hidden node problems, only a subset of channel gains are accounted in (4.1d) and (4.2).

Let $\mathbf{y}^*$ and $\mathbf{x}^*$ be a solution to the RLSP, and the optimal value be $t_{\mathrm{S}} = (\mathbf{y}^*)^{\mathrm{T}}\,\mathbf{1}$. The length of the schedule is $t_{\mathrm{T}} + t_{\mathrm{S}}$, which we normalize with the number of links, so that $t_{\mathrm{norm}} = \mathbb{E}\left\{(t_{\mathrm{T}} + t_{\mathrm{S}})/|E|\right\}$, is the expected normalized number of time slots, where the expectation is over shadowing realizations and location/channel estimates. As the actual channel gains are not known, certain scheduled links may not meet the SINR condition. We collect these links in a set $L$. The outage probability is defined as $P_{\mathrm{out}} = p\left(\mathrm{SINR}_{ij}(\mathbf{g}, \mathbf{x}^*) < \gamma\right) = \mathbb{E}\left\{\frac{|L|}{|E|}\right\}$. To capture the trade-off between schedule length and outage, we further introduce the normalized effective schedule length, which assumes that links in outage will be scheduled in a TDMA fashion as

$$t_{\mathrm{eff}} \;=\; \mathbb{E}\left\{\frac{t_{\mathrm{T}} + t_{\mathrm{S}}}{|E|} + \frac{|L|}{|E|}\right\} = t_{\mathrm{norm}} + P_{\mathrm{out}}. \tag{4.3}$$

We now describe two ways to obtain pessimistic ($\mathbf{g}^{-}$) and optimistic ($\mathbf{g}^{+}$) channel gain values. The first approach is based on direct channel estimation using beaconing signals called *gain based scheduler* (GBS). In GBS, nodes use $N_{\mathrm{tr}}$ unit-energy symbols to obtain channel estimates. Provided enough beaconing resources are available, GBS can rely on accurate channel information. However, it has two drawbacks: (i) certain links may be too weak to estimate, thus leading to hidden node problems. Channel estimation is only possible for links for which the SNR exceeds the so-called sensing threshold $\gamma_{\mathrm{sense}} \leq \gamma$; (ii) for a network with $N$ nodes, $\mathcal{O}\left(N^2\right)$ channel gains may need to be estimated, which is prohibitive for large-scale networks. To mitigate these problems, our second approach to the RLSP is based on location information and leads to the *location based scheduler* (LBS). Using positioning systems, each node can localize itself with an accuracy

[1] Observe that, equivalently, pessimistic gain values are used for transmitting link and optimistic gains are considered for interfering links in (4.1d).

of $\sigma_{\text{pos}}$, expressed in meters. Here, the scheduler collects the locations of all the nodes, which scales as $\mathcal{O}(N)$, and computes $\mathbf{g}^-$ and $\mathbf{g}^+$ for every pair of nodes. To have a consistent way to compare LBS and GBS, we introduce a robustness parameter $q \in [0, 1]$, such that

$$p(g_{ij}^- \leq g_{ij} \leq g_{ij}^+ | \text{observation}) = q, \tag{4.4}$$

where the "observation" may be either a channel estimate or the locations of nodes $i$ and $j$, as well as any available side information. When $q = 0$, there is no robustness and we revert to a traditional non-robust STDMA scheduler; when $q = 1$, all links in (4.1e) become infeasible, and as a result, they will be scheduled in TDMA, which is maximally robust.

**Numerical Results and Discussion** We consider a random network with 30 nodes and 38 links in a square area of 1250 m × 1250 m as shown in Fig. 4.3 (a). We set $\gamma_{\text{sense}}$ to $-6.5$ dB such that $P_{\text{out}} \approx 0.1$. Fig. 4.3 (b) shows, as a function of $q$, the normalized effective schedule length $t_{\text{eff}}$, which describes the trade-off between schedule length (as provided by the LBS or GBS) and the corresponding outages. We observe that for GBS (resp. LBS), $t_{\text{eff}}$ is around 17% (resp. 12%) larger than $t_{\text{norm}}$ when using the actual channel gains (resp. distances). In the presence of uncertainty an increase in $q$ leads to an initial reduction in $t_{\text{eff}}$ due to a reduction in outages. Further increase in $q$ leads to an increase in $t_{\text{eff}}$, due to the dominating effect of an excessively long schedule. For example, in GBS, it can be noticed that there is an optimal robustness parameter $q \approx 0.2$ for $N_{\text{tr}} = 5$ and $q \approx 0.7$ for $N_{\text{tr}} = 200$. Interestingly, GBS tends to favor large values of $q$, while LBS prefers low values of $q$, indicating the LBS is inherently more robust. While overall, LBS is outperformed by GBS, the gap between the two will shrink when $\gamma_{\text{sense}}$ is increased.

We have seen that link scheduling using channel gains suffers outage due to its limited sensing capability of interfering links, even when robustness is considered in the schedule. Such hidden node problems can be mitigated using location-based scheduling. Moreover, location information scales only linearly with number of nodes, whereas channel state information scales quadratically. However, the performance of LBS is limited by the amount of shadowing in the channel. The LBS performance can be improved by taking into consideration the uncertainty of shadowing.

### 4.2.3 Location-aware Routing for D2D

At the network layer, location information has been shown to improve scalability and reduce overhead and latency. A full-fledged location-based network architecture is proposed in [1] for cognitive wireless networks, dealing with dynamic spectrum management, network planning and expansion, and in handover. In particular, a location-aided handover mechanism significantly reduces the number of handovers compared to the signal strength-based methods [72].

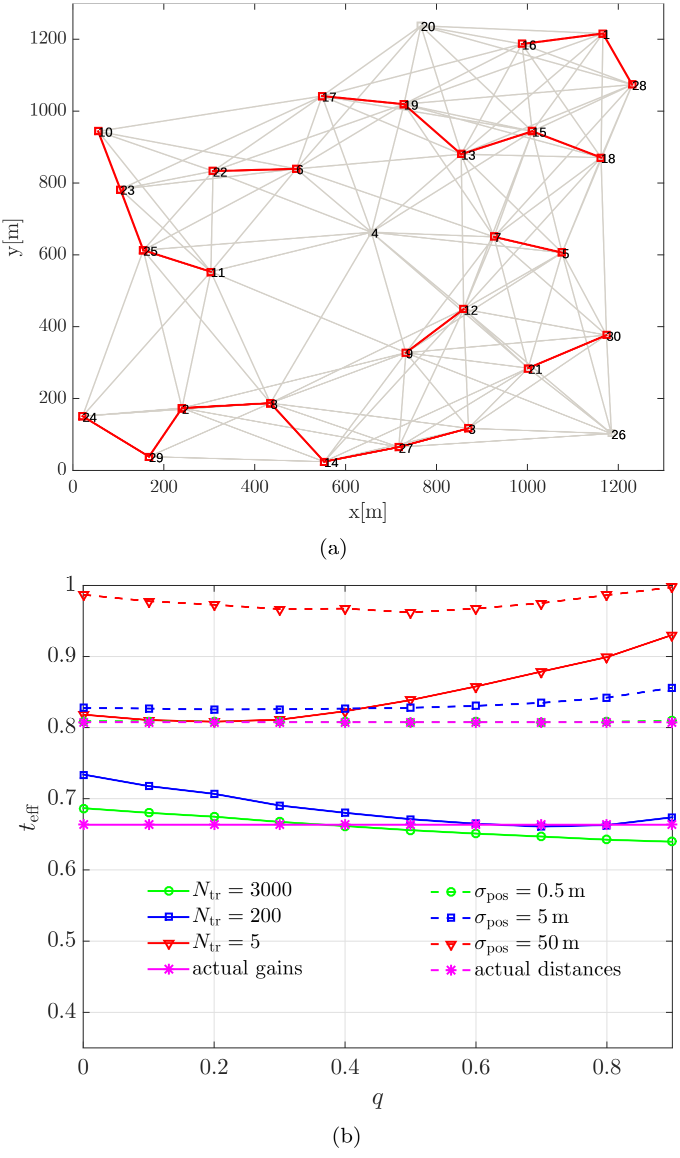


**Figure 4.3:** Inset (a) random network topology with 30 nodes and 38 bidirectional links (marked in red). The grey shaded links correspond to the links that can be sensed based on a threshold $\gamma_{\mathrm{sense}} = 0\,\mathrm{dB}$. Inset (b) effective schedule length for GBS (solid) and LBS (dashed) as a function of the robustness parameter $q$.

Most other works at the network layer have focused on the routing problem. A well-known technique in this area is geographic routing (geo-routing), which takes advantage of geographic information of nodes (actual geographic coordinates or virtual relative coordinates) to move data packets to gradually approach and eventually reach their intended destination. In its most basic form, given a destination $d$, a node $i$ with neighbors $\mathcal{N}_i$ will choose to forward data to a neighbor $j^* = \arg\min_{j \in \mathcal{N}_i} \|\mathbf{x}_j - \mathbf{x}_d\|$ . Recently, geo-routing has gained considerable attention, as it promises a scalable, efficient, and low latency solution for information delivery in wireless ad-hoc networks. For a comprehensive survey of the existing literature on geo-routing, investigating how location information can benefit routing, we refer to [73].

Geo-routing is mainly limited due to two factors: it is sensitive to localization errors and it does not exploit CQM, favoring latency (measured in this context in terms of progress towards the destination) over throughput. The first issue is investigated in [74], where it is shown that geo-routing quickly degrades as location information becomes imprecise. More robust routing mechanisms are proposed, combining progress towards the destination with an error measure in the locations. The second issue is treated in [75, 76]. In [75], where locations are mapped to a CQM, a centralized routing algorithm aims to maximize end-to-end flow. The mismatch between the estimated and true channels is mitigated using a distributed algorithm, whereby nodes locally adjust their rate, but not the routes. While [75] no longer directly optimizes progress towards the destination, [76] considers both throughput and latency in a fully distributed manner.

The focus in [74–76] is on relatively static networks, where there are no drastic topology changes. In certain applications, such as vehicular networks, this assumption is no longer valid, as is treated in [77, 78]. In [77], the use of mobility prediction to anticipate topology changes and perform rerouting prior to route breaks is considered. Routes that are the most stable, i.e., they do not become invalid due to node movements, and stay connected longest are chosen by utilizing the mobility prediction. The mobility characteristics of the mobile nodes are taken into account in [78], and a velocity-aided routing algorithm is proposed, which determines its packet forwarding scheme based on the relative velocity between the intended forwarding node and the destination node. The routing performance can further be improved by the proposed predictive mobility and location-aware routing algorithm, which incorporates the predictive moving behaviors of nodes in protocol design. The region for packet forwarding is determined by predicting the future trajectory of the destination node.

## 4.3 Location-aware Massive MIMO Communications

In this section, we show how location information is utilized for pilot allocation to improve the uplink channel estimation in massive MIMO systems.

### 4.3.1 Background

The use of very large antenna arrays at BS is considered as a promising technology for 5G communications in order to cope with the increasing demand of wireless services [55]. Such massive MIMO systems provide numerous advantages [79–84] including: (i) increase of spectral efficiency by supporting a higher number of users per cell; (ii) improvement of energy efficiency by radiating focused beams towards users; and (iii) averaging out small-scale fading resulting in the channel hardening effect. Furthermore, under the assumption of perfect channel estimation, massive MIMO provides asymptotic orthogonality between vector channels of the target and interfering users.

Pilot sequences are a scarce resource due to the fact that the length of pilot sequences (the number of symbols) is limited by the coherence time and bandwidth of the wireless channel. As a result, the number of separable users is limited by the number of the available orthogonal pilot sequences [81, 82]. Therefore, in multi-cell massive MIMO systems, the pilot sequences must be reused, which leads to interference between identical pilot sequences from users in either neighboring cells or even the same cell; this effect is known as pilot contamination [57]. The pilot contamination effect is explained in Fig. 4.4.

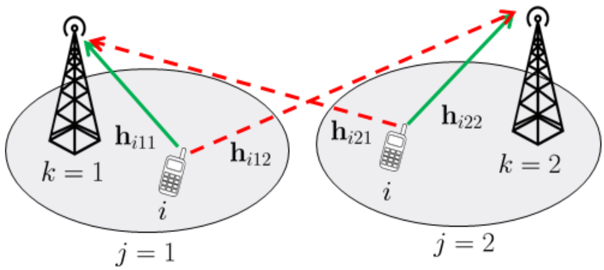


**Figure 4.4:** A 2-cell scenario is depicted with cell index $j = 1$ and $j = 2$. BSs ($k = 1, 2$) in each cell serve only one user. The uplink channels of the user $i$ in cell-1 and cell-2 are $\mathbf{h}_{i11}$ and $\mathbf{h}_{i22}$ respectively (shown in green solid arrows). For uplink channel estimation, the channels $\mathbf{h}_{i11}$ and $\mathbf{h}_{i22}$ generate interfering channels $\mathbf{h}_{i12}$ and $\mathbf{h}_{i21}$ at BS-2 and BS-1 respectively (shown in red dotted arrows) leading to pilot contamination.

Pilot contamination is known to degrade the quality of channel state information at the BS, which in turn degrades the performance in terms of the achieved spectral efficiency, BF gains, and cell-edge user throughput. Mitigation strategies for pilot contamination have been well studied in the literature. A comprehensive survey on pilot contamination in massive MIMO systems is provided in [85]. The existing pilot decontamination methods for time division duplex (TDD) MIMO systems are broadly grouped into two categories: pilot-based and subspace-based approaches. In pilot-based approaches, each BS takes turns in sending pilots in a non-overlapping fashion [86–90]. In these works, the frame structure is modified such that the pilots are transmitted in each cell in non-overlapping time slots [87,88], or pilots are transmitted in consecutive phases in which each BS keeps silent in one phase and repeatedly transmits in other phases [89], or combination of downlink and uplink scheduled training, where the frequency response obtained through downlink pilots is used to predistort the signal in uplink training [90]. In subspace-based approaches, methods exploit second-order statistics and utilize covariance-aided channel estimation [83, 91–98]. Second-order statistics of desired and interfering user channels are exploited in [83,91–93], the works in [57,91–93,99] considered spatial correlated fading, while earlier works assumed uncorrelated fading. In [94–96], blind channel estimation with power and power-controlled hand-off is studied with singular value decomposition of the received signal matrix. Blind channel estimation using eigenvalue-decomposition is described in [97].

### 4.3.2 Location-aware Pilot Contamination Avoidance

Location information is used for pilot allocation schemes to reduce interference in [100–102]. In [100], a location-aided channel estimation method is described to mitigate the inter-cell interference. The work employed a FFT-based post-processing step after the pilot-aided channel estimation. In [101], a location-aware novel pilot assignment algorithm is proposed for heterogeneous networks. The method ensures that users that are assigned to the same pilot sequence have distinguishable AoAs at the macro BSs, while maintaining large distances for the interfering users to the corresponding small BSs. The work in [102] proposed a location-aware pilot assignment scheme for Rician channel models and exploited the location-dependent LOS channel component during the pilot assignment procedure.

#### Case Study: Location-Aided User Selection for Pilot Contamination Reduction [103]

We considered $L$ arbitrary users that were assigned the same pilot sequence. We further considered that BSs are elevated and rarely obstructed, therefore the propagation can be dominated by scatterers in the vicinity of the users, giving rise a limited AoA spread [99, 104–108]. Therefore, each user's uplink channel is determined by AoA distribution $[\theta^{\min}, \theta^{\max}]$, where $\theta^{\min}$ and $\theta^{\max}$ are the minimum and maximum angle of the AoA distribution respectively. Finally, we assumed that a map exists in the BS, associating the user's location to the support of the AoA distribution.

The uplink channel of user $i$ from cell $j$ to BS $k$ equipped with $M$ antennas is denoted by $\mathbf{h}_{ijk} \in \mathbb{C}^M$. We note that the channel depends only on user $i$ and BS $k$, but the use of the additional index $j$ allows us to distinguish in which cell the users belong to. We consider the scenario of a given target user in cell 1, say user $n$, with desired channel $\mathbf{h}_{n11}$ determined by AoA distribution $[\theta_{n11}^{\min}, \theta_{n11}^{\max}]$. Our objective is to find $L-1$ users in the surrounding cells and assign them the same pilot sequence as user $n$. These users have AoAs in the ranges $\{[\theta_{ij1}^{\min}, \theta_{ij1}^{\max}]\}_{j\neq 1}$ for the corresponding channels $\{\mathbf{h}_{ij1}\}_{j\neq 1}$. It has been shown in [93, Theorem 1] that when the intervals $\{[\theta_{ij1}^{\min}, \theta_{ij1}^{\max}]\}_{j\neq 1}$ are strictly non-overlapping with $[\theta_{n11}^{\min}, \theta_{n11}^{\max}]$, then

$$\lim_{M\to\infty} \hat{\mathbf{h}}_{n11} = \hat{\mathbf{h}}_{n11}^{\text{no-int}}, \tag{4.5}$$

where $\hat{\mathbf{h}}_{n11}$ is the channel estimate of the desired signal and $\hat{\mathbf{h}}_{n11}^{\text{no-int}}$ denotes the channel estimate of the desired channel in the presence of no interfering pilot signals from other cells. We now consider two approaches for user assignment: random and location-based, both of which are detailed below.

**Random user assignment** In the random assignment, a single user is chosen randomly in each cell and assigned the same pilot sequence. A random assignment cannot always guarantee that $\{[\theta_{ij1}^{\min}, \theta_{ij1}^{\max}]\}_{j\neq 1}$ does not overlap with $[\theta_{n11}^{\min}, \theta_{n11}^{\max}]$, so that $\lim_{M\to\infty} \hat{\mathbf{h}}_{n11} \neq \hat{\mathbf{h}}_{n11}^{\text{no-int}}$, which in turn implies that in the large-antenna regime, the estimate of the channel will be limited by interference.

**Location-based user assignment** We assume each cell comprises $K$ users. Let us introduce the variables $y_{ij}^{(1)} \in \{0,1\}$, $y_{ij}^{(2)} \in \{0,1\}$, where they take on the value 1 if $i$-th user in $j$-th cell has been selected and 0 otherwise. The variables $y_{ij}^{(1)}$ and $y_{ij}^{(2)}$ distinguish whether the support of the interfering user's AoA is either to the left or right of the support of the desired user's AoA respectively. The user assignment can be written as an integer linear program:

$$\begin{aligned}
&\underset{\{y_{ij}^{(1)}, y_{ij}^{(2)}\}_{i=1,\dots K}^{j=2,\dots L}}{\text{maximize}} && \sum_{j=2}^{L}\sum_{i=1}^{K}\Big(\left(\theta_{ij1}^{\min} - \theta_{n11}^{\max}\right) y_{ij}^{(1)} + + \left(\theta_{n11}^{\min} - \theta_{ij1}^{\max}\right) y_{ij}^{(2)}\Big) && \text{(4.6a)}\\
&\text{subject to} && \sum_{i=1}^{K} y_{ij}^{(1)} + y_{ij}^{(2)} = 1, \; \forall j && \text{(4.6b)}\\
& && y_{ij}^{(1)} \in \{0,1\}, y_{ij}^{(2)} \in \{0,1\}. && \text{(4.6c)}
\end{aligned}$$

We note the following: (4.6a) maximizes the distance between the AoA supports of the desired and the interfering users; (4.6b) guarantees that only one user is selected from each cell; and (4.6c) imposes the binary integer requirements on the optimization variables.

To maximize the objective, (4.6) selects the interfering users in such a way that it provide minimal overlap with the support of the desired signal AoA. A toy example is given in Fig. 4.5 to show the user assignment based on (4.6).

**Numerical results and discussion** We consider a 7-cell network with the center cell being the target cell, i.e., cell 1. The performance metric considered for the numerical results is the normalized channel estimation error $\mathcal{E}$, which is defined in dB scale as

$$\mathcal{E}[\text{dB}] = 10\,\log_{10}\left(\frac{\|\hat{\mathbf{h}}_{n11} - \mathbf{h}_{n11}\|_{\text{F}}^2}{\|\mathbf{h}_{n11}\|_{\text{F}}^2}\right). \tag{4.7}$$

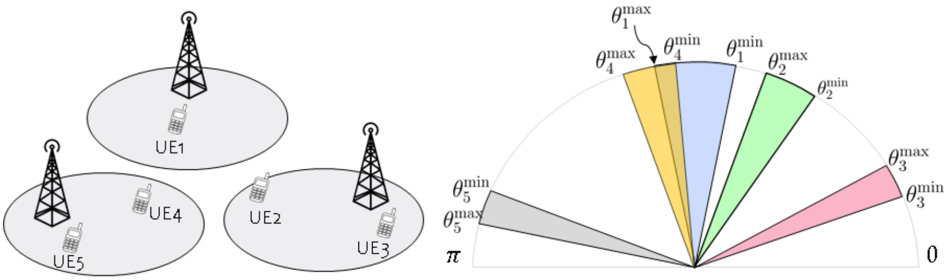


**Figure 4.5:** A 3-cell scenario is considered for demonstration, where cell-1 consists of UE1, and other two cells consist of two users each (shown in left panel). The objective is to find one user in each of the surrounding cells and assign them the same pilot sequence as user UE1. The AoAs of all desired and interfering users at BS-1 is depicted in the right panel. Of the AoAs of UE4 and UE5, UE5 AoA is non-overlapping therefore the optimization problem will select UE5. In the case of UE2 and UE3, both of them have non-overlapping AoA with UE1. In this case, the optimization problem will select the UE with maximal difference of AoA, so UE3 is selected.

In Fig. 4.6, the estimation error $\mathcal{E}$ as a function of the number of BS antennas is illustrated. It can be observed that $\mathcal{E}$ decreases with the increase in number of antennas $M$ at the BS. In the *random* assignment, $\mathcal{E}$ decreases initially and then saturates in the large antenna array regime. This is because it is not guaranteed that the AoA support of the interfering users is strictly non-overlapping with the AoA support of the desired user. On the other hand, in the *location-based* user assignment, the overlap between the desired and interfering users is minimized. As a consequence, $\mathcal{E}$ decreases rapidly and approaches the interference-free scenario channel estimation performance in the large antenna regime.

Now we discuss the limitations of the random and location-based assignments. First, we note that both the random and location-based assignments consider one user in target cell. Hence, after a set of users has been assigned a certain pilot, the process is repeated for a second user in the target cell, and so forth. This is a greedy approach, which provides the most benefit for the first user, and less benefit for later users, as there will be fewer users from the other cells to choose from. Hence, a one-shot joint assignment of all users in the target cell could lead to better performance. Second, we also note that the assignment aims to reduce the interference seen by the target cell users, with no regard to the interference that users in cells other than the target cell experience with respect to each other. Hence, a joint design across multiple cells is needed to benefit from the proposed scheme for all users in the system. Third, in practice, that the number of antennas can be limited such that the pilot contamination effect does not vanish. In Paper D, we address the aforementioned issues by considering a joint design across multiple cells for all users in the system when the number of BS antennas is not very large.

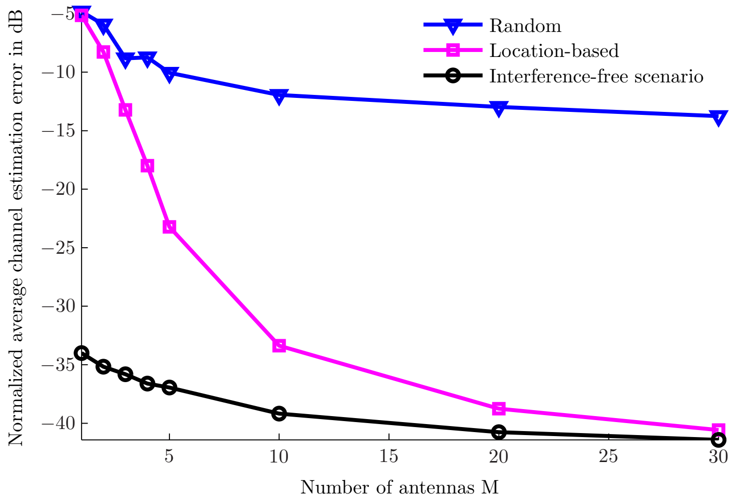


**Figure 4.6:** Comparison of normalized average channel estimation error $\mathcal{E}$ as a function of number of antennas for *random* and *location-based* user selection methods. For each value of $M$, the results of $\mathcal{E}$ are averaged over 200 channel realizations.

## 4.4 Location-aware mmWave Communications

In this section, we show how location information can aid during IA in mmWave communications.

### 4.4.1 Background

mmWave communications is one of the candidate technologies for 5G that has the vast potential to offer extremely high data rates which are needed for 5G networks [55]. mmWave communications can be utilized for multiple applications in 5G such as cellular access, wireless backhaul, and in small-cell networks. The range of frequencies from 30 GHz to 300 GHz constitute the mmWave band since the corresponding wavelengths are on the order of 10 to 100 mm [109]. The numerous advantages of mmWave communications are [110]: (i) offers data rates up to several Gbps due to the availability of extremely large bandwidth; (ii) provides very high spatial reuse of spectrum, same frequencies can be utilized over small distances due to very high signal attenuation; (iii) gives less form factor to bundle many antennas, the antennas size operating on mmWave tend to become small, thereby large number of antennas can be packaged within less area; (iv) offers better privacy and security due to narrow bandwidth and limited transmission range. However, it also possess several limitations [111]: very high attenuation of the signal due to high path-loss and atmospheric absorption of oxygen and water vapour; scattering due to rain; susceptible to blockages (buildings, trees, human body, etc.). Deafness is another blockage problem that occurs due to misalignment of transmitter and receiver beams. Due to these limitations coordination between transmitter and receiver becomes challenging during IA.

IA is the procedure to synchronize transmitter and receiver, and to establish a connection before starting to communicate. When compared to existing technologies such as LTE, IA search using mmWave communications could be challenging due to high directivity, high attenuation, and sensitivity to blockages. IA involves three steps [58]: cell search, extraction of system information, and random access. In the first step, the cell search phase, the UE searches for the BS that has the strongest signal. Then in the second step, the UE exchanges information (such as frequency band, cell ID etc.) with the detected BS. Finally, in the last step, the UE requests for a channel with the detected BS using a procedure called random access.

For the BS and UE to communicate, their transmitted beams must be aligned. Initially, the BS sends a beam in all possible directions, then the UE measures the received power of the transmitted beam and computes the SNR. For the establishing a link between BS and UE, the computed SNR should be more than a predefined threshold. The process of aligning beams between BS and UE takes time and there exist different beam alignment techniques. There are mainly four types of beam alignment algorithms available: namely, exhaustive, iterative, hybrid, and context-based. These methods differ on how the beams are constructed and how they are utilized for searching the UE. In the exhaustive method, based on the beam width the whole angular region is divided into many search sectors and then the BS sequentially sends beams in each search sector until the UE is found. Iterative method is an iterative procedure in which the beam width is reduced in each iteration to find the UE. There are also other iterative methods, without assuming reduced beam width in each iteration (see [112, 113] and the references therein). The hybrid method is a combination of iterative and exhaustive methods, where some stages of iterative procedure followed by exhaustive search with narrow beams. Lastly, the context-based method exploits context information such as UE location to aid in the beam alignment procedure [114]. The different search methods are shown in Fig. 4.7.

Exhaustive method offers finding UE at relatively larger distances from BS, therefore it is suitable for cell-edge users. However, exhaustive method takes more time to discover the UE [114]. Iterative method is limited to find UE at larger distances but takes less time to discover the UE. Iterative method is not suitable for cell-edge users [114]. Hybrid method performs in between exhaustive and iterative methods. Finally, context-based method needs low discovery time. It works only in LOS conditions due to availability of GPS.

The construction of beam patterns can be done in multiple ways. Mainly three architectures exist for BF namely: analog, digital, and hybrid. In analog BF, the transmitter and receiver consist of only one RF chain, and it uses one beam per time slot for searching. Due to the presence of only one RF chain, analog BF offers less complexity and also lower power consumption. However, it takes more time to discover the devices as only one beam is used for searching per time slot. In digital BF, each antenna element is connected to one RF chain. Therefore, it

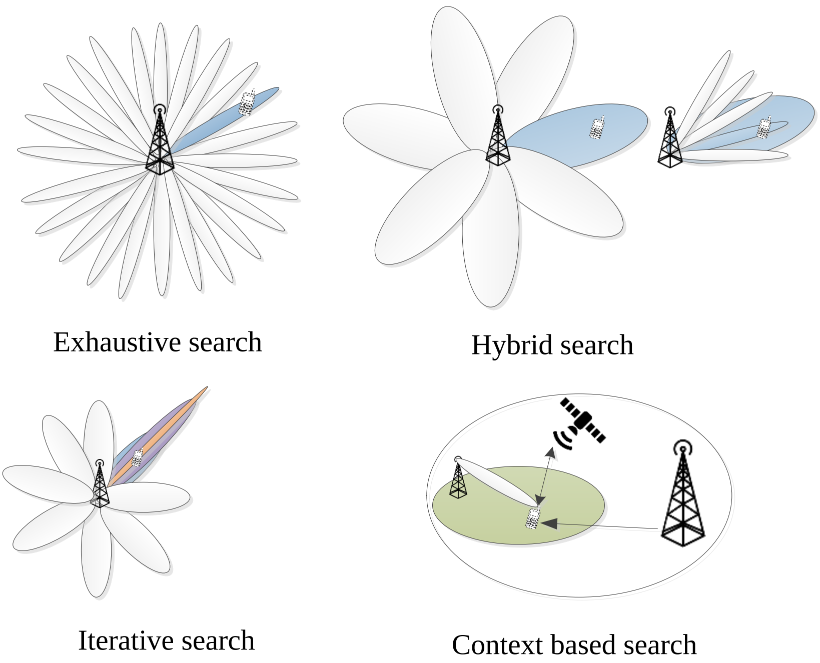


**Figure 4.7:** Comparison of different beam alignment search schemes (inspired from [114]).

offers greater flexibility and can create multiple beams in a time slot and use them to search simultaneously in multiple directions. As a result, the discovery time in digital BF is less compared to analog BF. Due to the presence of many RF chains, digital BF consumes more power and also involves high complexity. Lastly, hybrid BF provides the balance between analog and digital BF with a few RF chains, but less than the number of antennas. The transmitter and receiver chain of analog and digital BF is shown in Fig. 4.8.

As we have seen, IA is a very important issue in mmWave communications. This is a fairly recent topic and many researchers are investigating this issue. An overview of random access in mmWave BF is given in [116] and critical issues in random access and possible approaches to address them are discussed. The main drawback of the traditional methods is that they take more time to determine the beam alignment. In the next section, we review the latest works on beam alignment using location information.

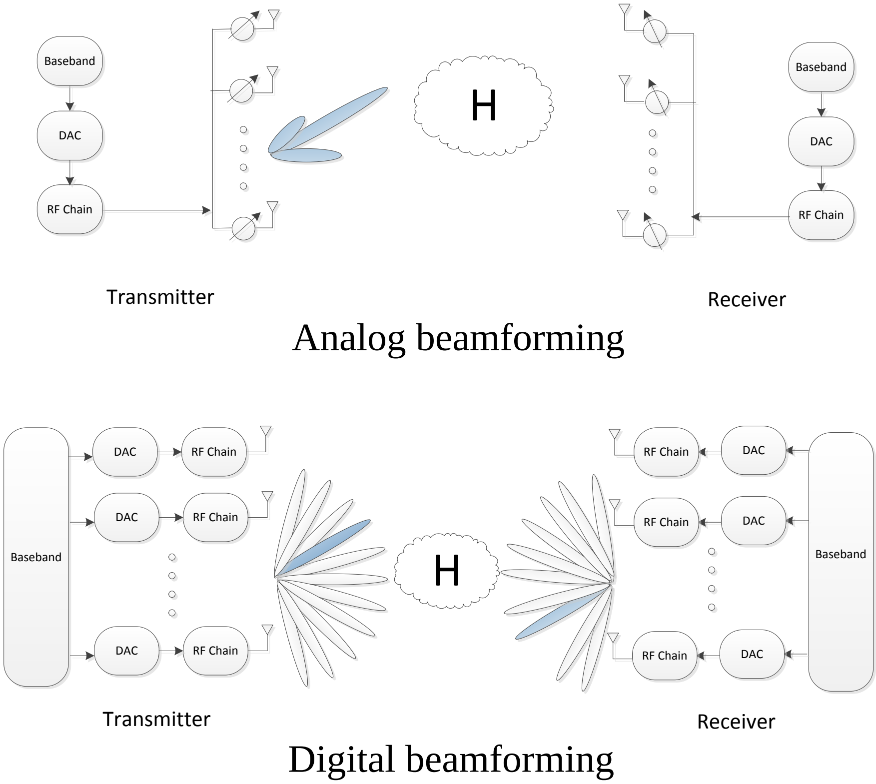


**Figure 4.8:** Transmitter and receiver chain of digital and analog BF (inspired from [115]).

### 4.4.2 Location-aware Beam Alignment in mmWave Communications

Context information has been exploited to point the beams to confined areas where the UE is located to speed up the beam alignment procedure. Mainly location information is used in the literature to compute the BF vectors [117, 118] and to preselect some transmitting beams [119–121].

Transmitter and receiver BF weights are computed based on AoD and AoA using location information in [117]. They consider an urban environment with connected-car scenario with vehicular speeds. The AoA and AoD information needed for the BF are tracked based on location information using an Extended Kalman filter. The proposed method reduces the uplink reference signals and provide very high throughput compared to traditional BF with full CSI. Beam alignment using location information for the backhaul in fixed networks in studied in [118]. Backhaul is the major bottleneck for small-cell networks. In small-cell networks, the nodes can be placed on lamp posts owing to displacement due to wind and disturbances which lead to uncertain location information. They consider analog BF and again location information is exploited in designing the BF vectors.

Another line of work is to preselect some beams using location information at BS and UE that maximizes the transmission rates. In [119], uncertain location information is used to preselect beams. First, an estimate of AoD and AoA is done based on the shared location information of BS and UE exchanged mutually. Then, the estimated AoD and AoA can be used to find a closer BF codebook that directs to the UE and BS, respectively. The beam alignment is cast as a team decision problem, wherein the beam is selected based on the node's location information and also the expected quality of the other node location information. In [121], UE location is used to guide the directional transmissions for synchronization. They argue that other context information can also be used for this purpose such as, channel gain predictions and UE spatial distribution. A fingerprint database with channel propagation knowledge tied to location is used to preselect some beams at the BS to direct towards the UE in [120].

Other works include faster adaptive channel estimation for vehicular communications [122]. The location information is used to compute the AoD and AoA based on geometry. This prior information is used then to discard AoD and AoA ranges that do not include the true AoD and AoA. Most of the works treat IA and localization separately. However, for IA, the location information is beneficial and vice versa. A joint location and beam selection procedure for mmWave is studied with in-band location information [123].

## 4.5 Location-aware HetNet Communications

In this section, we first introduce the basics of HetNets. Then we review various methods to mitigate one of the challenges of HetNets, interference management (IM). We showcase the shortcoming of the traditional methods and how it can be alleviated using location information.

### 4.5.1 Background

System capacity and coverage can be greatly increased by means of network densification. Network densification can be achieved by deploying more and more cell sites. Densifying macro cells might not be enough and it should be complemented by small-cell networks, such as WiFi, pico-, and femto-, cells, and these constitute a HetNet. Small-cells are low power, low cost, and low coverage BSs. The small-cells can be classified into pico- and femto-, cells based on their characteristics such as size, power and backhaul connections. HetNets is the combination and coexistence of macro and small-cells (see Fig. 4.9). Femtocells [124] are part of HetNets that are usually bought and deployed by users at offices and homes to increase the wireless connectivity. Furthermore, they are backhauled over the Internet to a femtocell gateway and then the core network. A survey on femtocells is presented in [125].

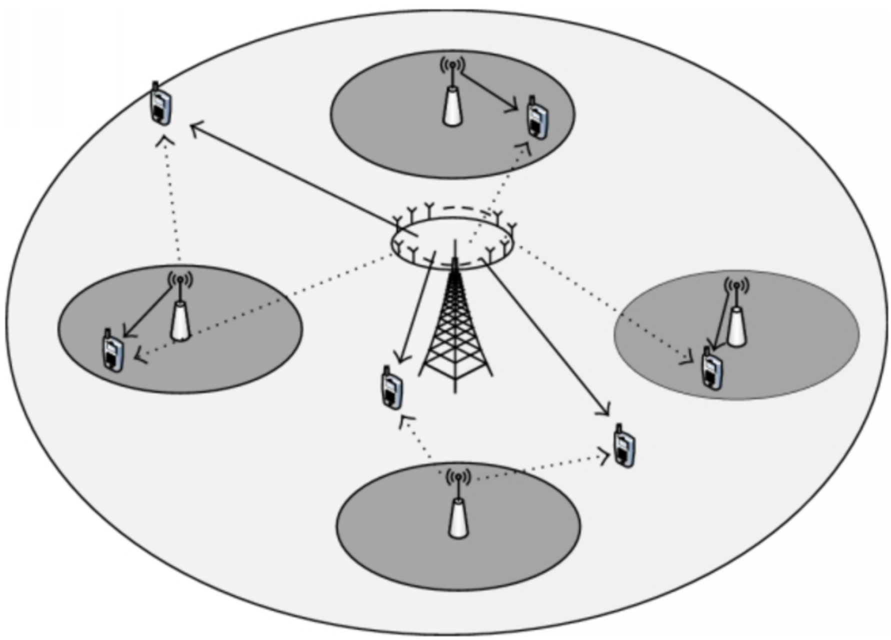

**Figure 4.9:** HetNets: network comprising of macro and small-cells serving their respective users. Solid line corresponds to the desired signal and the dotted line corresponds to interference signal.

HetNets have emerged as one of the promising technology to meet 5G requirements. Small-cells are usually deployed at dense locations to improve the coverage and to meet peak user data rates such as in hotspots. The small-cells and macro cells in HetNets can share the same channels, thereby leading to cross-tier co-channel interference. Furthermore, the small-cells can either be deployed by an operator or by an user. The user-deployed small-cells are done in ad-hoc fashion and this inefficient deployment can have a significant impact on the interference for the macro cell users and deteriorate the performance of the whole system [59]. Another reason for interference in HetNets is due to closed subscriber group cell association, wherein the UE is not allowed to connect to small-cell BS, even when the signal power to the UE from it is higher than the macro cell BS. Therefore, proper IM schemes are necessary to fully capitalize the benefits offered by the HetNets.

The main IM techniques for HetNets can be grouped into two categories; namely, coordination and cooperation [59]. In coordinated IM techniques, the BSs only share signaling information among the BSs. The main methods in coordinated schemes are inter-cell interference coordination (ICIC) and enhanced ICIC (eICIC). ICIC method performs scheduling of users on different frequency bands between macro and small-cell to mitigate the interference. The frequency reuse pattern could be static or dynamic based on the network load. Furthermore, some sub-bands are attenuated and some bands are boosted. Also, there are hard and soft frequency reuse schemes based on how much is the transmitted power in the attenuated sub-bands. In the hard frequency reuse, the power transmitted in the attenuated sub-band is zero. Users experiencing high interference are assigned boosted bands. The boosted sub-bands are chosen such that they do not overlap in the neighboring cells to minimize the interference. eICIC is an enhancement of ICIC, where the IM and resource partition is done in the time domain. eICIC introduces the concept of almost blank sub-frames (ABS). The ABS consists of vital information to maintain the connection and the remaining part of the ABS are left blank to minimize the interference. ABS are used by small-cells to communicate to vulnerable users who suffer alot of interference.

The other IM technique is a cooperative method called coordinated multipoint (CoMP) transmission [126, 127]. In cooperative IM techniques, the UE is allowed to connect to multiple BSs at the same time and macro and small-cells cooperate for data and signal transmission. There are variants in CoMP: in *joint transmission* all the connected BSs send data simultaneously at the same time to a UE to mitigate the interference; in *coordinated scheduling and beamforming* only the serving BS sends data to the UE but other BSs use beamforming to transmit data to spatially separated UEs. For the joint transmission both the data and signaling information be shared across BSs, on the other hand for coordinated scheduling and beamforming requires CSI and scheduling information.

The ICIC and eICIC techniques need limitedly coordination among BSs and need low signaling overhead, therefore backhaul is not constrained. However, for the cooperative IM schemes, signaling is higher and require fast and low latency backhaul links [59]. One way to decrease the exchange of signaling information in cooperative schemes is to use context information. The context information could be location, time, identity. In the next section, we review the literature where location information is exploited for IM in HetNets.

### 4.5.2 Location-aware Interference Management in HetNets

We find approaches [3, 128–130] that utilize location information for IM through REMs. REMs have been used for power, frequency and time controlled IM in HetNets [130].

The works in [3, 128] utilize REMs to manage interference in cross-tier networks through a power control mechanisms. In this power control mechanisms, the transmitter adjusts its power levels in order to meet the target SINR at the receiver. In [3] managing interference from femtocell AP (FAP) to the macro cell user (MUE) is considered. The FAP controls the power levels based on its distance from the macro BS. FAP uses higher power levels when it is close to the MBS and lower when it is on the cell edge. The femtocell measures the signal power and SINR from macro BS and other FAPs. The method assumes known location information about FAP, macro BS, and MUE. Then, based on the availability of

REM consisting of path-loss and shadowing information, the expected SINR can be computed.

**Table 4.1:** Summary of location-aware references for RRA in 5G technologies.

| Technology | Selected location-aware references | Remark |
|---|---|---|
| D2D | [6,62–64] | Location information is used in scheduling to achieve lower latency, higher throughput, reducing signalling overhead. |
| massive MIMO | [100–102] | Location information is used for pilot allocation schemes to reduce inter-cell interference. |
| mmWave | [117–121] | Location information is used to compute the BF vectors and to preselect some transmitting beams for IA. |
| HetNet | [3,128–130] | Location information is used to manage IM in HetNets through power control and time scheduling. |

Downlink interference at femtocell is severe if the macro BS is close to a FAP and the downlink interference at MUEs will be severe for the users at the cell-edge. Interference from macro BS to femtocell user is studied in [128]. In order to estimate the spatio-temporal interference they use the spatial Kriging interpolator followed by the temporal auto-regressive method.

In [130], how to chose different sub-bands based on REMs at macro BS and FAP for frequency controlled IM is discussed. FAP uses one sub-band, whereas macro cells use two sub-bands: one for the inner part of the cell and the other for the outer part of the cell. REM can also be used for muting period in macro cells to allow small-cell transmissions for time controlled IM. While in [129], REMs are used for deployment of small-cells such that the transmitting power of these small-cells do not interfere with the primary receivers.

## 4.6 Summary

In this chapter, we showed the use of location information as in RRA for various RAs in 5G. We reviewed the works from the literature where location information has been used for various RAs in 5G candidate technologies. We have provided two use cases on the use of location information for RRA: scheduling in D2D communications in unlicensed spectrum, and pilot allocation in massive MIMO networks. Table 4.1 summarizes the main location-aware references and how location information has been utilized in various 5G candidate technologies.

# Chapter 5

# Location-aware Proactive Resource allocation

In this chapter, we give a detailed introduction of PRA. First, we introduce the basic components necessary for a PRA. We then discuss how PRA strategies are utilized in the literature for various applications. In particular, we provide a case study on media streaming and proactive caching in which we showcase the advantage of PRA using the channel measurements detailed in Chapter 2.

## 5.1 Background

A PRA system is described in [56] as *"The Proactive Resource Allocation design pattern maintains the performance of a computing system within required bounds by anticipating critical changes in the system state, pre-planning resource allocations appropriate to those changes, monitoring the system state for those changes, and implementing the appropriate pre-planned resource allocation when the system state changes."* For example, the system could be a network provider serving the users, the state of the system could be network load, user trajectories and their CQMs, and user traffic demand. In this case, the system resources could be time, frequency, power, and the system performance can be measured by means of network load, throughput, and QoS.

The difference between PRA and RRA is as follows. In RRA, the RA starts when a user requests for a service, where as in PRA, the RA is planned before the user requests for service. Specifically, a proactive network system, can track, learn, and then predict the user service requests ahead of time, and hence offers more flexibility in scheduling these requests before their actual time of arrival [131]. Moreover, PRA can only be applied for delay tolerant services where users can wait for the service [131]. The main disadvantage of RRA is that it allocates resources without consideration to the user's future channel conditions. Instead of waiting for better channel conditions of the user, it continues to serve the users even though their current channel conditions are poor. This translates to a high operating cost during peak network load [28]. The other disadvantage is that the reactive systems must be designed for very high network capacity in order to be able to satisfy all the users during the peak period. On the other hand, PRA schemes exploit users' future channel conditions, thereby are capable of sending bulk transmissions when the channel conditions are good. Scenarios where PRA could be beneficial are [22, 132]: (i) a user moving towards a BS can delay the transmission until getting closer; (ii) a user approaching a poor coverage will be pre-allocated additional content to make smooth playback of the media streaming; (iii) BS can prioritize users that are heading towards poor channel conditions such as a cell-edge or a tunnel. From these examples, we can infer that the three key ingredients necessary for PRA are mechanisms to predict the user mobility, CQM along the navigation path, and user traffic demands.

Four proactive approaches are discussed in [25], where location information can be utilized for providing better QoS, namely: (i) adaptive video planning; (ii) in-network caching; (iii) content prefetching; (iv) long-term predictive RA.

- In adaptive video planning, the video quality is adjusted based on network conditions, and users' location information is exploited to adjust the video quality levels based on predicted future transmission rates.

- It is a known fact that a popular content is requested by many users. Therefore, instead of requesting the content every time from the server, it is stored temporarily closer to the end user. This is called in-network caching (see Fig. 5.2). User mobility and their trajectories might help in deciding where the content needs to be cached. The in-network caching helps to reduce the content server and core network load.

- Content prefetching is an extreme form of caching, wherein the content is directly downloaded at the UE storage for its consumption (see Fig. 5.3). The main challenge here is, which content needs to be cached. The main difference compared to in-network caching, is that prefetching requires insights on user specific consumption preferences. Moreover, there could also be wastage of resources as the user might not consume the downloaded content. For cases where it is not important to distinguish whether the content is cached at the network provider or at the user we simply call it *proactive caching*.

- Long-term predictive RA (see Fig. 5.6) optimizes the radio resources to minimize the streaming interruptions by exploiting the users future CQM. The main advantage is that it intelligently utilizes the available resources so that users are given more resources during their peak channel conditions.

From the aforementioned methods, we can infer that a PRA system benefits from user predictability, i.e., user mobility, user demand preferences, and user channel conditions. The next section is dedicated to user predictability, which is the main ingredient of PRA. In the later sections, we discuss how the user predictability is utilized in various location-aware PRA strategies.

## 5.2 Components of User Predictability

People's behavior is highly predictable. For example, most people generally take the same route to work every day. Furthermore, users mostly read and watch content from the same sources, such as for news (BBC, CNN, etc.) and video (Netflix, YouTube, etc.). In the following, we review works on the user mobility, user demand, and channel prediction which are necessary for PRA.

### 5.2.1 Mobility

User mobility is highly predictable, and both long-term and short-term user mobility have been studied extensively [27,133–135]. In [134], an algorithm is developed that can predict a vehicle's end-to-end route. The work is based on Microsoft Multiperson Location Survey (MSMLS), which is a measurement campaign where drivers volunteer to record their GPS traces for a couple of weeks. The database contains about 2.2 million GPS locations from 252 drivers. The proposed algorithm tries to match the first part of the driver's current trip with that of the recorded GPS traces from the database. The main focus of the algorithm is to predict the entire trip rather than predicting near term road segments. From the numerical results, it was found that for some trips the algorithm completely predicts with 100% accuracy within first two miles of the trip. In another work [133], a study is conducted to know where exactly a user will be based on historical data. The study is based on Four square application, wherein users check-in their geographical location. For the study, 5 million geo-tagged check-in points are used to extract features such as historical visits and social ties. Using these features, an algorithm is proposed to predict the user's next check-in place. Short-term route prediction of vehicles is described in [135]. The basic idea is to construct Markov models based on user driving paths and then use it for route prediction. For example, a 2nd order Markov model will use two previous road segments to predict the next road segment. As expected, the accuracy of the prediction is improved as the order of the Markov model is increased. Another measurement campaign to predict the user location along with their channel strength is presented in [27]. The campaign is conducted on a public transport along a bus route of 23.4 Km involving urban and suburban areas of Kingston, Canada. Based on the 33 repeated bus trips, an analysis is provided on the impact of location and signal strength errors on the signal strength predictability. Moreover, today's smart phones are equipped with plenty of applications that allow for reporting user's current location and destination. The above studies indicate that it is possible to predict user future navigation path based on database consisting of historic vehicle drive paths.

### 5.2.2 Demand

User demand predictability is another important ingredient necessary for successful application of PRA. To be able to provide the necessary content to the user in advance, the network needs to estimate the user content preferences. The demand prediction depends on the type of location-aware proactive strategy. For example, in in-network caching the ratings of the content are needed and the network stores the highly popularity content. On the other hand, for the content prefetching, content that is very specific to the user is to be predicted. Lastly, for long-term predictive RA the network should be aware of user multimedia traffic, but it can only be served on a real time basis.

Recommendation system is a filtering system which is used to predict rating of a content. Collaborative filtering [136–138] is the most widely used recommendation system for in-network caching to predict the popular contents. A collaborative recommendation system rates user content based on other people who have similar content preferences liked in the past. Other recommendation systems apart from collaborative filtering are content-based and hybrid recommendation systems. In content-based recommendation systems, the ratings are based on the user preferences in the past and hybrid recommendation systems combine content-based and collaborative methods. For further details on recommendation systems, the reader is referred to [139], which provides a comprehensive survey of the recommendation systems and their extensions.

There is growing evidence that user specific content can be predicted with the advent of Google Instant and from the findings of predictable user mobility patterns [140]. As it is hard to predict perfectly the demand of the user, we consider that network can only know with a certain probability whether a user will request demand in a specific time slot. So, the service provider is only probabilistically aware of user demand characteristics. The probabilistic demand characteristics with time-invariant statistics for proactive caching is treated in Paper E and a case study is described in Section 5.3. We also consider the case where the service provider is perfectly aware of the user multimedia demand, a long-term predictive RA with perfect user demand is described in Section 5.4.

### 5.2.3 Channel

The third ingredient of PRA is channel prediction. We know from Chapter 2 that the wireless propagation channel is predictable and in Chapter 3 we presented a GP framework for channel prediction. In the following, we review various channel prediction methods from the literature. In [37], GP was shown to model spatially correlated shadowing to predict shadowing and path-loss at any arbitrary location. In [141], a cognitive network setting was evaluated, in which the transmit powers of the primary users were tracked with cooperation among the secondary users. For this purpose, a distributed radio channel tracking framework using a Kriged Kalman filter was developed with location information. A study on the impact of underlying channel parameters on the spatial channel prediction variance using GP was presented in [142]. The work [143], extends [142] to include the effect of localization errors on spatial channel prediction. In [41], location information is used to predict the spatial correlation between the links of a multi-hop network. A channel gain predictor using a Kalman filter in combination with expectation maximization is proposed in [144]. The proposed method performs better than the Auto regressive integrated moving average (ARIMA) and polynomial approximation methods. A Bayesian approach is considered in [145] for channel prediction by exploiting the spatial and temporal correlation properties of the channel. Two methods are studied for predicting signal strength in robotic networks using few channel measurements [146]. The first one is a model based on a GP framework and the second one, which is sparsity-based, utilizes the compressibility feature in the frequency domain. An algorithm to reconstruct a complete channel map based on sparse measurements of channel coverage data is given in [147]. Predicting wireless channel quality based on path-loss values using street and coverage maps is described in [148]. From these works, we can conclude that long-term channel prediction is possible with location information.

We have considered two types of channel models in this thesis. In the first model, we have considered complete knowledge of the channel values including uncertanties (see Fig. 5.1 (a)). This model is used in Paper B and in the case study in Section 5.4. In the second model, we quantize the channel values and probabilities of the channel states are considered (see Fig. 5.1 (b)). We can clearly observe channel state probabilities varying with the location. Depending on the velocity of the user, the channel state probabilities can be mapped to time. This time-variant channel statistics model (see Fig. 5.1) is used for proactive caching in Paper E and also in the case study in Section 5.3.

Proactive caching and long-term predictive RA are well studied topics in PRA and are detailed next.

## 5.3 Location-aware Proactive Caching

Proactive caching is the combination of in-network caching (see Fig. 5.2) and content prefetching (see Fig. 5.3).

### Background

A comprehensive survey on proactive networking is provided in [149]. The basic three ingredients of a proactive network namely context, prediction, and optimization are discussed. Context defines the type of information considered for the prediction. The prediction mechanism predicts the context based on current and past context information. Finally, the optimization utilizes the predicted context to meet the network objectives. As an example, context could be CQM, prediction could be GP, and optimization could be a simple linear programming problem to enhance user QoS.

Most of the works on in-network caching assumes that backhaul is the bottleneck [16–18]. In these works, the user predictability is exploited to reduce the backhaul load by caching the popular content at the network edge. Ideally, the capacity of the backhaul should be of the same order as the wireless links. However, deploying backhaul is very expensive. Therefore, to satisfy the user demand the content is cached at the edge of the network [18]. Furthermore, all the data content cannot be stored at network edge possibly due to storage constraints. Therefore,

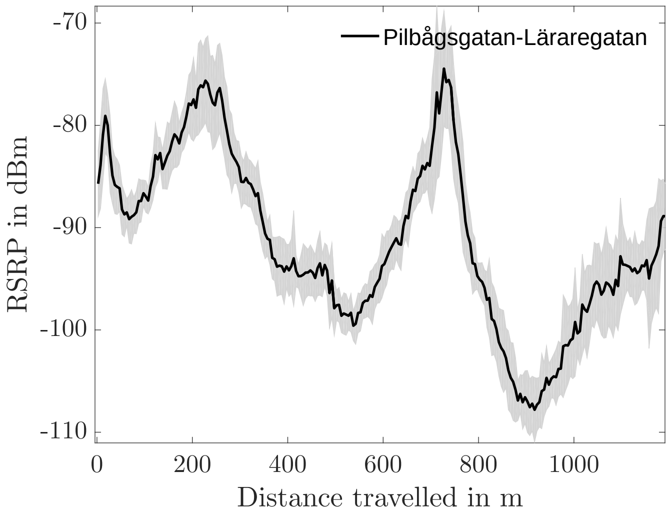


(a)

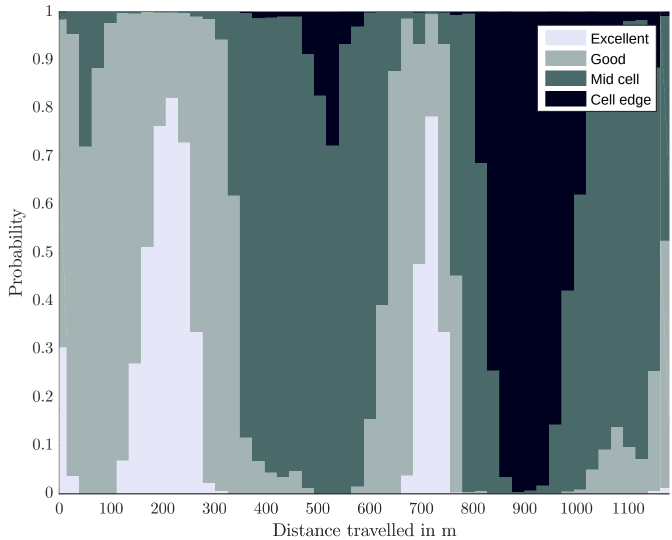


(b)

**Figure 5.1:** Inset(a): RSRP measurements of a user walking along a pedestrian path (Pilbågsgatan-Läraregatan). The solid line is the mean RSRP with measurements averaged over different times of the day and on different days. The shaded region captures the standard deviation of the measurements. Inset (b): The channel measurements of the left panel are categorized in four channel states namely, excellent (RSRP $\geq -80\,$dBm), good ($-80\,$dBm $<$ RSRP $\leq -90\,$dBm), mid-cell ($-90\,$dBm $<$ RSRP $\leq -100\,$dBm), and cell-edge (RSRP $\leq -100\,$dBm). The figure depicts the channel state probabilities along the path.

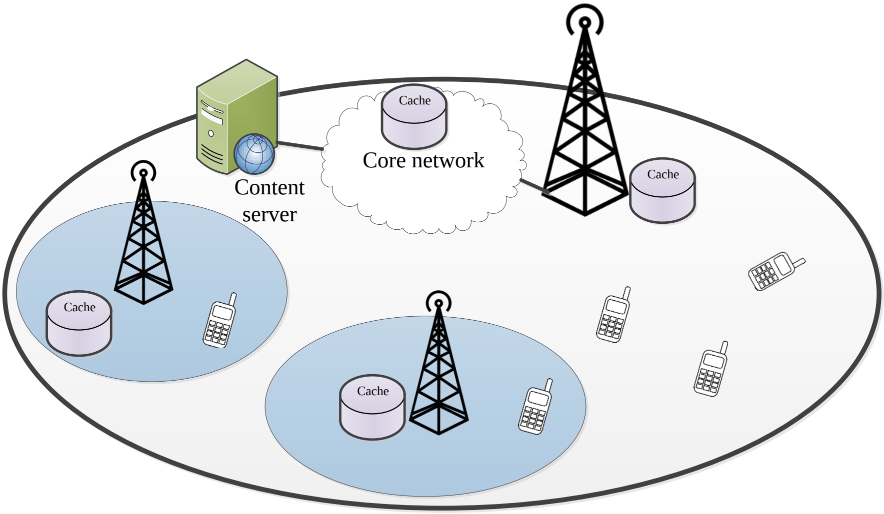


**Figure 5.2:** In in-network caching, popular content is stored temporarily at the BSs, so that when the user requests for the specific content, it is served from the local cache of BS rather than requesting it every time from the server.

there is a necessity to devise algorithms which smartly store the most popular content until capacity is achieved. An algorithm is proposed in [17], which offers 85% higher user satisfaction than random caching and also reduces the backhaul usage by 10%. Based on the popularity matrix of the contents, the proposed algorithm caches content with high probability until the storage capacity is reached. The traditional reactive networks do not possess any intelligence and hence they just act upon user demand request. On the other hand, proactive networks are smart, so they track, learn and then predict the user demand requests before they occur. As a result, they have a greater flexibility in deciding which content to store. In another work [16], the backhaul load is reduced by proactively caching the users' content during off-peak demands based on the content popularities. The proposed architecture exploits social networks, where the files are cached at the influential users and D2D communications is used for content sharing. From the above works, we can conclude that user predictability can be harnessed to alleviate the backhaul load by in-network caching.

The other approach in location-aware proactive caching is content prefetching. In content prefetching, the user content is pushed into the UE storage before its actual request. When the user requests for the content, the application directly pulls the data from the UE local memory rather than accessing it from the network provider. In [150], a novel PRA paradigm that exploits the user predictability is introduced. The basic assumption is that UE terminals predict future data requests $T$ slots in advance. It is shown that the outage probability decreases with

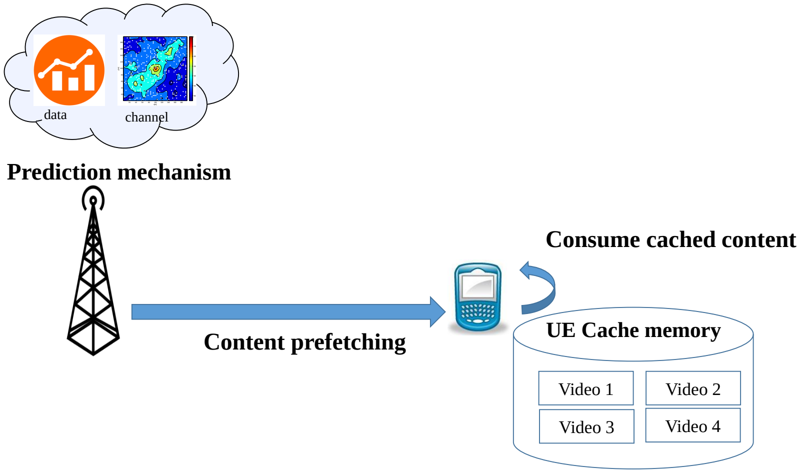


**Figure 5.3:** Content prefetching: the user content is pushed into the UE storage before its actual request. When the user requests for the content, the application directly pulls the data from the UE local memory rather than accessing it from the network provider.

prediction window $T$. The works [131, 151] studied content prefetching under the knowledge of user demand and channel statistics. While the work [131] developed optimal proactive policies under time-invariant and time-varying demand statistics, the work [151] included the predictable channel statistics of the users and studied its effect on the proactive scheduling. However, [151] assumes time-invariant channel statistics for the users. In the following, we give a brief case study on proactive content prefetching with the inclusion of time-varying channel statistics of the users and show its effect on the proactive scheduling. In Paper E, we develop stationary and cyclostationary asymptotically optimal proactive service policies based on demand and channel statistics.

## Case Study: Location-aware Content Prefetching (Paper E)

We consider a network equipped with a service provider (SP) and consisting of a set of $N$ users, $n \in \mathcal{N} = \{1, 2, \ldots, N\}$. The network operates on time slots basis indexed by $t$. We denote $g_{n,t} \in \mathbb{R}_+$ to capture the user experienced channel quality and $d_{n,t} \in \{0, 1\}$ to capture the data request generation at time $t$. The system is further described by the statistics of $d_{n,t}$ and $g_{n,t}$. In addition, we assume time-invariant demand statistics, i.e., $\mathbb{E}[d_{n,t}] = \bar{\pi}_n$, where $\pi_{n,t} = p(d_{n,t} = 1)$, and denote demand profile for all users $\bar{\boldsymbol{\pi}} = \{\bar{\pi}_1, \ldots, \bar{\pi}_N\}$. User demand requests cannot be delayed but can be serviced beforehand and $S$ amount of resources are utilized to serve the request. The channel gain $g_{n,t}$ is from a finite set $\mathcal{C}_n = \{g_n^{(k)}, k =$

$1, \ldots, K_n\}$ with statistics described by $\psi_{n,t} = \{\psi_{n,t}^{(k)}, k = 1, \ldots, K_n\}$. The channel is considered to be cyclo-stationary, so that the $\psi_{n,t}$ is periodic in $t$ with period $Q$, which is assumed to be the same for all users. Hence, the channel statistics of all users are determined by $\mathbf{\Psi}^Q = \{\mathcal{C}_n, \psi_{n,0}, \ldots, \psi_{n,Q-1}\}_{n=1}^N$. The time-invariant demand statistics and time-varying channel statistics model is shown in Fig. 5.4.

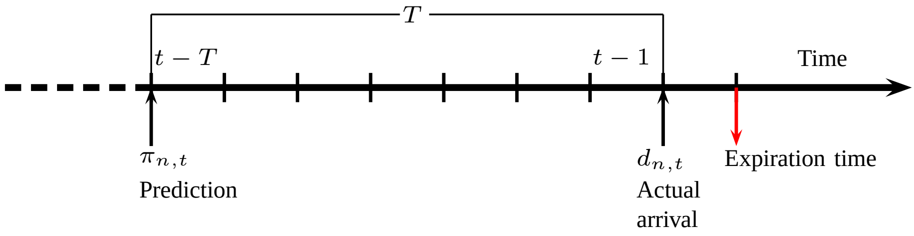


(a)

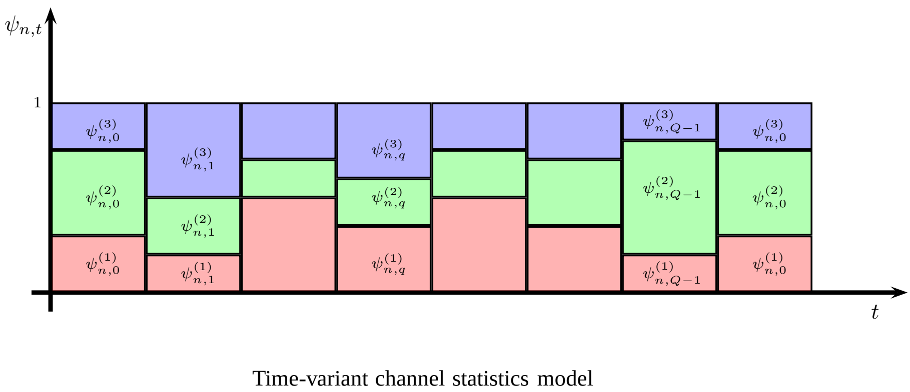


(b)

**Figure 5.4:** Inset (a): demand statistics model. A user request $d_{n,t}$ is proactively served $T$ (proactive service window) slots ahead, where $\pi_{n,t}$ is the probability of request $d_{n,t}$ being realized at time $t$. Inset (b): channel statistics model. Time-varying channel statistics, wherein channels exhibit a cyclo-stationarity behavior with period $Q$.

We denote the cost associated with load $L \geq 0$ as $C_d(L)$. The load $L$ is a function of the amount of service $S$ that is provided to each user $n$, as well as the channels $g_n$ for each user. In particular, $L = \sum_{n=1}^N L_n$, where

$$L_n = S\, C_c(g_n), \tag{5.1}$$

in which $C_c(g)$, $C_c : \mathbb{R}_+ \to \mathbb{R}_+$, is the channel cost function for utilizing the channel $g \geq 0$ in a time slot.

### Reactive network model

We consider a reactive network as the baseline scenario in which the requests are served upon their arrival. The load of a user $n$ in time slot $t$ for a reactive network under channel realization $g_{n,t}$, (5.1) is written as

$$L^{\mathcal{R}}_{n,t}(g_{n,t}) = S\, d_{n,t}\, C_c(g_{n,t}). \tag{5.2}$$

The time-averaged expected cost of all users under reactive operation is

$$c^{\mathcal{R}}(\bar{\boldsymbol{\pi}}, \boldsymbol{\Psi}^Q) = \limsup_{t\to\infty} \frac{1}{t} \sum_{l=0}^{t-1} \mathbb{E}\Big[C_d\Big(\sum_{n=1}^{N} L^{\mathcal{R}}_{n,t}(g_{n,t})\Big)\Big], \tag{5.3}$$

where expectation is over the demand and channel statistics of the users.

### Proactive network model

We assume the SP is aware of the demand $\bar{\boldsymbol{\pi}}$ and channel $\boldsymbol{\Psi}^Q$ profile of the users, and aims to spread out the load over the $T$ time-slot proactive service window. To this end, we denote by $u_{n,t}(\tau)$ the amount of *proactive service* applied to a user $n$ at time slot $t$ for a possible request $\tau$ slots in the future, i.e., at time $t+\tau$, where $1 \leq \tau \leq T$.[1] The proactive service at time $t-\tau$ for a future request at time $t$ cannot exceed the total demand of $S$ units of service, i.e., $\sum_{\tau=1}^{T} u_{n,t-\tau}(\tau) \leq S$ and the proactive service can never be negative, i.e., $u_{n,t}(\tau) \geq 0$. With the total proactive service at time $t$ denoted by $\mathbf{u}_{n,t} = [u_{n,t}(1), \ldots, u_{n,t}(T)]$, the load of user $n$ is written as

$$L^{\mathcal{P}}_{n,t}(\mathbf{u}_{n,t}, g_{n,t}) = \big((S - \sum_{\tau=1}^{T} u_{n,t-\tau}(\tau))d_{n,t} + \sum_{\tau=1}^{T} u_{n,t}(\tau)\big)C_c(g_{n,t}), \tag{5.4}$$

in which $\sum_{\tau=1}^{T} u_{n,t-\tau}(\tau)$ corresponds to the past applied proactive services for user $n$ and $\sum_{\tau=1}^{T} u_{n,t}(\tau)$ captures the proactive service to be applied at time $t$ for user $n$, over the next $T$ slots. The goal of the proactive controller is to determine the optimal online proactive service policy that minimizes the time averaged expected cost while delivering the content on time:

$$\min_{\{u_{n,t}(\tau)\}_{n,t,\tau}} \quad \limsup_{t\to\infty} \frac{1}{t} \sum_{t'=0}^{t-1} \mathbb{E}\Big[C_d\Big(\sum_{n=1}^{N} L^{\mathcal{P}}_{n,t'}(\mathbf{u}_{n,t'}, g_{n,t'})\Big)\Big] \tag{5.5a}$$

$$\text{s.t.} \quad \sum_{\tau=1}^{T} u_{n,t-\tau}(\tau) \leq S, \tag{5.5b}$$

$$u_{n,t}(\tau) \geq 0, \tag{5.5c}$$

[1] The notation of the proactive service $u_{n,t}(\tau)$ can best be understood with an example. Consider the case with $t=1$ and $\tau=2$, then $u_{n,1}(2)$ indicates the proactive service applied in time slot 1 for a future possible request in time slot 3, i.e., two slots ahead of the current time slot.

the optimal value of which is denoted by $c_T^{\mathcal{P}}(\bar{\boldsymbol{\pi}}, \boldsymbol{\Psi}^Q)$. In Paper E, we establish a global lower bound for the proactive scheduler and develop an optimal proactive service policy that approaches such a bound as the proactive service window size $T$ grows. Note that the reactive model is recovered when $u_{n,t}(\tau) \equiv 0$.

**Numerical results and discussion**

We consider $N = 2$ users and we set demand probability $\bar{\pi}_1 = 0.42$, $\bar{\pi}_2 = 0.42$. for this scenario in the system. For the time-varying channel statistics, we consider $Q = 14$ different channel state probability levels for each state. We consider two channel states and set $\{g_n^{(1)} = 0.5, g_n^{(2)} = 2\}$. We use channel probabilities of the channel state $g_n^{(1)}$ as (0.4,0.55,0.7,0.8,0.9,0.7,0.55,0.4,0.25,0.36,0.53,0.67,0.7,0.78). We compare the proactive scheduler for various proactive service window sizes ($T = 14, 168, 672$) against the reactive on-time service and the asymptotically optimal lower bound. We can observe in Fig. 5.5 (a), that the cost of the reactive service varies considerably with changing statistics over time. The reactive service does not possess the flexibility and has to offer service irrespective of the channel conditions. However, it can be observed that the average cost offered by the proactive scheduler is constant. This is due to the fact that the proactive scheduler exhibits flexibility in scheduling and shifts the loads based on the channel conditions. This can be seen in Fig. 5.5 (b) where the load for the proactive scheduler is less when the channel conditions are worse (i.e., channel time periods $q = 1, 2, 3, 4, 5$). It can be seen that the load curves of the proactive schemes look like upside down version of reactive load. Furthermore, the load and cost levels of the proactive scheduler approach to the corresponding asymptotically optimal limits with increase in $T$. For $T = 672$, the proactive scheduler load and cost approach to that of the asymptotically optimal (see Fig. 5.5)

## 5.4 Location-aware Long-term Predictive RA

In this section, we review the works on long-term predictive RA (see Fig. 5.6) that optimizes the radio resources to minimize the streaming interruptions by exploiting the users' future CQMs. A case study will be provided later for a media streaming application using the real channel measurements that are collected as part of a measurement campaign (see Section 2.2).

### Background

As video constitutes a major chunk of the load carried out by a BS, most of the works in the literature about media streaming concentrate on methods to enhance the user experience by providing an uninterrupted video streaming [19–22, 24, 26, 28, 132, 152, 153]. For uninterrupted video streaming, user terminals are equipped with a buffer which stores the data content that needs to be played. When the users move to places with low available data rates, this will degrade the video quality and video stalls occur as there is insufficient data available at the user

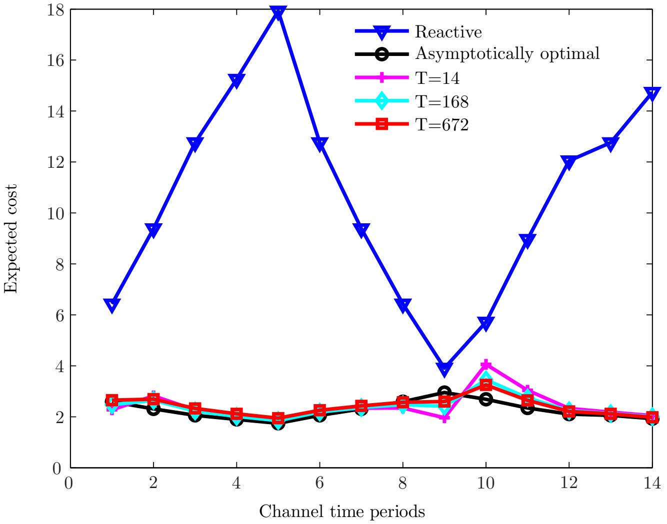


(a)

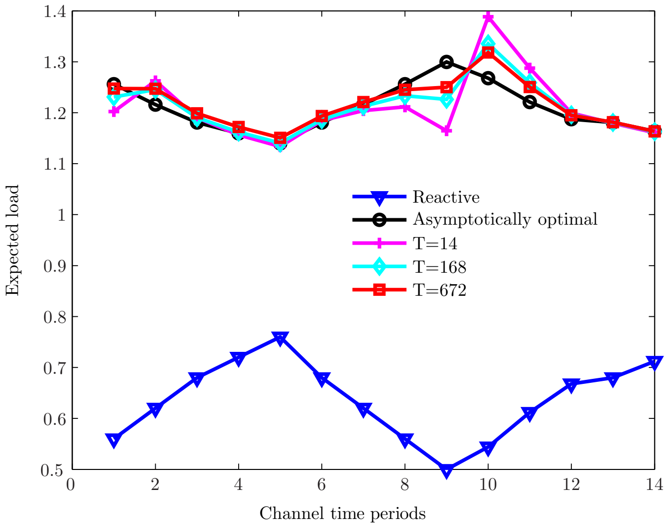


(b)

**Figure 5.5:** Inset (a): average cost levels under reactive and proactive services for time-varying channel statistics. Inset (b): average load levels under reactive and proactive services for time-varying channel statistics.

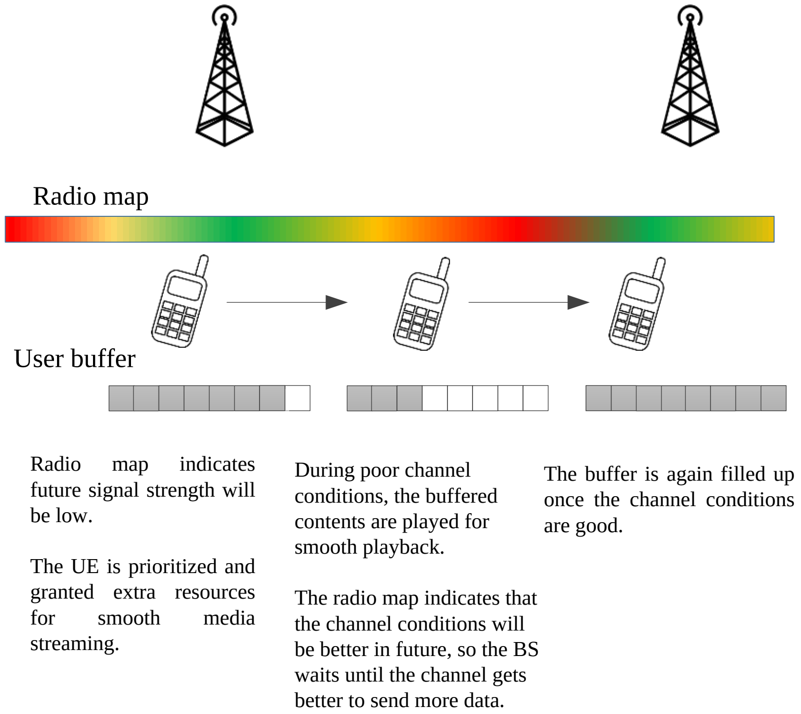


**Figure 5.6:** Long-term predictive RA optimizes the radio resources to minimize the streaming interruptions by exploiting the users future transmission rates. The BS exploits the users' peak channel conditions to fill up the user data buffer for streaming.

terminal to play due to buffer underruns. Therefore, a lot of research has been done on how to utilize the user mobility and to exploit the REMs. The methods perform long-term RA on the order of seconds to minutes.

Most of the works employ multi-user and multi-cell long-term RA strategies to overcome video quality degradation [19–21]. In [19], users' future transmission rates, based on REMs, are utilized for pre-allocation to fill up the user buffers. Usually, the rate predictions involve uncertainty and therefore the RA based on the predicted data rates will lead to buffer overruns (more data is downloaded than necessary) and buffer underruns (less data is downloaded than needed). Both cases should be avoided and it is the study of the work in [152]. The trade-off between BS power consumption and video quality degradation is studied in [28]. The power consumption can be reduced by half and video degradation can be improved up to 40% in comparison to traditional schemes when the BS exploits users future transmission rates and transmit more data when the user has better channel conditions. In [20,21], methods for long-term fairness in multi-cell networks are studied. When the users move from one cell to another cell, the rates that are allocated to users in the previous cell are not known to the next cell. Therefore, all the users are treated equally, although some users might have got good data rates when compared with some users who had low data rates. In [20], a proportional fair scheduling algorithm is proposed in which it keeps track of average rates received by each user while traversing the cells. A generic proportional fairness algorithm is proposed in [21] and different utility functions can be obtained based a single parameter.

An interesting study is done in [153], where they quantify the performance of current existing streaming algorithms when the bandwidth is known for the full video session. They report that existing methods only achieve 69%-86% of optimal quality and have proposed to incorporate both rate predictions as well as rate stability functions to improve the performance. Since the rate predictions involve uncertainty, [132] proposed a fuzzy based resource allocation for video streaming. A triangular fuzzy membership function is used to model the uncertainty of the REM measurements. In [24], an optimization problem is proposed to minimize both the network wide video degradation as well as each individual user video degradation. The algorithm tracks the users' allocated accumulated rates and then finds the users who will experience video degradation and then allocates the resources accordingly. The intuition of this allocation metric is to prioritize users with both a high current channel quality and a high future video degradation. Finally, in [26] a framework is implemented on a simulator using the rate predictions for LTE networks.

We have seen from the aforementioned works that users' future transmission rates can be exploited to minimize the video quality degradation experienced by the users when they are in bad channel conditions. In this section, we show a location-aware long-term predictive RA for media streaming application using the real channel data that is collected as part of the physical campaign by a smart phone (Section 2.2).

## Case Study: Location-aware long-term Predictive RA for Media Streaming [154]

We consider a network which consists of a set of $N$ users, $n \in \{1, 2, \dots, N\}$ and a set of $K$ BSs, $k \in \{1, 2, \dots K\}$. Time slots have a fixed duration of size $\tau$ and are indexed by $t$. We further assume that the users' video streams are available at the BS and are ready to be served to users. Let $U_{t,k}$ denote the set of users associated to BS $k$ at time $t$ and assume that it is known for all times. The received power at time $t$ at user $n$ is denoted by $P_{\mathrm{RX},t,n}$. We assume that the BSs know the received powers of the users for the next $T$ slots, known as the prediction window. Therefore, at time $t = 1$, the received powers $\{P_{\mathrm{RX},t,n}\}_{t=1,\dots T}^{n=1,\dots N}$ of all users are known for $T$ time slots in the future. The supported rate of user $n$ at time $t$ in bits/sec/Hz can be computed as

$$r_{t,n} = \tau\, B\, \log_2\left(1 + \frac{P_{\mathrm{RX},t,n}}{N_0 B}\right), \tag{5.6}$$

where $B$ is the bandwidth and $N_0$ is the noise power spectral density.

The rates of user $n$ at time $t = 1$ and for next $T$ slots are collected in $\mathbf{r}^{\mathrm{LA}}_{1,n} = [r_{t,n}]_{t=1}^{T}$ and $\mathbf{r}^{\mathrm{LA}} = [\mathbf{r}^{\mathrm{LA}}_{1,n}]_{n=1}^{N}$ holds the rates of all the users. The superscript stands for long term allocation. We further introduce $\mathbf{x}$, of same dimensionality as $\mathbf{r}$, with $x_{t,n} \in [0,1]$ denoting the fraction of airtime that user $n$ is assigned from a BS in time slot $t$. Hence, for an allocation $\mathbf{x}$, the predicted rate of user $n$ at time $t$ is given by $x_{t,n}\, r_{t,n}$.

All users request video content at time $t = 1$, with the same streaming rate $A$ (bps). Hence, the minimum video content available in the buffer of user $n$, expressed in bits, at each time slot $t$, required for smooth streaming is calculated to be $D_{t,n} = A\tau t$. For smooth playback, we require $\sum_{t'=1}^{t} x_{t',n} r^{\mathrm{LA}}_{t',n} \geq D_{t,n}$. We define the video degradation (VD) experienced by user $n$ at time $t$ as

$$\mathsf{deg}_{t,n}(\mathbf{x}) = \max\left(A\tau t - \sum_{t'=1}^{t} x_{t',n} r^{\mathrm{LA}}_{t',n}, 0\right). \tag{5.7}$$

### Resource Allocation and Performance Metrics

Our goal is to find $\mathbf{x}$ to provide good QoS to each user. To this end, we use three resource allocation methods: equal share and rate proportional are traditional resource allocation schemes, whereas PRA is a proactive resource allocation scheme which exploits the future channel knowledge. The performance of the methods are compared in terms of video degradation, power consumption and throughput of the network. First, the three resource allocation methods are described.

1. *Equal share:* each user gets the same amount of time in each time slot. This can be written as $x_{t,n} = \tau/T$.

2. *Rate proportional:* each user gets an amount of time in each time slot, proportional to its rate: $x_{t,n} = \tau/T \times r^{\mathrm{LA}}_{t,n}/(\sum_n r^{\mathrm{LA}}_{t,n})$.

3. *PRA:* the allocation accounts for the QoS of each user. For one formulation [28] of this, we have

$$\begin{aligned}
\text{min.} \quad & \sum_{n=1}^{N}\sum_{t=1}^{T}\left(\frac{1}{D_{\mathrm{tot}}}\mathsf{deg}_{t,n}(\mathbf{x}) + \frac{\lambda}{NT} x_{t,n}\right) && \text{(5.8a)}\\
\text{s.t.} \quad & \sum_{n \in U_{t,k}} x_{t,n} \leq 1, \forall t, k && \text{(5.8b)}\\
& \sum_{t'=1}^{t} x_{t',n} r^{\mathrm{LA}}_{t',n} \geq A\tau t, t \in \{1, \dots, T\}, && \text{(5.8c)}\\
& x_{t,n} \in [0,1], \forall t, n && \text{(5.8d)}
\end{aligned}$$

in which $\lambda$ is a trade-off parameter that indicates the importance of minimizing air time over video degradation. Both components of the objective are normalized, where $D_{\text{tot}} = NA\tau T(T+1)/2$ is the total cumulative demand. We note that (5.8) is a linear program, which can be solved efficiently.

Second, three performance metrics are considered, based on the solution $\mathbf{x}^*$ of (5.8), i.e., throughput, degradation, and power consumption. These are defined as follows:

- *Throughput*, defined as

$$\mathsf{throughput} = \sum_{n=1}^{N}\sum_{t=1}^{T} x^*_{t,n} r_{t,n}, \tag{5.9}$$

  in which $r_{t,n}$ is the actual rate supported by the channel (which may be different from the predicted rate, due to location errors).

- *Average video degradation*, defined as [28]

$$\mathsf{degradation} = \frac{1}{TN}\sum_{n=1}^{N}\sum_{t=1}^{T} \mathsf{deg}_{t,n}(\mathbf{x}^*). \tag{5.10}$$

- *Time-averaged BS power consumption*, defined as

$$P_{\text{avg}} = \frac{1}{T}\sum_{t=1}^{T}\sum_{k=1}^{K} \big(P_{\min} + (P_{\max} - P_{\min}) \sum_{n\in U_{t,k}} x^*_{t,n}\big) \tag{5.11}$$

  where we recall that $U_{t,k}$ is the set of users assigned to BS $k$ at time $t$. $P_{\min}$ and $P_{\max}$ are the power consumption under no load and under maximum load, respectively. Here $P_{\min}$ is set to zero, so that the degradation simplifies to

$$P_{\text{avg}} = \frac{1}{T}\sum_{t=1}^{T}\sum_{n=1}^{N} P_{\max} x^*_{t,n}. \tag{5.12}$$

  We set $P_{\max}$ to 1000 W. This yields a power consumption of $K \times 1000$ W if all $K$ BSs are transmitting during an entire time slot.

**Numerical results and discussion** We evaluate the performance of the three resource allocation methods using the data described in Section 2.2. We use the Pilbågsgatan-Läraregatan path for the evaluation. The average received power is used for the evaluation. Users are randomly placed along the path and they move independently with different user velocities for 35 seconds. The user velocities are drawn uniformly between 1 m/s and 10 m/s. To study the impact of location errors in the PRA method, we generate a uniformly distributed location error between 1 m and 10 m and shift the initial location of the user. The parameters used in the simulation are given in Table 5.1.

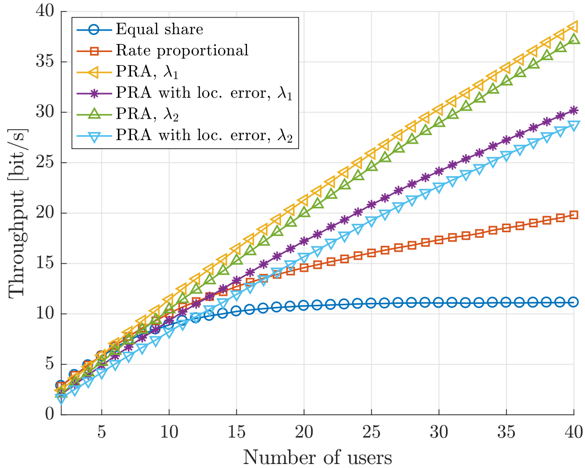


**Figure 5.7:** Throughput comparison as a function of the number of users for equal share, rate proportional and predictive resource allocation. For PRA, $\lambda_1 < \lambda_2$.

**Table 5.1:** Simulation parameters.

| Parameter | Value | Parameter | Value |
|---|---|---|---|
| $T$ | 35 sec. | $\lambda_1$ | 1.3 |
| $B$ | 1Hz | $\lambda_2$ | 2.5 |
| $A$ | 0.055 | $N_0$ | -80 dBm |

In Fig. 5.7, we show the throughput performance of the three resource allocation schemes with a varying number of users. We can clearly observe that PRA offers higher throughput, which grows approximately linearly with the number of users. However, for a fewer number of users, PRA offers similar throughput as equal share and rate proportional schemes, as the system is under-utilized. The throughput offered by the equal share scheme gets saturated after 15 users. The rate proportional scheme fares better than the equal share scheme, however the rate of increase of throughput decreases after 10 users. As expected, the location uncertainty degrades the performance of the PRA scheme, especially when there are more users.

Fig. 5.8 shows the average power consumption of the BS for the three resource allocation schemes. The PRA scheme uses less BS power for transmission compared to other schemes. This is due to the fact that PRA exploits future channel knowledge to satisfy user data demands. The equal share scheme consumes highest BS power and after 15 users it consumes the maximum available BS power. The power consumption of Rate proportional scheme is in between equal share and PRA schemes. The location uncertainty has a negligible impact on the power consumption for the PRA scheme.

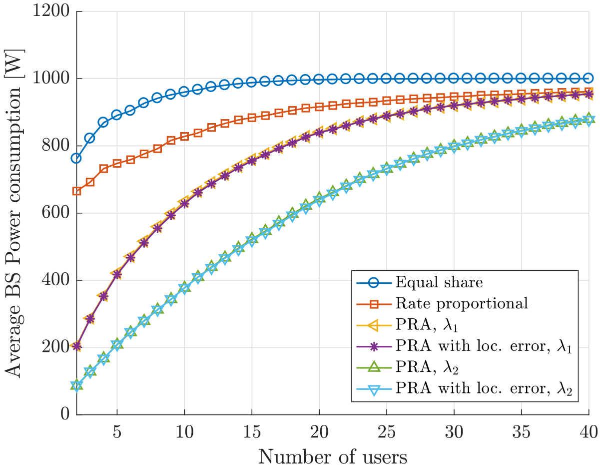


**Figure 5.8:** BS power consumption for different number of users for equal share, rate proportional and predictive resource allocation. For PRA, $\lambda_1 < \lambda_2$.

In Fig. 5.9, we depict the video degradation performance. In contrast to throughput and power consumption, PRA does not always offer the best performance. For a lower number of users, equal share and rate proportional schemes have lower video degradation. However, when the number of users is increased, both the schemes suffer and the video degradation increases very quickly. On the other hand, for a higher number of users, video degradation increases slowly for PRA scheme. When the system has a light load, PRA can obtain a lower objective function by reducing the airtime which translates to lower power consumption. Recall $\lambda$, which represents the trade-off between video degradation and power consumption. For the case with a maximum number of users (i.e., 40 users), we can see that PRA has a significant gain compared to other schemes while PRA with location error offers a somewhat reduced gain. Also for more number of users, there is not much difference between $\lambda_1$ and $\lambda_2$.

## 5.5 Summary

In this chapter, we focused on the role of location information for PRA. We first described the three basic ingredients necessary for PRA namely prediction of user demand, mobility, and channel. We then reviewed four proactive strategies where location information can be utilized for PRA. Specifically, we had provided two use cases where in location information is useful in the context of content prefetching and long-term predictive RA.

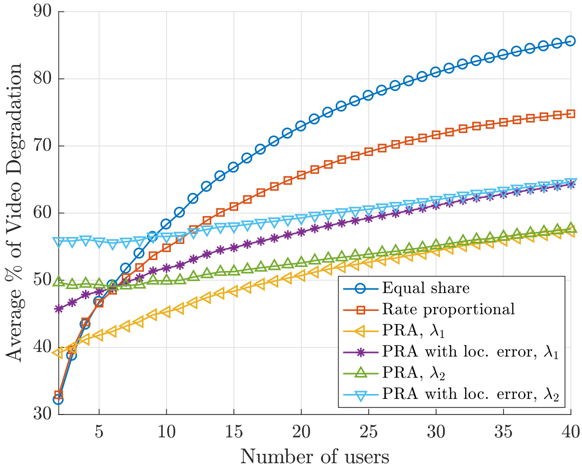


**Figure 5.9:** Video degradation comparison for varying number of users for equal share, rate proportional and predictive resource allocation. For PRA, $\lambda_1 < \lambda_2$.

# Chapter 6

# Contributions and Future Work

This chapter summarizes the contributions of the appended papers which fall under the category of location-aware communications.

## Paper A: "Location-aware Communications for 5G Networks"

5G networks will be the first generation to benefit from location information that is sufficiently precise to be leveraged in wireless network design and optimization. In this paper, we argue that location information can aid in addressing several of the key challenges in 5G, complementary to existing and planned technological developments. These challenges include an increase in traffic and number of devices, robustness for mission-critical services, and a reduction in total energy consumption and latency. We first present technologies providing seamless and ubiquitous location awareness for 5G devices, identify associated signal processing challenges, and describe at a high level how location information can be utilized across the protocol stack. We then zoom in on each layer of the protocol stack, and provide an overview of recent and relevant research on location-aware communications. We conclude the paper by identifying a number of issues and research challenges that must be addressed before 5G technologies can successfully utilize location information and achieve the predicted performance gains.

## Paper B: "Spatial Wireless Channel Prediction under Location Uncertainty"

In this paper, we develop a spatial wireless channel prediction framework incorporating the location uncertainty of the terminals. We show that not considering location uncertainty leads to poor learning of the channel parameters and poor prediction of CQM values at other locations, especially when location uncertainties are heterogeneous. We investigate two channel prediction frameworks, classical Gaussian processes (cGP) and uncertain Gaussian processes (uGP), and analyze the impact of location uncertainty during learning/training and prediction/testing, for scenarios where measurements uncertainty are dominated by large-scale fading. We observe that cGP generally fails both in terms of learning the channel parameters and in predicting the channel in the presence of location uncertainties. In contrast, uGP explicitly considers the location uncertainty. Using simulated data, we show that uGP is able to learn and predict the wireless channel. We also demonstrate the use of the proposed framework for a spatial resource allocation application.

## Paper C: "Channel Gain Prediction for Multi-agent Networks in the Presence of Location Uncertainty"

The channel prediction framework in Paper B is mainly for cellular networks. In this paper, we extend the channel prediction framework for ad-hoc networks. We present a GP framework to learn channel parameters and predict the channel between arbitrary transmitter and receiver locations. We explicitly incorporate location uncertainty in both learning and prediction phases. Our framework is able to deal with channel measurements recorded at uncertain locations and to incorporate this location uncertainty into the predictive distribution of the wireless channel at a given (possibly uncertain) test location.

## Paper D: "Location-aided Pilot Contamination Avoidance for Massive MIMO Systems"

In this paper, we exploit location for a reactive resource allocation in massive MIMO systems. One of the key limitations of massive MIMO systems is pilot contamination, which is defined as the interference during uplink channel estimation due to reusing the same pilot sequences in surrounding cells. We propose a location-based approach to mitigating the pilot contamination problem for uplink MIMO systems. Our approach makes use of the approximate locations of mobile devices to provide good estimates of the channel statistics between the mobile devices and their corresponding BSs. Specifically, we aim at avoiding pilot contamination even when the number of BS antennas is not very large, and when multiple users from different cells, or even in the same cell, are assigned the same pilot sequence. First, we characterize a desired angular region of the target user at the serving BS based on the number of BS antennas and the location of the target user, and make the observation that in this region the interference is close to zero due to the spatial separability. Second, based on this observation, we propose pilot coordination methods for multi-user multi-cell scenarios to avoid pilot contamination. In particular, we propose multi-cell multi-user joint optimization problems such that it takes into consideration during the pilot assignment the mutual interference seen by the target users at their respective BSs. We also propose a heuristic approach for assigning users to BSs to decrease the computational complexity of the proposed joint optimization schemes. We show proposed pilot assignment strategies offer improved channel estimation performance as well as enhanced downlink sum rate even when the number of antennas is finite.

## Paper E: "Proactive Resource Allocation with Predictable Channel Statistics"

In this paper, we utilize location information for proactive resource allocation. This work falls in the category of location-aware content prefetching. Since the data demand patterns and channel qualities of mobile users along their navigation paths are largely predictable, this work aims at fusing the statistically predictable demand and channel patterns in devising proactive resource allocation strategies that alleviate network congestion. Specifically, we establish global lower bounds on the proactive scheduling cost that capture the impact of demand and channel uncertainties. Driven by insights from the obtained lower bounds, we develop stationary and cyclostationary asymptotically optimal proactive service policies that approach such bounds as proactive service window size grows. We demonstrate the designed proactive schedulers offer better performance in terms of cost and load, in contrast to a baseline reactive scheduler.

## Paper F: "LAPRA: Location-aware Proactive Resource Allocation"

In this paper, we show another application of location information for proactive resource allocation. We treat a very specific use case of large crowded areas (airports, conferences), where networks get congested and users may suffer from poor QoS. To mitigate this, we propose and evaluate a location-aware user-centric proactive resource allocation approach (LAPRA), in which the users are proactive and seek good channel quality by moving to locations where the signal quality is good. In particular, we evaluate a spatial user-in-the-loop resource allocation method that utilizes GP for channel prediction by exploiting user location information. We formulate a decentralized binary integer optimization problem for the user assignment. Each user decides where to move by solving an optimization problem. We analyze the performance of the proposed method, compared to a network-centric reactive approach and baseline network-centric proactive approach. We show that our proposed method improves the number of satisfied users and the overall network throughput.

# Future work

- An important challenge which is not covered in this thesis is to identify the right tradeoff between relying on location-based information and on pilot-based CQM information.

- In PaperB, we mentioned one of the drawbacks for GPs is its computational complexity. It is worth studying the sparse approximations as well as online learning of GPs along with location uncertainty.

- In Paper D, we formulated several centralized pilot assignment schemes to address the pilot contamination issue in massive MIMO. It would be interesting to focus on developing distributed implementations based on local information. Distributed implementations for pilot contamination avoidance under a game theoretic framework have been proposed using coalition games [49] and non-cooperative games [27]. However, none of the aforementioned approaches exploits the location information.

- In Paper E, we have studied optimal proactive policies under the time-varying channel statistics keeping the demand statistics being time-invariant. However, it would be interesting to extend the case to time-varying demand and channel statistics case. In that case, one should develop optimal proactive policies that run on a more longer time periods such on a day basis.

- In Paper F, we have considered the availability of perfect location information during channel prediction for the LAPRA scheme. The analysis of uncertain location information is left as future work. Furthermore, tools from game theory can be utilized to study the behaviour of the users for the proactive schemes.

# References


[1] H. Celebi and H. Arslan, "Utilization of location information in cognitive wireless networks," *IEEE Wireless Commun.*, vol. 14, no. 4, pp. 6–13, 2007.

[2] Y. Zhao, L. Morales, J. Gaeddert, K. K. Bae, J.-S. Um, and J. H. Reed, "Applying radio environment maps to cognitive wireless regional area networks," in *2nd IEEE International Symposium on New Frontiers in Dynamic Spectrum Access Networks*, 2007, pp. 115–118.

[3] A. Zalonis, N. Dimitriou, A. Polydoros, J. Nasreddine, and P. Mahonen, "Femtocell downlink power control based on radio environment maps," in *IEEE Wireless Communications and Networking Conference (WCNC)*, 2012, pp. 1224–1228.

[4] A. Galindo-Serrano, B. Sayrac, S. Ben Jemaa, J. Riihijarvi, and P. Mahonen, "Harvesting MDT data: Radio environment maps for coverage analysis in cellular networks," in *8th International Conference on Cognitive Radio Oriented Wireless Networks (CROWNCOM)*, 2013, pp. 37–42.

[5] J. Li and Y. Zhao, "Radio environment map-based cognitive doppler spread compensation algorithms for high-speed rail broadband mobile communications," *EURASIP Journal on Wireless Communications and Networking*, vol. 2012, no. 1, pp. 1–18, 2012.

[6] A. Dammann, G. Agapiou, J. Bastos, L. Brunel, M. García, J. Guillet, Y. Ma, J. Ma, J. J. Nielsen, L. Ping, R. Raulefs, J. Rodriguez, D. Slock, D. Yang, and N. Yi, "WHERE2 location aided communications," in *Proc. European Wireless Conf*, Apr. 2013.

[7] S. Sand, R. Tanbourgi, C. Mensing, and R. Raulefs, "Position aware adaptive communication systems," in *Forty-Third Asilomar Conference on Signals, Systems and Computers*, 2009, pp. 73–77.

[8] A. Osseiran, F. Boccardi, V. Braun, K. Kusume, P. Marsch, M. Maternia, O. Queseth, M. Schellmann, H. Schotten, H. Taoka, "Scenarios for 5G mobile and wireless communications: the vision of the METIS project," *IEEE Communications Magazine*, vol. 52, no. 5, pp. 26–35, 2014.

[9] R. Di Taranto, S. Muppirisetty, R. Raulefs, D. Slock, T. Svensson, and H. Wymeersch, "Location-Aware Communications for 5G Networks: How location information can improve scalability, latency, and robustness of 5G," *IEEE Signal Processing Magazine*, vol. 31, no. 6, pp. 102–112, Nov 2014.

[10] M. Z. Win, A. Conti, S. Mazuelas, Y. Shen, W. M. Gifford, D. Dardari, and M. Chiani, "Network localization and navigation via cooperation," *IEEE Communications Magazine*, vol. 49, no. 5, pp. 56–62, 2011.

[11] M. de Reuver, D. Skournetou, and E.-S. Lohan, "Impact of Galileo commercial service on location-based service providers: business model analysis and policy implications," *Journal of Location Based Services*, vol. 7, no. 2, pp. 67–78, 2013.

[12] M. Koivisto, A. Hakkarainen, M. Costa, P. Kela, K. Leppanen, and M. Valkama, "High-efficiency device positioning and location-aware communications in dense 5G networks," *IEEE Communications Magazine*, 2017.

[13] J. Johansson, W. Hapsari, S. Kelley, and G. Bodog, "Minimization of drive tests in 3GPP release 11," *IEEE Communications Magazine*, vol. 50, no. 11, pp. 36–43, 2012.

[14] M. S. Grewal, L. R. Weill, and A. P. Andrews, *Global positioning systems, inertial navigation, and integration.* John Wiley & Sons, 2001.

[15] Z. Sahinoglu, S. Gezici, and I. Guvenc, *Ultra-wideband positioning systems.* Cambridge university press, Cambridge, UK, 2008, vol. 2.

[16] E. Bastug, M. Bennis, and M. Debbah, "Living on the edge: The role of proactive caching in 5G wireless networks," *IEEE Communications Magazine*, vol. 52, no. 8, pp. 82–89, Aug 2014.

[17] E. Bastug, J.-L. Guénégo, and M. Debbah, "Proactive small cell networks," in *20th International Conference on Telecommunications (ICT)*, 2013, pp. 1–5.

[18] E. Bastug, M. Bennis, and M. Debbah, "Think before reacting: Proactive caching in 5G small cell networks," *Towards 5G: Applications, Requirements and Candidate Technologies, Wiley(Submitted)*, 2014.

[19] H. Abou-zeid, H. Hassanein, and S. Valentin, "Optimal predictive resource allocation: Exploiting mobility patterns and radio maps," in *Proc. IEEE Global Telecommunications Conference (GLOBECOM)*, 2013, pp. 4714–4719.

[20] H. Abou-zeid, S. Valentin, and H. S. Hassanein, "Long-term proportional fairness over multiple cells," in *37th Conference on Local Computer Networks Workshops (LCN Workshops)*, 2012, pp. 807–813.

[21] H. Abou-zeid, H. S. Hassanein, and N. Zorba, "Long-term fairness in multi-cell networks using rate predictions," in *GCC Conference and Exhibition*, 2013, pp. 131–135.

[22] H. Abou-Zeid and H. S. Hassanein, "Predictive green wireless access: Exploiting mobility and application information," *IEEE Wireless Communications*, vol. 20, no. 5, pp. 92–99, 2013.

[23] H. Abou-zeid, H. S. Hassanein, and S. Valentin, "Energy-efficient adaptive video transmission: Exploiting rate predictions in wireless networks," *IEEE Transactions on Vehicular Technology*, vol. 63, no. 5, pp. 2013–2026, 2014.

[24] H. Abou-zeid, H. S. Hassanein, and N. Zorba, "Enhancing mobile video streaming by lookahead rate allocation in wireless networks," in *11th Consumer Communications and Networking Conference (CCNC)*, 2014, pp. 471–476.

[25] H. Abou-Zeid and H. Hassanein, "Toward green media delivery: location-aware opportunities and approaches," *IEEE Wireless Communications*, vol. 21, no. 4, pp. 38–46, 2014.

[26] H. Abou-zeid, H. S. Hassanein, and R. Atawia, "Towards mobility-aware predictive radio access: Modeling; simulation; and evaluation in LTE networks," in *17th ACM international conference on Modeling, analysis and simulation of wireless and mobile systems*, 2014, pp. 109–116.

[27] H. Abou-zeid, H. S. Hassanein, Z. Tanveer, and N. AbuAli, "Evaluating mobile signal and location predictability along public transportation routes," in *IEEE Wireless Communications and Networking Conference (WCNC)*, 2015, pp. 1195–1200.

[28] H. Abouzeid and H. S. Hassanein, "Efficient lookahead resource allocation for stored video delivery in multi-cell networks," in *IEEE Wireless Communications and Networking Conference (WCNC)*, 2014, pp. 1909–1914.

[29] A. Goldsmith, *Wireless communications.* Cambridge university press, 2005.

[30] T. S. Rappaport, *Wireless communications: principles and practice.* prentice hall PTR New Jersey, 1996, vol. 2.

[31] G. L. Stüber, *Principles of mobile communication.* Springer, 2001, vol. 2.

[32] D. Tse and P. Viswanath, *Fundamentals of wireless communication.* Cambridge university press, 2005.

[33] A. F. Molisch, *Wireless communications.* John Wiley & Sons, 2012, vol. 34.

[34] S. S. Szyszkowicz, H. Yanikomeroglu, and J. S. Thompson, "On the feasibility of wireless shadowing correlation models," *IEEE Transactions on Vehicular Technology*, vol. 59, no. 9, pp. 4222–4236, 2010.

[35] M. Gudmundson, "Correlation model for shadow fading in mobile radio systems," *Electronics letters*, vol. 27, no. 23, pp. 2145–2146, 1991.

[36] S. Ahmad, *Predictive resource allocation based on real channel measurements.* Department of Signals and Systems, Communication Systems, Chalmers University of Technology,, 2016.

[37] J. Fink, "Communication for teams of networked robots," Ph.D. dissertation, Elect. Syst. Eng., Univ. Pennsylvania, Philadelphia, PA, Aug 2011.

[38] M. Neiman, "The principle of reciprocity in antenna theory," *Proceedings of the IRE*, vol. 31, no. 12, pp. 666–671, 1943.

[39] Z. Li, R. Wang, and A. F. Molisch, “Shadowing in urban environments with microcellular or peer-to-peer links,” in *6th European Conference on Antennas and Propagation (EUCAP)*, 2012, pp. 44–48.

[40] Z. Wang, E. K. Tameh, and A. R. Nix, “Joint shadowing process in urban peer-to-peer radio channels,” *IEEE Transactions on Vehicular Technology*, vol. 57, no. 1, pp. 52–64, 2008.

[41] P. Agrawal and N. Patwari, “Correlated link shadow fading in multi-hop wireless networks,” *IEEE Transactions on Wireless Communications*, vol. 8, no. 8, pp. 4024–4036, 2009.

[42] N. Patwari and P. Agrawal, “Effects of correlated shadowing: Connectivity, localization, and RF tomography,” in *International Conference on Information Processing in Sensor Networks*, 2008, pp. 82–93.

[43] M. Fröhle, *Channel Gain Prediction for Cooperative Multi-Agent Systems.* Department of Signals and Systems, Communication Systems, Chalmers University of Technology,, 2016.

[44] M. Fröhle, T. Charalambous, I. Nevat, and H. Wymeersch, “Channel prediction with location uncertainty for ad-hoc networks,” *IEEE Transactions on Signal and Information Processing over Networks*, vol. PP, no. 99, pp. 1–1, 2017.

[45] C. Rasmussen and C. Williams, *Gaussian processes for machine learning.* MIT Press, 2006.

[46] L. S. Muppirisetty, “Wireless channel prediction with location uncertainty,” Department of Signals and Systems, Communication Systems, Chalmers University of Technology, 2014.

[47] J. Quiñonero-Candela and C. E. Rasmussen, “A unifying view of sparse approximate Gaussian process regression,” *The Journal of Machine Learning Research*, vol. 6, pp. 1939–1959, 2005.

[48] L. Csató and M. Opper, “Sparse on-line Gaussian processes,” *Neural computation*, vol. 14, no. 3, pp. 641–668, 2002.

[49] E. Snelson and Z. Ghahramani, “Sparse Gaussian processes using pseudo-inputs,” *Advances in neural information processing systems*, vol. 18, p. 1257, 2006.

[50] S. Sarkka, A. Solin, and J. Hartikainen, “Spatiotemporal learning via infinite-dimensional bayesian filtering and smoothing: A look at Gaussian process regression through Kalman filtering,” *IEEE Signal Processing Magazine*, vol. 30, no. 4, pp. 51–61, 2013.

[51] P. Dallaire, C. Besse, and B. Chaib-draa, "An approximate inference with Gaussian process to latent functions from uncertain data," *Neurocomputing*, vol. 74, no. 11, pp. 1945–1955, 2011.

[52] A. Girard, "Approximate methods for propagation of uncertainty with Gaussian process models," Ph.D. dissertation, University of Glasgow, 2004.

[53] A. McHutchon and C. E. Rasmussen, "Gaussian process training with input noise," in *Advances in Neural Information Processing Systems*, 2011, pp. 1341–1349.

[54] A. Girard and R. Murray-Smith, "Learning a Gaussian process model with uncertain inputs," 2003.

[55] F. Boccardi, R. W. Heath, A. Lozano, T. L. Marzetta, and P. Popovski, "Five disruptive technology directions for 5G," *IEEE Communications Magazine*, vol. 52, no. 2, pp. 74–80, Feb 2014.

[56] J. K. Cross and P. J. Lardieri, "Proactive and reactive resource allocation," in *Proc. 9th Conf. Pattern Languages of Programming (PLOP 02)*, 2002.

[57] J. Hoydis, S. Ten Brink, and M. Debbah, "Massive MIMO in the UL/DL of cellular networks: How many antennas do we need?" *IEEE Journal on Selected Areas in Communications*, vol. 31, no. 2, pp. 160–171, 2013.

[58] S. Habib, "Novel insights for smart cell search in millimeter wave cellular networks," Ph.D. dissertation, Department of Electrical Engineering, National University of Sciences and Technology, 2017.

[59] D. Marabissi and R. Fantacci, *Cognitive Interference Management in Heterogeneous Networks.* Springer, 2015.

[60] M. N. Tehrani, M. Uysal, and H. Yanikomeroglu, "Device-to-device communication in 5G cellular networks: challenges, solutions, and future directions," *IEEE Communications Magazine*, vol. 52, no. 5, pp. 86–92, 2014.

[61] G. Fodor, E. Dahlman, G. Mildh, S. Parkvall, N. Reider, G. Miklós, and Z. Turányi, "Design aspects of network assisted device-to-device communications," *IEEE Communications Magazine*, vol. 50, no. 3, 2012.

[62] M.-t. Sun, L. Huang, S. Wang, A. Arora, and T.-H. Lai, "Reliable MAC layer multicast in ieee 802.11 wireless networks," *Wireless Communications and Mobile Computing*, vol. 3, no. 4, pp. 439–453, 2003.

[63] N. Wen and R. Berry, "Information propagation for location-based MAC protocols in vehicular networks," in *40th Annual Conference on Information Sciences and Systems*, 2006, pp. 1242–1247.

[64] S. B. Kodeswaran and A. Joshi, "Using location information for scheduling in 802.15.3 MAC." in *2nd International Conference on Broadband Networks*, 2005, pp. 718–725.

[65] A. Dammann, J. Bastos, L. Brunel, M. García, J. Guillet, J. Ma, J. J. Nielsen, L. Ping, R. Raulefs, J. Rodriguez, D. Slock, D. Yang, and S. Zazo, "Location aided wireless communications," *IEEE Commun. Mag., submitted Nov. 2013.*

[66] S. Katragadda, C. Ganesh Murthy, R. Rao, S. Mohan Kumar, and R. Sachin, "A decentralized location-based channel access protocol for inter-vehicle communication," in *IEEE Vehicular Technology Conference-Spring*, vol. 3, 2003, pp. 1831–1835.

[67] Y.-B. Ko and N. H. Vaidya, "Geocasting in mobile ad hoc networks: Location-based multicast algorithms," in *Second IEEE Workshop on Mobile Computing Systems and Applications*, 1999, pp. 101–110.

[68] P. Djukic and S. Valaee, "Link scheduling for minimum delay in spatial re-use TDMA," *INFOCOM*, pp. 28–36, 2007.

[69] R. Nelson and L. Kleinrock, "Spatial TDMA: A collision free multihop channel access protocol," *IEEE Transactions on Communications*, vol. 33, no. 9, pp. 934–944, Sep 1985.

[70] L. Muppirisetty, R. Di Taranto, and H. Wymeersch, "Robust link scheduling with channel estimation and location information," in *Forty-Seventh Asilomar Conference on Signals, Systems and Computers*, 2013.

[71] K. Papadaki and V. Friderikos, "Robust scheduling in spatial reuse TDMA wireless networks," *IEEE Transactions on Wireless Communication*, vol. 7, no. 12, pp. 4767–4771, 2008.

[72] J. J. Nielsen, "Location based network optimizations for mobile wireless networks — a study of the impact of mobility and inaccurate information," Ph.D. dissertation, Aalborg University, Mar 2011.

[73] F. Cadger, K. Curran, J. Santos, and S. Moffett, "A survey of geographical routing in wireless ad-hoc networks," *IEEE Communications Surveys & Tutorials*, vol. 15, no. 2, 2013.

[74] A. Popescu, N. Salman, and A. Kemp, "Geographic routing resilient to location errors," *IEEE Wireless Communicaiton Letters*, vol. 2, no. 2, 2013.

[75] R. Di Taranto and H. Wymeersch, "Simultaneous routing and power allocation using location information," in *Forty-Seventh Asilomar Conference on Signals, Systems and Computers*, 2013.

[76] M. J. Neely, E. Modiano, and C. E. Rohrs, "Dynamic power allocation and routing for time-varying wireless networks," *IEEE Journal on Selected Areas in Communications*, vol. 23, no. 1, pp. 89–103, 2005.

[77] W. Su, S.-J. Lee, and M. Gerla, "Mobility prediction and routing in ad hoc wireless networks," *International Journal of Network Management*, vol. 11, no. 1, pp. 3–30, 2001.

[78] K.-T. Feng, C.-H. Hsu, and T.-E. Lu, "Velocity-assisted predictive mobility and location-aware routing protocols for mobile Ad Hoc Networks," *IEEE Transactions on Vehicular Technology*, vol. 57, no. 1, pp. 448–464, 2008.

[79] Y.-G. Lim, C.-B. Chae, and G. Caire, "Performance analysis of massive MIMO for cell-boundary users," *IEEE Transactions on Wireless Communications*, vol. 14, no. 12, pp. 6827–6842, Dec 2015.

[80] E. G. Larsson, O. Edfors, F. Tufvesson, and T. L. Marzetta, "Massive MIMO for next generation wireless systems," *IEEE Communications Magazine*, vol. 52, no. 2, pp. 186–195, Feb 2014.

[81] F. Rusek, D. Persson, B. K. Lau, E. G. Larsson, T. L. Marzetta, O. Edfors, and F. Tufvesson, "Scaling up MIMO: Opportunities and challenges with very large arrays," *IEEE Signal Processing Magazine*, vol. 30, no. 1, pp. 40–60, Jan 2013.

[82] E. Bjornson, E. G. Larsson, and M. Debbah, "Optimizing multi-cell massive MIMO for spectral efficiency: How many users should be scheduled?" in *Proc. IEEE Global Conference on Signal and Information Processing*, Dec 2014, pp. 612–616.

[83] T. L. Marzetta, "Noncooperative cellular wireless with unlimited numbers of base station antennas," *IEEE Transactions on Wireless Communications*, vol. 9, no. 11, pp. 3590–3600, Nov 2010.

[84] A. Osseiran, J. F. Monserrat, and P. Marsch, N. Rajatheva, S. Suyama, W. Zirwas, L. Thiele, G. Fodor, A. Tolli, E. D. Carvalho, and J. H. Sorensen, *5G Mobile and Wireless Communications Technology.* Cambrdige University Press, 2016, no. ISBN 9781107130098.

[85] O. Elijah, C. Y. Leow, T. A. Rahman, S. Nunoo, and S. Z. Iliya, "A comprehensive survey of pilot contamination in massive MIMO-5G system," *IEEE Communications Surveys &Tutorials*, vol. 18, no. 2, pp. 905–923, 2016.

[86] F. Fernandes, A. Ashikhmin, and T. L. Marzetta, "Inter-cell interference in noncooperative TDD large scale antenna systems," *IEEE Journal on Selected Areas in Communications*, vol. 31, no. 2, pp. 192–201, 2013.

[87] K. Appaiah, A. Ashikhmin, and T. L. Marzetta, "Pilot contamination reduction in multi-user TDD systems," in *Proc. IEEE International Conference on Communications*, May 2010.

[88] W. A. W. M. Mahyiddin, P. A. Martin, and P. J. Smith, "Pilot contamination reduction using time-shifted pilots in finite massive MIMO systems," in *Proc. IEEE Vehicular Technology Conference (Fall)*, Sep 2014.

[89] T. X. Vu, T. A. Vu, and T. Q. S. Quek, "Successive pilot contamination elimination in multiantenna multicell networks," *IEEE Wireless Communications Letters*, vol. 3, no. 6, pp. 617–620, Dec 2014.

[90] J. Zhang, B. Zhang, S. Chen, X. Mu, M. El-Hajjar, and L. Hanzo, “Pilot Contamination Elimination for Large-Scale Multiple-Antenna Aided OFDM Systems,” *IEEE Journal of Selected Topics in Signal Processing*, vol. 8, no. 5, pp. 759–772, Oct 2014.

[91] H. Yin, D. Gesbert, M. C. Filippou, and Y. Liu, “Decontaminating pilots in massive MIMO systems,” in *IEEE International Conference on Communications (ICC)*, 2013, pp. 3170–3175.

[92] M. Filippou, D. Gesbert, and H. Yin, “Decontaminating pilots in cognitive massive MIMO networks,” in *International Symposium on Wireless Communication Systems (ISWCS)*, 2012, pp. 816–820.

[93] H. Yin, D. Gesbert, M. Filippou, and Y. Liu, “A coordinated approach to channel estimation in large-scale multiple-antenna systems,” *IEEE Journal on Selected Areas in Communications*, vol. 31, no. 2, pp. 264–273, Feb 2013.

[94] R. R. Mueller, M. Vehkaperae, and L. Cottatellucci, “Blind pilot decontamination,” in *17th International ITG Workshop on Smart Antennas*, Mar 2013, pp. 1–6.

[95] R. R. Muller, M. Vehkapera, and L. Cottatellucci, “Analysis of blind pilot decontamination,” in *Asilomar Conference on Signals Systems and Computers*, 2013, pp. 1016–1020.

[96] L. Cottatellucci, R. R. Muller, and M. Vehkapera, “Analysis of pilot decontamination based on power control,” in *77th Vehicular Technology Conference (VTC Spring)*, 2013, pp. 1–5.

[97] H. Q. Ngo and E. G. Larsson, “EVD-based channel estimation in multicell multiuser MIMO systems with very large antenna arrays,” in *Proc. IEEE International Conference on Acoustics, Speech and Signal Processing*, Mar 2012, pp. 3249–3252.

[98] L. You, X. Gao, X.-G. Xia, N. Ma, and Y. Peng, “Pilot reuse for massive MIMO transmission over spatially correlated Rayleigh fading channels,” *IEEE Transactions on Wireless Communications*, vol. 14, no. 6, pp. 3352–3366, 2015.

[99] A. Adhikary, J. Nam, J.-Y. Ahn, and G. Caire, “Joint spatial division and multiplexing: The large-scale array regime,” *IEEE Transactions on Information Theory*, vol. 59, no. 10, pp. 6441–6463, Oct 2013.

[100] Z. Wang, C. Qian, L. Dai, J. Chen, C. Sun, and S. Chen, “Location-based channel estimation and pilot assignment for massive MIMO systems,” in *IEEE International Conference on Communication Workshop (ICCW)*, June 2015, pp. 1264–1268.

[101] P. Zhao, Z. Wang, C. Qian, L. Dai, and S. Chen, "Location-aware pilot assignment for massive MIMO systems in heterogeneous networks," *IEEE Transactions on Vehicular Technology*, vol. 65, no. 8, pp. 6815–6821, Aug 2016.

[102] N. Akbar, S. Yan, N. Yang, and J. Yuan, "Mitigating pilot contamination through location-aware pilot assignment in massive MIMO networks," in *IEEE Globecom Workshops (GC Wkshps)*, Dec 2016, pp. 1–6.

[103] L. S. Muppirisetty, H. Wymeersch, J. Karout, and G. Fodor, "Location-aided pilot contamination elimination for massive MIMO systems," in *Proc. IEEE Global Communications Conference*, Dec 2015.

[104] D. S. Shiu, G. Foschini, M. J. Gans, and J. M. Kahn, "Fading correlation and its effect on the capacity of multi element antenna systems," *IEEE Transactions on Communications*, vol. 48, no. 3, pp. 502–513, March 2000.

[105] A. Abdi and M. Kaveh, "A space-time correlation model for multi element antenna systems in mobile fading channels," *IEEE Journal on Selected Areas in Communications*, vol. 20, no. 3, pp. 550–560, April 2002.

[106] C. Oestges, B. Clerckx, D. Vanhoenacker-Janvier, and A. J. Paulraj, "Impact of diagonal correlations on MIMO capacity: Application to geometrical scattering models," in *Proc. 58th IEEE Vehicle Technology Conference*, vol. 1, October 2003, pp. 394–398.

[107] C. Oestges and A. J. Paulraj, "Beneficial impact of channel correlations on MIMO capacity," *IEEE Electronics Letters*, vol. 40, no. 10, May 2004.

[108] M. Zhang, P. J. Smith, and M. Shafi, "An extended one-ring MIMO channel model," *IEEE Transactions on Wireless Communications*, vol. 6, no. 8, pp. 2759–2764, August 2007.

[109] T. S. Rappaport, S. Sun, R. Mayzus, H. Zhao, Y. Azar, K. Wang, G. N. Wong, J. K. Schulz, M. Samimi, and F. Gutierrez, "Millimeter wave mobile communications for 5G cellular: It will work!" *IEEE access*, vol. 1, pp. 335–349, 2013.

[110] L. Wei, R. Q. Hu, Y. Qian, and G. Wu, "Key elements to enable millimeter wave communications for 5G wireless systems," *IEEE Wireless Communications*, vol. 21, no. 6, pp. 136–143, 2014.

[111] Y. Niu, Y. Li, D. Jin, L. Su, and A. V. Vasilakos, "A survey of millimeter wave communications (mmwave) for 5G: opportunities and challenges," *Wireless Networks*, vol. 21, no. 8, pp. 2657–2676, 2015.

[112] H. Guo, B. Makki, and T. Svensson, "A genetic algorithm-based beamforming approach for delay-constrained networks, " *15th International Symposium on Modeling and Optimization in Mobile, Ad Hoc, and Wireless Networks (WiOpt)*, pp. 1–7, May 2017.

[113] H. Guo, B. Makki, and T. Svensson, "A Comparison of Beam Refinement Algorithms for Millimeter Wave Initial Access, " *28th Annual IEEE International Symposium on Personal, Indoor and Mobile Radio Communications (PIMRC)*, Oct 2017.

[114] M. Giordani, M. Mezzavilla, and M. Zorzi, "Initial access in 5G mmWave cellular networks," *IEEE Communications Magazine*, vol. 54, no. 11, pp. 40–47, November 2016.

[115] A. Ali, N. González-Prelcic, and R. W. Heath Jr, "Millimeter wave beam-selection using out-of-band spatial information," *arXiv preprint arXiv:1702.08574*, 2017.

[116] C. Jeong, J. Park, and H. Yu, "Random access in millimeter-wave beamforming cellular networks: issues and approaches," *IEEE Communications Magazine*, vol. 53, no. 1, pp. 180–185, 2015.

[117] P. Kela, M. Costa, J. Turkka, M. Koivisto, J. Werner, A. Hakkarainen, M. Valkama, R. Jantti, and K. Leppanen, "Location based beamforming in 5G ultra-dense networks," in *84th IEEE Vehicular Technology Conference (VTC-Fall),* , 2016, pp. 1–7.

[118] G. C. Alexandropoulos, "Position aided beam alignment for millimeter wave backhaul systems with large phased arrays," *arXiv preprint arXiv:1701.03291*, 2017.

[119] F. Maschietti, D. Gesbert, P. de Kerret, and H. Wymeersch, "Robust location-aided beam alignment in millimeter wave massive MIMO," *arXiv preprint arXiv:1705.01002*, 2017.

[120] J. C. Aviles and A. Kouki, "Position-aided mm-wave beam training under NLOS conditions," *IEEE Access*, vol. 4, pp. 8703–8714, 2016.

[121] A. Capone, I. Filippini, and V. Sciancalepore, "Context information for fast cell discovery in mm-wave 5G networks," in *21th European Wireless Conference*, 2015, pp. 1–6.

[122] N. Garcia, H. Wymeersch, E. G. Ström, and D. Slock, "Location-aided mm-wave channel estimation for vehicular communication," in *17th IEEE International Workshop on Signal Processing Advances in Wireless Communications (SPAWC)*, 2016, pp. 1–5.

[123] G. E. Garcia, G. Seco-Granados, E. Karipidis, and H. Wymeersch, "Transmitter beam selection in millimeter-wave mimo with in-band position-aiding," *arXiv preprint arXiv:1705.05668*, 2017.

[124] J. G. Andrews, H. Claussen, M. Dohler, S. Rangan, and M. C. Reed, "Femtocells: Past, present, and future," *IEEE Journal on Selected Areas in Communications*, vol. 30, no. 3, pp. 497–508, 2012.

[125] V. Chandrasekhar, J. G. Andrews, and A. Gatherer, “Femtocell networks: a survey,” *IEEE Communications magazine*, vol. 46, no. 9, 2008.

[126] R. Irmer, H. Droste, P. Marsch, M. Grieger, G. Fettweis, S. Brueck, H. P. Mayer, L. Thiele, and V. Jungnickel, “Coordinated multipoint: Concepts, performance, and field trial results,” *IEEE Communications Magazine*, vol. 49, no. 2, pp. 102–111, February 2011.

[127] D. Lee, H. Seo, B. Clerckx, E. Hardouin, D. Mazzarese, S. Nagata, and K. Sayana, “Coordinated multipoint transmission and reception in LTE-advanced: deployment scenarios and operational challenges,” *IEEE Communications Magazine*, vol. 50, no. 2, pp. 148–155, February 2012.

[128] D. M. Gutierrez-Estevez, B. Canberk, and I. F. Akyildiz, “Spatio-temporal estimation for interference management in femtocell networks,” in *23rd International Symposium on Personal Indoor and Mobile Radio Communications (PIMRC)*, 2012, pp. 1137–1142.

[129] A. Umbert, J. Pérez-Romero, F. Casadevall, A. Kliks, and P. Kryszkiewicz, “On the use of indoor radio environment maps for HetNets deployment,” in *9th International Conference on Cognitive Radio Oriented Wireless Networks and Communications (CROWNCOM)*, 2014, pp. 448–453.

[130] J. Perez-Romero, A. Zalonis, L. Boukhatem, A. Kliks, K. Koutlia, N. Dimitriou, and R. Kurda, “On the use of radio environment maps for interference management in heterogeneous networks,” *IEEE Communications Magazine*, vol. 53, no. 8, pp. 184–191, 2015.

[131] J. Tadrous and A. Eryilmaz, “On optimal proactive caching for mobile networks with demand uncertainties,” *IEEE/ACM Transactions on Networking*, vol. 24, pp. 2715–2727, Oct. 2016.

[132] R. Atawia, H. Abou-zeid, H. S. Hassanein, and A. Noureldin, “Robust resource allocation for predictive video streaming under channel uncertainty,” in *IEEE Global Communications Conference (GLOBECOM)*, 2014, pp. 4683–4688.

[133] A. Noulas, S. Scellato, N. Lathia, and C. Mascolo, “Mining user mobility features for next place prediction in location-based services,” in *12th IEEE international conference on Data mining (ICDM)*, pp. 1038–1043.

[134] J. Froehlich and J. Krumm, in *Route Prediction from Trip Observations*, April 2008.

[135] J. Krumm, in *A Markov Model for Driver Turn Prediction.* SAE 2008 World Congress, April 2008.

[136] M. Balabanović and Y. Shoham, “Fab: content-based, collaborative recommendation,” *Communications of the ACM*, vol. 40, no. 3, pp. 66–72, 1997.

[137] J. Salter and N. Antonopoulos, "Cinemascreen recommender agent: combining collaborative and content-based filtering," *IEEE Intelligent Systems*, vol. 21, no. 1, pp. 35–41, 2006.

[138] Z. Huang, D. Zeng, and H. Chen, "A comparison of collaborative-filtering recommendation algorithms for e-commerce," *IEEE Intelligent Systems*, vol. 22, no. 5, 2007.

[139] G. Adomavicius and A. Tuzhilin, "Toward the next generation of recommender systems: A survey of the state-of-the-art and possible extensions," *IEEE transactions on knowledge and data engineering*, vol. 17, no. 6, pp. 734–749, 2005.

[140] C. Song, Z. Qu, N. Blumm, and A.-L. Barabási, "Limits of predictability in human mobility," *Science*, vol. 327, no. 5968, pp. 1018–1021, 2010.

[141] S.-J. Kim, E. Dall'Anese, and G. Giannakis, "Cooperative spectrum sensing for cognitive radios using kriged Kalman filtering," *IEEE Journal of Selected Topics in Signal Processing*, vol. 5, no. 1, pp. 24–36, 2011.

[142] M. Malmirchegini and Y. Mostofi, "On the spatial predictability of communication channels," *IEEE Transactions on Wireless Communications*, vol. 11, no. 3, pp. 964–978, 2012.

[143] Y. Yan and Y. Mostofi, "Impact of localization errors on wireless channel prediction in mobile robotic networks," in *IEEE Globecom, Workshop on Wireless Networking for Unmanned Autonomous Vehicles*, Dec. 2013.

[144] S. Mekki, M. Amara, A. Feki, and S. Valentin, "Channel gain prediction for wireless links with Kalman filters and expectation-maximization," in *IEEE Wireless Communications and Networking Conference (WCNC)*, 2016, pp. 1–7.

[145] Q. Liao, S. Valentin, and S. Stańczak, "Channel gain prediction in wireless networks based on spatial-temporal correlation," in *16th IEEE International Workshop on Signal Processing Advances in Wireless Communications (SPAWC)*, 2015, pp. 400–404.

[146] Y. Mostofi, M. Malmirchegini, and A. Ghaffarkhah, "Estimation of communication signal strength in robotic networks," in *IEEE International Conference onRobotics and Automation (ICRA)*, 2010, pp. 1946–1951.

[147] S. Chouvardas, S. Valentin, M. Draief, and M. Leconte, "A method to reconstruct coverage loss maps based on matrix completion and adaptive sampling," in *2016 IEEE International Conference on Acoustics, Speech and Signal Processing (ICASSP)*, 2016, pp. 6390–6394.

[148] N. Barman, S. Valentin, and M. G. Martini, "Predicting link quality of wireless channel of vehicular users using street and coverage maps," in *IEEE*

*27th Annual International Symposium on Personal, Indoor, and Mobile Radio Communications (PIMRC)*, 2016, pp. 1–6.

[149] N. Bui, M. Cesana, S. A. Hosseini, Q. Liao, I. Malanchini, and J. Widmer, "A survey of anticipatory mobile networking: Context-based classification, prediction methodologies, and optimization techniques," *IEEE Communications Surveys & Tutorials*, 2017.

[150] J. Tadrous, A. Eryilmaz, and H. El Gamal, "Proactive resource allocation: Harnessing the diversity and multicast gains," *IEEE Transactions on Information Theory*, vol. 59, no. 8, pp. 4833–4854, 2013.

[151] L. S. Muppirisetty, J. Tadrous, A. Eryilmaz, and H. Wymeersch, "On proactive caching with demand and channel uncertainties," in *53rd Annual Allerton Conference on Communication, Control, and Computing (Allerton)*, 2015, pp. 1174–1181.

[152] M. Dräxler, J. Blobel, and H. Karl, "Anticipatory download scheduling in wireless video streaming with uncertain data rate prediction," in *8th IFIP Wireless and Mobile Networking Conference (WMNC)*, 2015, pp. 136–143.

[153] X. K. Zou, J. Erman, V. Gopalakrishnan, E. Halepovic, R. Jana, X. Jin, J. Rexford, and R. K. Sinha, "Can accurate predictions improve video streaming in cellular networks?" in *Proceedings of the 16th International Workshop on Mobile Computing Systems and Applications*, 2015, pp. 57–62.

[154] S. Ahmad, R. Reinhagen, L. S. Muppirisetty, and H. Wymeersch, "Predictive resource allocation evaluation with real channel measurements," in *IEEE International Conference on Communications (ICC)*, May 2017, pp. 1–5.